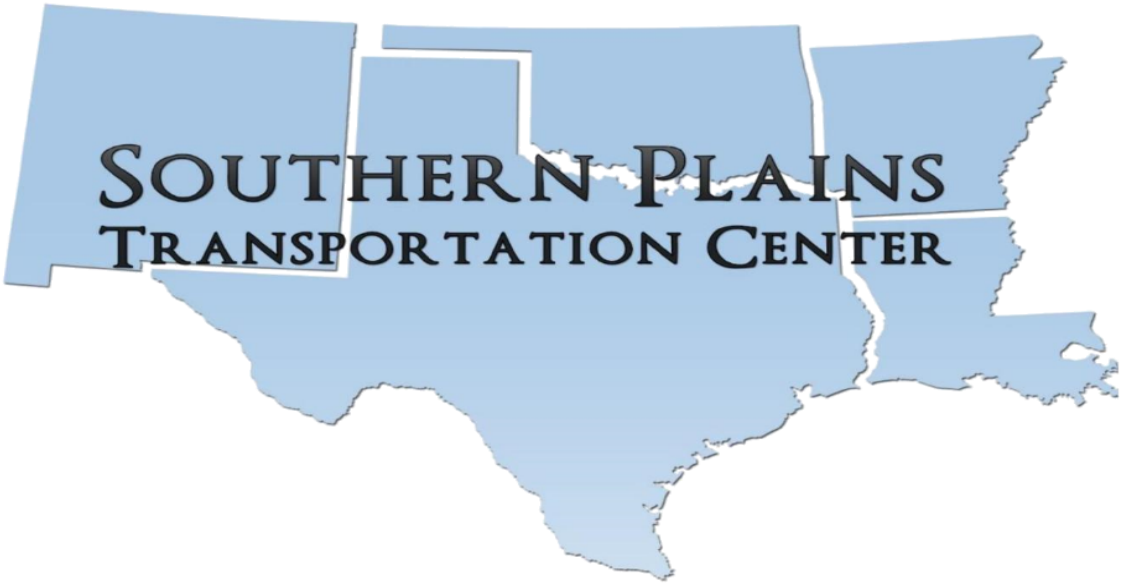

Evaluating Rutting/Stripping Potentials of Asphalt Mixes Using Hamburg Wheel Tracking Device

Rafiqul A. Tarefder, PhD, PE
Md Mehedi Hasan

SPTC14.1-69-F

Southern Plains Transportation Center
201 Stephenson Pkwy, Suite 4200
The University of Oklahoma
Norman, Oklahoma 73109

DISCLAIMER

The contents of this report reflect the views of the authors, who are responsible for the facts and accuracy of the information presented herein. This document is disseminated under the sponsorship of the Department of Transportation University Transportation Centers Program, in the interest of information exchange. The U.S. Government assumes no liability for the contents or use thereof.

Technical Report Documentation Sheet

1. REPORT NO.	2. GOVERNMENT ACCESSION NO.	3. RECIPIENTS CATALOG NO.
SPTC14.1-69		

4. TITLE AND SUBTITLE	5. REPORT DATE
Evaluating Rutting/Stripping Potentials of Asphalt Mixes Using Hamburg Wheel Tracking Device	October 30, 2018
	6. PERFORMING ORGANIZATION CODE
7. AUTHOR(S)	8. PERFORMING ORGANIZATION REPORT
Dr. Rafiqul A. Tarefder and Md Mehedi Hasan	
9. PERFORMING ORGANIZATION NAME AND ADDRESS	10. WORK UNIT NO.
School of Civil Engineering The University of New Mexico 220 University Blvd NE MSC01 1070, Room 3020 Albuquerque, NM 87131-0001	11. CONTRACT OR GRANT NO. DTRT13-G-UTC36
12. SPONSORING AGENCY NAME AND ADDRESS	13. TYPE OF REPORT AND PERIOD COVERED
Southern Plains Transportation Center 201 Stephenson Pkwy, Suite 4200 The University of Oklahoma Norman, OK 73019	Final February 2015 – June 2018 14. SPONSORING AGENCY CODE

15. SUPPLEMENTARY NOTES

University Transportation Center

16. ABSTRACT

A comprehensive study was conducted to evaluate the rutting and stripping potentials of asphalt mixes using Hamburg Wheel Tracking Device (HWTD). A total of forty-two asphalt concrete (AC) mixes, of which thirty-three were SP-III and nine were SP-IV, were collected from different construction sites in cooperation with the New Mexico Department of Transportation (NMDOT). Cylindrical specimens were prepared in the laboratory using superpave gyratory compactor and the HWTD testing was conducted on the laboratory prepared specimens. The test results revealed that SP-IV mixes are less susceptible to rutting and stripping potentials compared to SP-III mixes. The binder grade, Reclaimed Asphalt Pavement (RAP) content, and aggregate type have significant influences on the stripping and rutting performances. Tensile Strength Ratio (TSR) test was also conducted on the laboratory prepared specimen to measure the moisture damage of the AC mixes. No strong correlation was observed between TSR value and the stripping potentials of HWTD data. This research also investigated the effects of warm mix additives on the mixture's rutting performance by performing Multiple Stress-Creep Recovery (MSCR) tests on binders. The test results show that warm mix asphalt modification improves the rutting potential of the mixtures. Several pavement sections were analyzed by Pavement ME software using level 2 design inputs. The rut values obtained from ME analysis after twenty years of pavement design life were compared with that of HWTD test results. The ME analysis yields higher rut depth after 20 years of pavement service life compared to the laboratory measured value. Based on the HWTD laboratory test results, a detailed specification for rutting of SP-III and SP-IV mixes was developed to be implemented by the NMDOT during the mix design stage.

17. KEY WORDS	18. DISTRIBUTION STATEMENT
Rutting, Stripping, HWTD, TSR, MEPDG	No restrictions. This publication is available at www.sptc.org and from the NTIS.

19. SECURITY CLASSIF. (OF THIS REPORT)	20. SECURITY CLASSIF. (OF THIS PAGE)	21. NO. OF PAGES	22. PRICE
Unclassified	Unclassified	89 + cover	

SI* (MODERN METRIC) CONVERSION FACTORS

APPROXIMATE CONVERSIONS TO SI UNITS

SYMBOL	WHEN YOU KNOW	MULTIPLY BY	TO FIND	SYMBOL
		LENGTH		
in	inches	25.4	millimeters	mm
ft	feet	0.305	meters	m
yd	yards	0.914	meters	m
mi	miles	1.61	kilometers	km
		AREA		
in^2	square inches	645.2	square millimeters	mm^2
ft^2	square feet	0.093	square meters	m^2
yd^2	square yard	0.836	square meters	m^2
ac	acres	0.405	hectares	ha
mi^2	square miles	2.59	square kilometers	km^2
		VOLUME		
fl	fluid ounces	29.57	milliliters	m
oz	gallons	3.785	liters	L
gal	cubic feet	0.028	cubic meters	L
ft^3	cubic yards	0.765	cubic	m^3
yd^3	meters NOTE: volumes greater than 1000 L shall be shown in m^3			m^3
		MASS		
oz	ounces	28.35	grams	g
lb	pounds	0.454	kilograms	kg
T	short tons (2000 lb)	0.907	megagrams (or "metric ton")	Mg (or "t")
		TEMPERATURE (exact degrees)		
^oF	Fahrenheit	5 (F-32)/9 or (F-32)/1.8	Celsius	^oC
		ILLUMINATION		
fc	foot-candles	10.76	lux	lx
fl	foot-Lamberts	3.426	$candela/m^2$	cd/m^2
		FORCE and PRESSURE or STRESS		
lbf	poundforce	4.45	newtons	N
lbf/in^2	poundforce per square inch	6.89	kilopascals	kPa

APPROXIMATE CONVERSIONS FROM SI UNITS

SYMBOL	WHEN YOU KNOW	MULTIPLY BY	TO FIND	SYMBOL
		LENGTH		
mm	millimeters	0.039	inches	in
m	meters	3.28	feet	ft
m	meters	1.09	yards	yd
km	kilometers	0.621	miles	mi
		AREA		
mm^2	square millimeters	0.0016	square inches	in^2
m^2	square meters	10.764	square feet	ft^2
m^2	square meters	1.195	square yards	yd^2
ha	hectares	2.47	acres	ac
km^2	square kilometers	0.386	square miles	mi^2
		VOLUME		
mL	milliliters	0.034	fluid ounces	fl oz
L	liters	0.264	gallons	gal
m^3	cubic meters	35.314	cubic feet	ft^3
m^3	cubic meters	1.307	cubic yards	yd^3
		MASS		
g	grams	0.035	ounces	oz
kg	kilograms	2.202	pounds	lb
Mg (or "t")	megagrams (or "metric ton")	1.103	short tons (2000 lb)	T
		TEMPERATURE (exact degrees)		
^oC	Celsius	1.8C+32	Fahrenheit	^oF
		ILLUMINATION		
lx	lux	0.0929	foot-candles	fc
cd/m^2	$candela/m^2$	0.2919	foot-Lamberts	fl
		FORCE and PRESSURE or STRESS		
N	newtons	0.225	poundforce	lbf
kPa	kilopascals	0.145	poundforce per square h	lbf/in^2

ACKNOWLEDGEMENTS

The authors would like to express their sincere gratitude and appreciation to the Southern Plain Transportation Center (SPTC) and NMDOT for financially supporting this research project. The UNM research team would like to thank the Project Technical Panel for their valuable suggestions during the quarterly meetings. Special thanks go to project sponsor James Gallegos, Materials Bureau Chief, project advocate Mr. Parveez Anwar, Former State Asphalt Engineer; Jeff Mann, Pavement Management and Design Bureau Chief, Panel Members Jeremy Rocha, Materials Bureau, and Kelly Montoya, Materials Bureau.

Evaluating Rutting/Stripping Potentials of Asphalt Mixes Using Hamburg Wheel Tracking Device

Final Report

October 2018

Dr. Rafiqul A. Tarefder
Md Mehedi Hasan
SPTC14.1-69-F

Southern Plains Transportation Center
201 Stephenson Pkwy, Suite 4200
The University of Oklahoma
Norman, Oklahoma 73109

TABLE OF CONTENTS

LIST OF TABLES

LIST OF FIGURES

EXECUTIVE SUMMARY

Rutting is one of the primary distresses in the flexible pavement and defined as the longitudinal depression in the wheel path. Stripping, on the other hand, is defined as the adhesive failure between the asphalt binder and aggregate. Rutting and stripping have become potential distresses for New Mexico's asphalt pavement. This research project has conducted a comprehensive study to evaluate the rutting and stripping potentials of asphalt mixes using Hamburg Wheel Tracking Device (HWTD). A total of forty-two asphalt concrete (AC) mixes, of which thirty-three were SP-III and nine were SP-IV, were collected from different construction sites in cooperation with the NMDOT. Cylindrical specimens were prepared in the laboratory using superpave gyratory compactor and the HWTD test was conducted on the laboratory prepared specimens. The test results revealed that SP-IV mixes showed less rutting and stripping potentials compared to SP-III mixes. The binder grade, RAP content, aggregate type etc. have significant influences on the stripping and rutting performance of the AC mixes. Tensile Strength Ratio (TSR) test was also conducted on the laboratory prepared specimen to measure the moisture damage of the AC mixes. No strong correlation was observed when the moisture susceptibility of the AC mixes obtained from the TSR test was compared with the stripping potentials from HWTD test data.

This research investigated the effects of warm mix additives on the mixture's rutting performance by performing MSCR and Dynamic Shear Rheometer (DSR) tests. The test results show that warm mix asphalt modification improves the rutting potential of the AC mixtures.

Several pavement sections were analyzed in Pavement ME software for level 2 design. The rut deformation values obtained from the analysis after twenty years of pavement design life were compared with that of HWTD test results. The ME analysis yields higher rut depth after 20 years of pavement service life compared to the laboratory measured value.

Finally, based on the HWTD laboratory test results, a detailed specification for NMDOT was developed to measure the quality of rut resistance of both the SP-III and SP-IV mixes.

INTRODUCTION

Rutting is one of the major distresses in the flexible pavement and defined as the longitudinal depression in the wheel path formed by the accumulation of permanent deformations caused by repeated heavy load, and shear failure of the asphalt concrete (AC) materials. Stripping of flexible pavement indicates the adhesive fracture between the asphalt binder and the aggregate. Rutting and stripping have become potential distresses for New Mexico's asphalt pavement. Until now, New Mexico Department of Transportation (NMDOT) evaluates the resistance of Asphalt Concrete (AC) to moisture damage by determining the Tensile Strength Ratio (TSR). Asphalt Concrete (AC) is also susceptible to permanent deformation (rutting) under traffic loading which is affected by AC temperature, aggregate type, and binder type. There is no complete research in the literature which examined all these factors at the same time to understand rutting and stripping. The following section described a comprehensive literature review on several factors that have significant effect on the rutting and stripping potential of AC materials.

Effect of Aggregate

Aggregates play an important role on the performance of asphalt mixtures since most of it is composed with different type of aggregates. Aggregate mineralogy and durability properties are keys to determine the influence of aggregates in HWTD test. Aggregate type is closely related to permanent deformation (rutting) since its composition influences the behavior of this distress. The interplay between aggregates type, binder type and temperature are significant properties to increase the susceptibility to rutting. Otherwise, the aggregate properties such as particle shape, angularity and texture also play an important role. Understand the effect of aggregate is difficult to quantify since any aggregate properties will differ the results. In terms of degradation, limestone aggregates shows higher level of degradation and lower levels of stripping different than gravel aggregates. The correlation between HWTD and Los Angeles abrasion test showed good results, harder aggregates tend to perform better in the HWTD test [1].

Effect of Anti-Stripping Agents

The use of additives such as anti-stripping agents changes the binder properties in addition to the intended modification; it proved resistance against moisture damage. The use of anti-stripping agents in AC mixtures has become useful to several transportation agencies to avoid moisture damage [2]. It is believed the stripping potential of asphalt mixtures is potentially reduced with the use of anti-stripping agents. New Mexico department of transportation uses hydrated lime and Versabind as potential anti-stripping additives in their AC mixtures. A comparison between hydrated lime and liquid anti-stripping agents was made by some researches; they found that hydrated lime has better results than liquid anti-stripping agents in terms of HWTD results [3]. In addition, Lu observed that effectiveness of hydrated lime does not decrease, but instead in some cases increases with conditioning time, while the effectiveness of the liquid anti-stripping agents generally does not change with time. It was also found that percentage content of anti-stripping agent it is not related to

performance, if additives are used incorrectly or when not needed adverse effects may occur and maintenance may be needed early than expected. Higher anti-stripping content in the mixture can result in worse results since these agents affect the deformation characteristics of the mixture.

Anyways, the amount of anti-stripping agent is also related to gradation of the aggregate. Usually a 1 to 1.5 percent of additive is needed but this may change if presence of fines is high in the aggregate. Tensile strength ratio is the indicator that most of the transportation agencies adopt to analyze the striping effect in AC mixtures. Previous research has shown a poor correlation between TSR and HWTD results [4]. Hamburg wheel tracking device can closely identify the effect of anti-stripping agents but it may underestimate the performance of mixes containing soft binder at fixed water test temperatures. Hydrated lime became the only anti-stripping agent used by CDOT since it has given positive results at the time to prevent moisture damage in the HWTD test. Anyways, CDOT states that some other anti-stripping agents may work as well as hydrated lime or better with some type of aggregates. Properties measured by the HWTD test of the mixtures modified with anti-stripping agents did not always show improvement in comparison with mixtures with no anti-stripping agents [5].

Effect of Gradation and Air Voids (AV)

HWTD results are affected by different mixture design properties and test inputs as mentioned. Throughout the past of year's research to understand coarse and finer gradation to understand rutting and stripping distresses was performed. Kandhal and Cooley [6] defined gradations below and above the restriction zone to define finer and coarser mixtures. Mixtures tested in three different rutting susceptibility tests showed no significant difference between gradations. Gokhale et al. [7] used the accelerated pavement testing and asphalt pavement analyzer to evaluate coarse and fine superpave mixtures. Same findings as Khandal and Colley were observed. Golalipour et al. [8] defined three variations in mixtures gradation. Better rutting results were observed in upper limit variations (coarser gradation). In addition, a variation in testing results was observed when AV contents changed. Manal and Attia [9] tested three different types of aggregates using the wheel tracker test. Results shown improvement when coarse gradation was used in the AC mixture. Differently, Habbeb et al. [10] found less rutting when finer gradation mixtures were tested in the wheel tracker test. Kanitpong et al. [11] found that finer and coarser mixtures permanent deformation performance is related to the type of aggregate. In addition, finer mixtures appear to have greater stripping resistance. Studies showed mixtures with lower AV performed better. Permanent deformation and other distresses were sensitive to AV contents. Tarefder and Zamman [12] observed that AV contents and gradation are important rutting factors in AC mixtures using the asphalt pavement analyzer. Results showed an improvement in rutting resistance for lower AV contents and coarser gradations. Aschenbrener and Curier [13] tested 4 types of mixtures at different AV contents using the HWTD. Based on the results, a recommendation of 5 to 7 percent AV contents range was defined. Kassem et al. [14] stated that AV contents are less sensitive to HWTD results.

Effect of Warm Mix Asphalt Agents

In the past years, the effort of industries to reduce the emission of carbon dioxide and other greenhouses was conducted by different research. WMA is being an alternative to HMA in order to reduce environmental effects and increase the benefits in terms of production, workability and economics. WMA can be classified by degree of temperature reduction or by technologies used to reduce temperature. Mostly, the technologies used to reduce temperature are foaming techniques, organic or wax additives and chemical additives. Variation of temperatures in the production of WMA has a wide range. From temperatures 10 °C to 20 °C below HMA to even temperatures close to boiling water. Research using HWTD was conducted to understand the effect of agents in WMA deformation. Influence of curing time at the time of using WMA agents was found. Short term aging (2 hours) is less critical to HMA mixtures compared to WMA using HWTD test and Evotherm showed better results in terms of cycles to failure when the curing time was increased from 2 to 4 hours [15]. Perkins [16] found the use of anti-stripping agents improved WMA mixtures in terms of rutting distresses. Liva and MacBroom [17] tested WMA mixtures with different agents. AC with a PG 64-28 binder was tested using different Synthetic Zeolite Products (SZP), Evotherm agents and Sasobit. SZP did not show improvement for rutting distresses and stripping was observed. Otherwise, Evotherm 3G showed improvement in rutting and stripping was not observed. Finally, improvement was observed for Evotherm DAT modified and Sasobit for rutting and stripping behavior. Hurley and Prowell [18] have tested WMA mixtures with two different binder grades and type of aggregates. PG 64-22 and PG 76-22 binder grades were used with limestone and granite as type of aggregates. Four mixes were tested with and without Evotherm WMA agent. Results showed an improvement in the rutting rate (mm/hr.) when WMA mixtures were in presence of Evotherm agent. In addition, their study observed that Evotherm improves the compactability in the SGC and vibratory compactor.

Colorado department of transportation tested WMA mixtures with a PG58-28 binder grade and three WMA technologies (Advera, Evotherm and Sasobit). Results showed no improvement between WMA technologies and HMA control mixtures [19]. Jones et al. [20] conducted a comparison between WMA mixtures with Cecabase, Gencor and Evotherm DAT agents and a control HMA mixture. AV range was between 6.3 and 7.0 %. Results showed that HMA mixture and WMA mixtures with Evotherm DAT and Cecabase RT behaved similar with a maximum rutting depth of 10 mm. Otherwise, WMA mixture with Gencor exceeded the 12.5 mm maximum impression point set by most of transportation state agencies.

The specific objective of this research project is to measure and minimize the impact of rutting and stripping on asphalt concrete pavements. Due to climate and materials variability between different regions, separate specification is needed to determine the suitability of HWTD in New Mexico. This study involves testing, interpretation of laboratory data, and MEPDG evaluations to assess the effectiveness of HWTD testing criteria, and develop detailed specifications needed to ensure proper testing for implementation of HWTD in New Mexico.

MIX COLLECTION, PREPARATION, AND TESTING

Mix Collection

A total of forty two mixes were collected according to the AASHTO T 2 [21] and AASHTO T 168 [22] standards from various construction sites in different districts of New Mexico in cooperation with the NMDOT. Figure 1 shows the AC materials collection from the field.

Figure 1: AC materials collection from the field

The collected materials are listed in Table 1. Table 1 presents the properties of the collected AC materials including the aggregate type and performance grade (PG) binder. It is seen from Table 1 that four different PG binder grade were used in the collected mixes. These are PG 64-28, PG 70-22, PG 76-22, and PG 76-28. The pavement section of mixtures 8, 9, 10, 11 and 12 was one of the Specific Pavement Study Section-10 (SPS-10) of the nationwide Long-Term Pavement Performance (LTPP) monitoring program. Five WMA/HMA mixtures were collected, where these mixes having the same mixture designs but only differing in the type of mixture, WMA agent and polymer modified binder. The SPS-10 project consists of pavement test sections including i) Control HMA, ii) Terex Foaming, iii) Evotherm®, iv) Cecabase® 1, and v) Cecabase® 2 (polymerized).

Table 1: Collected materials

Test Code	Project	Mixture	Type	Gradation	Aggregate	Binder PG Used
D1A1	1C00003	1	WMA	SP-III	Sand and Gravel	76-22
D2A1	2100880	2	WMA	SP-III	Limestone	76-22
D2A2	2100250/2100251	3	WMA	SP-III	River Deposits	70-22
D4A1	4100650	4	HMA	SP-III	Basalt	64-28
D4A2	4100660	5	WMA	SP-III	River Deposits	76-22
D4A3	4100450	6	HMA	SP-III	Shale	64-28
D6A1	6100451	7	WMA	SP-III	Dacite	76-28
D4A4	4100600	8	HMA	SP-III	Sand & Gravel	76-22
D4A5	4100600	9	WMA	SP-III	Sand & Gravel	76-22
D4A6	4100600	10	WMA	SP-III	Sand & Gravel	76-22
D4A7	4100600	11	WMA	SP-III	Sand & Gravel	76-22
D4A8	4100600	12	WMA	SP-III	Sand & Gravel	76-22*
D4A9	4100670	13	WMA	SP-III	Sand & Gravel	76-22
D1A2	1100900	14	WMA	SP-III	Sand & Gravel	76-22
D3A1	3100460	15	HMA	SP-III	Basalt	76-22
D4A10	4100590	16	WMA	SP-III	Sand & Gravel	64-28
D3A2	A301010/A301610	17	WMA	SP-III	Basalt	76-22
D3A3	A300411	18	HMA	SP-III	Quartzite	70-22
D3A4	A300380	19	WMA	SP-III	Sand & Gravel	76-22
D2A3	G3A92	20	HMA	SP-III	River Deposits	70-22
D2A4	2100900	21	WMA	SP-IV	Sand & Gravel	70-22
D5A1	5100411	22	HMA	SP-III	Quartzite	64-28

*Modified Polymer

Table1: Collected materials (Continued)

Test Code	Project	Mixture	Type	Gradation	Aggregate	Binder PG Used
D4A11	4100800	23	WMA	SP-III	Sand & Gravel	64-28
D3A5	3100300	24	HMA	SP-III	Sand & Gravel	70-22
D5A2	F100110	25	HMA	SP-III	Sand & Gravel	70-22
D3A6	3100340	26	HMA	SP-III	Sand & Gravel	70-22
D6A2	6100223	27	HMA	SP-III	Crushed Granite	76-28
D4A12	4100810	28	WMA	SP-III	Sand & Gravel	70-22
D5A3	S100140	29	HMA	SP-III	Sand & Gravel	64-28
D2A5	2101370	30	WMA	SP-III	Limestone	76-22
D1A3	1100890	31	WMA	SP-IV	Limestone	76-22
D4A13	4100780	32	WMA	SP-III	Basalt	64-28
D3A10	A300420	33	HMA	SP-III	Limestone	70-22
D6A3	6100783	34	HMA	SP-III	Crushed Granite	70-22
D6A4	6100783	35	HMA	SP-III	Crushed Granite	70-22
D3A8	A301010/A301610	36	WMA	SP-IV	Basalt	76-22
D1A4	1100570	37	HMA	SP-IV	Limestone	76-22
D1A5	1100641	38	WMA	SP-IV	Volcanic	76-22
D2A6	2100890	39	WMA	SP-IV	Limestone	76-22
D5A4	5100440	40	HMA	SP-IV	Sand & Gravel	64-22
D1A6	1101460	41	HMA	SP-IV	Sand & Gravel	70-28
D3A9	A300280	42	WMA	SP-IV	Basalt	70-22

Gradation

As mentioned previously, AC mixtures 8 to 12 only differ in the WMA agent used within the mixes. For gradation purposes, only thirty-eight mixtures were analyzed since SPS-10 mixtures have the same gradation and mixture properties. The combined aggregate gradation shall be classified as coarse-graded when it passes below the Primary Control Sieve (PCS) control point as defined in the Table 2 [23].

Table 2: Gradation classification

	PCS Control Point for Mixture Nominal Maximum Aggregate Size (% Passing)				
Nominal Maximum Aggregate Size (NMAS)	37.5 mm	25.0 mm	19.0 mm	12.5 mm	9.5 mm
PCS	9.5 mm	4.75 mm	4.75 mm	2.36 mm	2.36 mm
PCS Control Point (% Passing)	47	40	47	39	47

Table 3 presents the aggregate gradation classification based on the Federal Highway Administration (FHA) [24-25].

Table 3: Gradation classification based on FHA

Mixture NMAS	Coarse-Graded	Fine Graded
37.5 mm (1 ½")	< 35% Passing 4.75 Sieve	>35% Passing 4.75 Sieve
25.0 mm (1")	< 40% Passing 4.75 Sieve	>40% Passing 4.75 Sieve
19.0 mm (3/4")	<35% Passing 2.36 Sieve	>35% Passing 2.36 Sieve
12.5 mm (1/2")	<40% Passing 2.36 Sieve	>40% Passing 2.36 Sieve
9.5 mm (3/8")	<45% Passing 2.36 Sieve	>45% Passing 2.36 Sieve
4.75 mm (No. 4 Sieve)	N/A (No standard super pave gradation)	

Figure 2 illustrates the gradation plot for the first sixteen SP-III mixes whereas Figure 3 shows the gradation plot for the rest of the mixes. Figure 4 depicts the gradation plot for the nine SP-IV mixes. This plot illustrates the maximum density line along with the gradation of the mixes. The maximum density gradation line represents the tightest arrangement that particles can fit together. When designing mix, the maximum density line will be used as a guide for increasing or decreasing Voids in Mineral Aggregate (VMA). Sufficient inter-particle space must be available for a minimum amount of asphalt binder and the aggregate must have a sufficiently strong skeleton to carry the traffic loads.

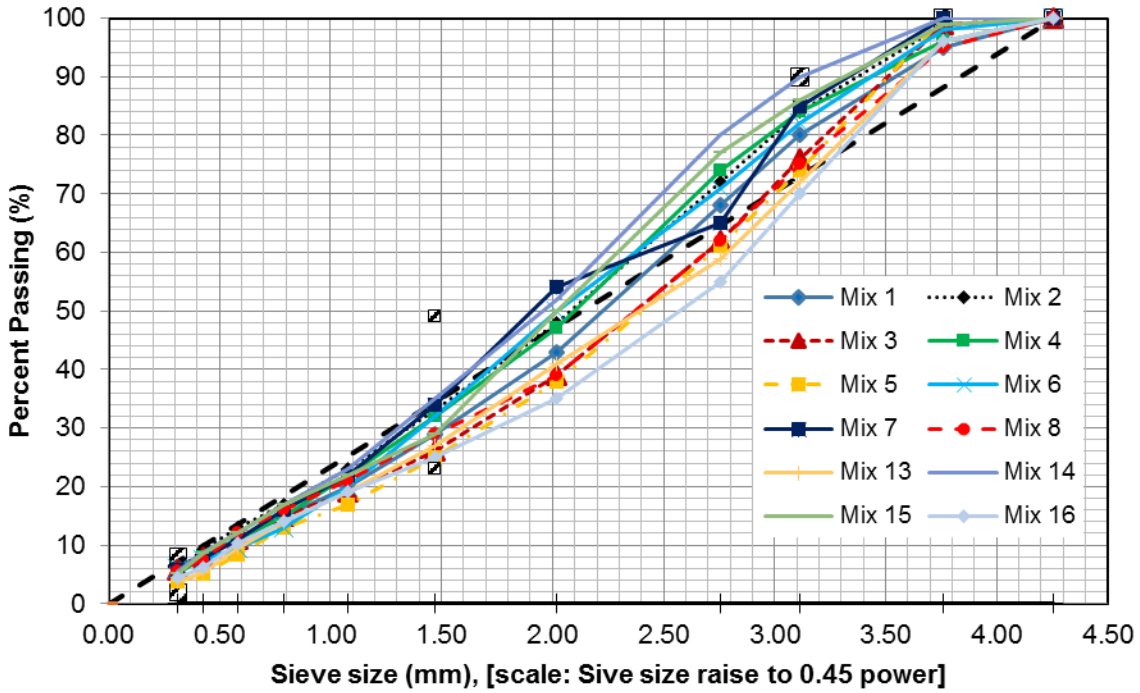

Figure 2: Gradation curve for the first sixteen SP-III mixes

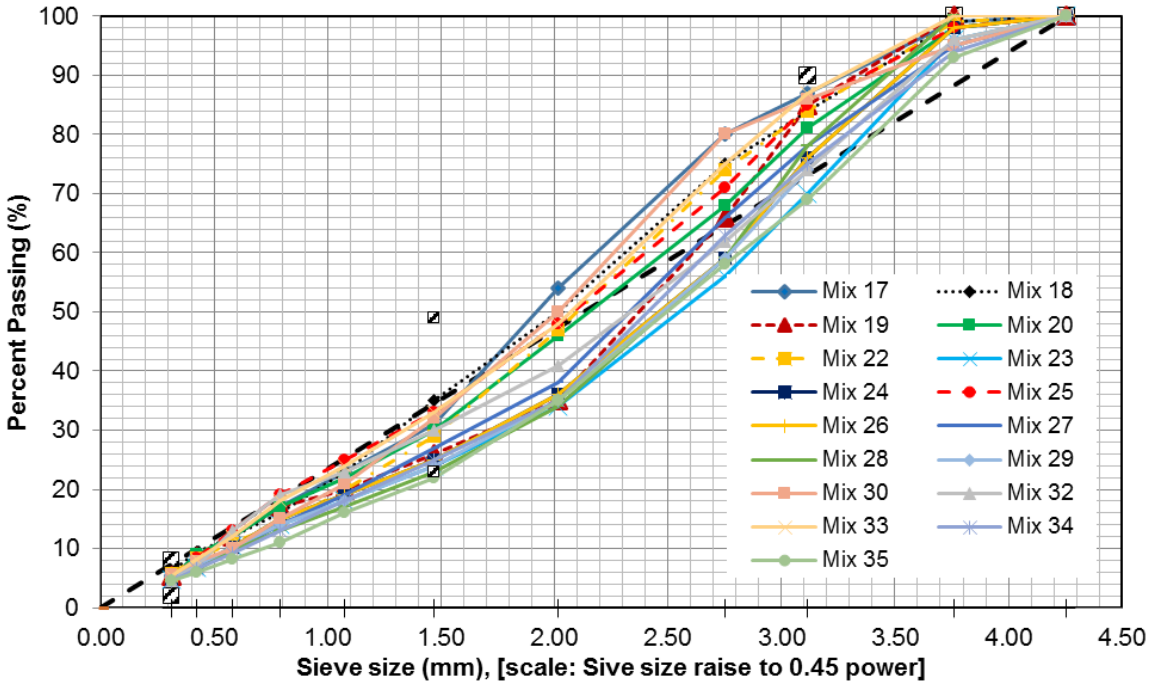

Figure 3: Gradation curve for the rest of the SP-III mixes

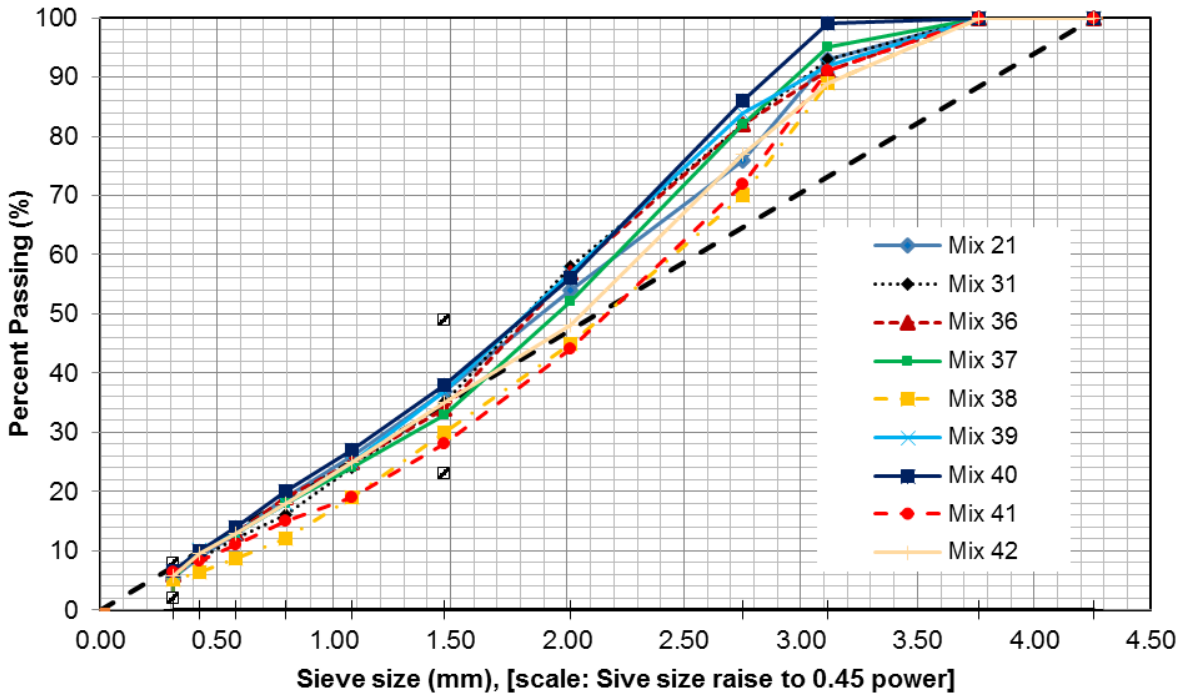

Figure 4: Gradation curve for the SP-IV mixes

Based on the gradation plot the materials are classified as finer or coarse materials. For a mixture with a nominal maximum aggregate size (NMAS) of 12.5 mm that is for SP-IV mixes the primary control sieve number is #8 which has an opening size of 2.36 mm. The combined aggregate gradation is classified as coarse graded when it passes below the PCS. For SP IV mixes if percent passing in sieve # 8 is found to be less than 39 the aggregate would be classified as coarse graded. As can seen from Figure 4 that percent passing #8 sieve was found to be < 39 for all of the SP-IVmixes, Therefore, all of the mixes were classified as coarse materials. The SP-III mixes are also classified according to the standard. The materials classification are summarized in table 4.

Table 4: Mixtures gradation

Mixture	NMAS (mm)	% Passing #4 (4.75mm)	% Passing #8 (2.36 mm)	AASHTO Classification	FHWA Classification
1	19	43	29	Coarser	Coarser
2	19	48	33	Finer	Coarser
3	19	39	26	Coarser	Coarser
4	19	47	32	Finer	Coarser
5	19	38	25	Coarser	Coarser
6	19	50	32	Finer	Coarser
7	19	66	54	Finer	Finer
8	19	39	29	Coarser	Coarser
9	19	39	29	Coarser	Coarser
10	19	39	29	Coarser	Coarser
11	19	39	29	Coarser	Coarser
12	19	39	29	Coarser	Coarser
13	19	41	27	Coarser	Coarser
14	19	52	35	Finer	Finer
15	19	50	29	Finer	Coarser
16	19	35	25	Coarser	Coarser
17	19	54	31	Finer	Coarser
18	19	50	35	Finer	Finer
19	19	35	26	Coarser	Coarser
20	19	46	30	Coarser	Coarser
21	12.5	54	37	Coarser	Coarser
22	19	47	29	Coarser	Coarser
23	19	34	24	Coarser	Coarser
24	19	36	25	Coarser	Coarser
25	19	48	33	Coarser	Coarser
26	19	36	25	Coarser	Coarser
27	19	38	27	Coarser	Coarser
28	19	34	23	Coarser	Coarser
29	19	35	24	Coarser	Coarser
30	19	50	32	Coarser	Coarser

Table 4: Mixtures gradation (Continued)

Mixture	NMAS (mm)	% Passing #4 (4.75mm)	% Passing #8 (2.36 mm)	AASHTO Classification	FHWA Classification
31	12.5	58	35	Coarser	Coarser
32	19	41	30	Coarser	Coarser
33	19	48	33	Coarser	Coarser
34	19	35	25	Coarser	Coarser
35	19	32	22	Coarser	Coarser
36	12.5	57	34	Coarser	Coarser
37	12.5	52	33	Coarser	Coarser
38	12.5	45	30	Coarser	Coarser
39	12.5	57	37	Coarser	Coarser
40	12.5	56	38	Coarser	Coarser
41	12.5	44	28	Coarser	Coarser

Sample Preparation

About 713 samples were prepared using the Superpave gyratory compactor following the AASHTO T 312 [26] test standard. The samples were then cut into specific dimensions using a laboratory cutting saw as shown in Figure 5. Cylindrical samples are prepared to a height of 62±1 mm (Figure 6).

Samples' volumetric properties, theoretical maximum specific gravity (G_{mm}), air voids and bulk specific gravity (G_{mb}) were determined at the UNM laboratory. The G_{mm}, G_{mb} and air void were determined according to the AASHTO T 209 [27], AASHTO T 166 [28], AASHTO T 269 [29] test protocols respectively. The resulting air void range is 5-7%; this meets the desired criteria.

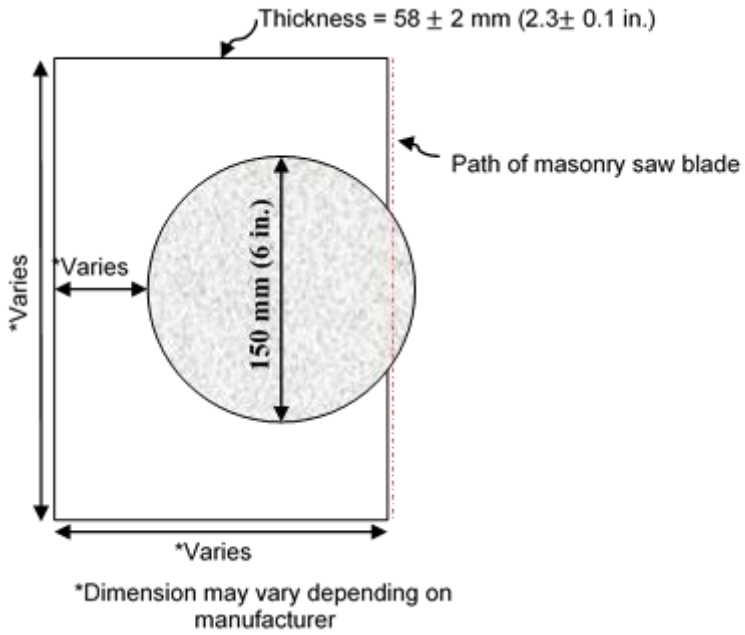

Figure 5: Sample-trimming process

Figure 6: Sample-trimming process

A defined standard configuration for the HWTD test does not exist. AASHTO T 324-11 [30] only addresses the preparation of cylindrical samples, but configuration of the test is not defined. Configuration inputs and samples parameters will affect the results of the HWTD. Variation of test temperature, conditioning time, loading and frequency of loading are configuration parameters that will have significant effect on the test results. The most common setup for the HWTD used in most transportation agencies as follows:

- 20,000 passes along the test track
- 12.5 mm. (0.5 in.) maximum rutting depth
- 52 rpm
- 50°C constant water bath temperature
- 158 lb. (700 N approx.)

Several departments' of transportation have implemented HWTD test in their specifications as an alternative to Tensile Strength Ratio (TSR) test. Researchers found that binder PG is related to HWTD; stiffer asphalt binder showed better results. In their specifications, transportation agencies defined the water temperature test and number of passes according to the binder PG grade of the AC mixture. In addition, a maximum rutting depth was adopted when binder PG varies.

ASPHALT CONCRETE HWTD TESTING

A total of four mixtures (4 sets each Approx.) were tested at 50 ˚C at using UNM HWTD. Wheels of 158 lb. weight rolled over the sample for 20,000 cycles. The resulting deflections were recorded at different intervals of loading. The testing of one set of samples (2 pairs) is shown in Figure 7. For the purpose of this study, orientation of sample placement in polyethylene molds is shown in Figure 8, where the specimen consisting of the lowest air void will be positioned at location 1 and the specimen with the highest air void will be positioned at location 4.

Figure 7: UNM Hamburg Wheel Tracking Testing

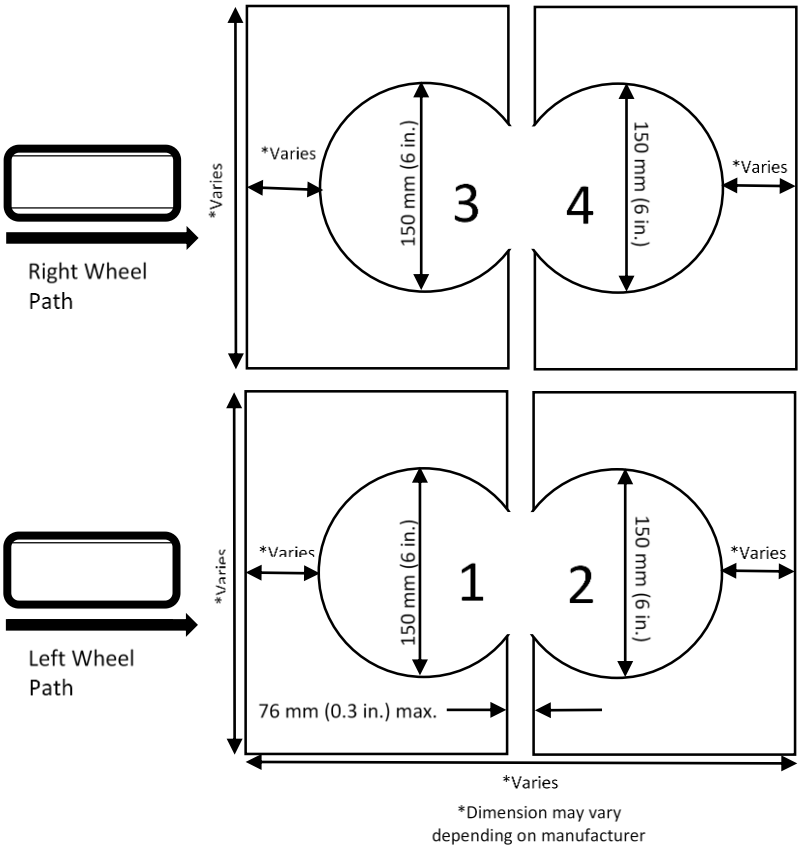

Figure 8: Top view of test specimen configuration

HWTD test is conducted following the AASHTO T 324-11 [30] test standard. It includes the method to determine the premature failure susceptibility of HMA/WMA due to weakness in the aggregate structure, inadequate binder stiffness, or moisture damage. This test method measures the rut depth and number of passes to failure. In addition, it describes the procedure for testing rutting and moisture susceptibility of WMA/HMA AC samples in the HWTD. HWTD results are expressed in post-compaction consolidation, creep slope, stripping inflection point and stripping slope shown in Figure 9**.**

The post-compaction consolidation is the rut depth at 1000 wheel passes and occurs at the very beginning of the test. It is called post-compaction consolidation because the load applied by the wheel increase the density of an asphalt mixture. Post Compaction slope is the inverse of the rate of deformation in the linear region of the deformation curve at 1,000 wheel passes. The creep slope is related to the permanent deformation (rutting) of the asphalt mixture. It is the inverse of the rate of deformation in the linear region of the deformation curve, after post compaction and before stripping [13]. The stripping slope is related to the moisture damage (stripping) of an asphalt mixture. It is the inverse of the rate of deformation in the linear region of the deformation curve, after starting stripping to the end of the test. It is the number of passes required to create a 1 mm impression from stripping [13]. The lower the creep slope and the stripping slope the most severe rutting and moisture damage the mixture experiences. The Striping Inflection Point (SIP) is the number of wheel passes that intersects the creep slope and

the stripping slope. This mark is related to the resistance of the asphalt mixture to moisture damage. Once the stripping inflection is reached moisture damage dominates the performance of the mixture.

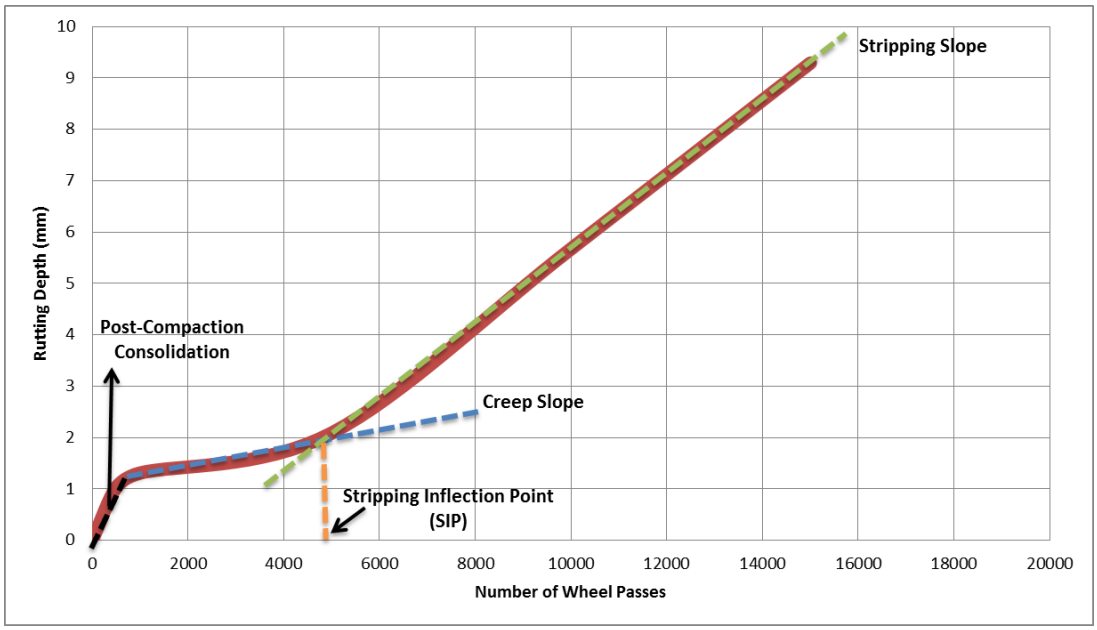

Figure 9: HWTD results curve

The shape of the curve in Figure 9 is the same as creep and repeated load tests which determines the typical permanent deformation curve [31]. The tertiary region is related to moisture damage and is when the samples tend to fail rapidly. Based on the examination of many slabs and pavement cores, the tertiary regions of the curves produced by the HWTD appear to be primarily related to moisture damage, rather than to other mechanisms that cause permanent deformation, such as viscous flow [32]. They state that mixtures that are susceptible to moisture damage tend to start losing fine aggregates around the stripping inflection point, and coarse aggregate particles may become dislodged. The data reported includes the number of passes, maximum impression, test temperature; samples air void content, post-compaction point, creep slope, stripping slope and stripping inflection point.

Test Results and Discussions

Table 5 presents the results of all the AC mixtures tested in the HWTD. Due to repeatability of results, each mixture data set was generalized.

Table 5: HWTD test results

Mixture	Average Number of Passes	Maximum Impression (mm)	Samples Air Voids Average (%)	Post-Compaction Point Slope (pass/mm)	Creep Slope (pass/mm)	Stripping Slope (pass/mm)	SIP
1	20,000	2.57	6.2	962	18,518	N/A	N/A
2	20,000	1.81	5.6	1178	26231	N/A	N/A
3	20,000	2.92	6.3	906	18,151	N/A	N/A
4	20,000	2.48	6.1	763	27,273	N/A	N/A
5	20,000	2.30	5.3	1174	15946	N/A	N/A
6	15,000	15.27	5.8	420	1,794	938	4,990
7	15,827	15.96	6.1	648	2,089	866	5,100
8	20,000	4.72	5.8	677	8,929	N/A	N/A
9	20,000	3.07	5.7	640	7,224	N/A	N/A
10	20,000	3.99	6.0	511	9,359	N/A	N/A
11	20,000	3.59	6.7	837	11,387	N/A	N/A
12	20,000	2.44	6.7	1,171	17,494	N/A	N/A
13	20,000	3.46	6.5	699	20926	N/A	N/A
14	20,000	2.28	5.3	953	13879	N/A	N/A
15	20,000	2.63	5.5	806	21418	N/A	N/A
16	20,000	5.02	5.9	613	11955	N/A	N/A
17	20,000	3.02	5.7	810	15692	N/A	N/A
18	20,000	3.40	5.4	824	12747	N/A	N/A
19	20,000	3.70	5.0	762	10695	N/A	N/A
20	20,000	1.99	6.4	945	19811	N/A	N/A
21	20,000	3.99	5.6	705	11367	3851	14,250
22	20,000	2.84	5.7	761	14029	N/A	N/A
23	20,000	6.34	6.8	540	5476	4174	10,200
24	20,000	4.16	5.4	687	11498	3961	14,800
25	20,000	5.85	5.5	712	9438	2224	13050
26	20,000	5.47	5.3	474	5197	8898	8600

Table 5: HWTD test results (Continued)

Mixture	Average Number of Passes	Maximum Impression (mm)	Samples Air Voids Average (%)	Post-Compaction Point Slope (pass/mm)	Creep Slope (pass/mm)	Stripping Slope (pass/mm)	SIP
27	20,000	2.85	5.8	733	15279	N/A	N/A
28	20,000	3.35	6.6	659	9650	N/A	N/A
29	20,000	11.42	5.8	478	2949	1459	12075
30	20,000	3.99	6.2	734	8520	6910	15100
31	20,000	3.03	5.3	897	8958	N/A	N/A
32	20,000	8.47	5.8	354	4024	2953	13450
33	20,000	4.4	5.4	675	6207	5441	13550
34	20,000	5.63	6.4	540	7475	3602	14200
35	20,000	3.20	5.5	706	14855	N/A	N/A
36	20,000	3.27	5.8	766	9886	N/A	N/A
37	20,000	1.83	6.7	911	22420	N/A	N/A
38	20,000	4.16	6.3	693	8512	N/A	N/A
39	20,000	4.98	5.6	631	9031	N/A	N/A
40	20,000	3.45	5.7	451	8093	8957	10100
41	20,000	4.0	6.3	468	12453	N/A	N/A
42	20,000	3.12	6.9	743	16909	N/A	N/A

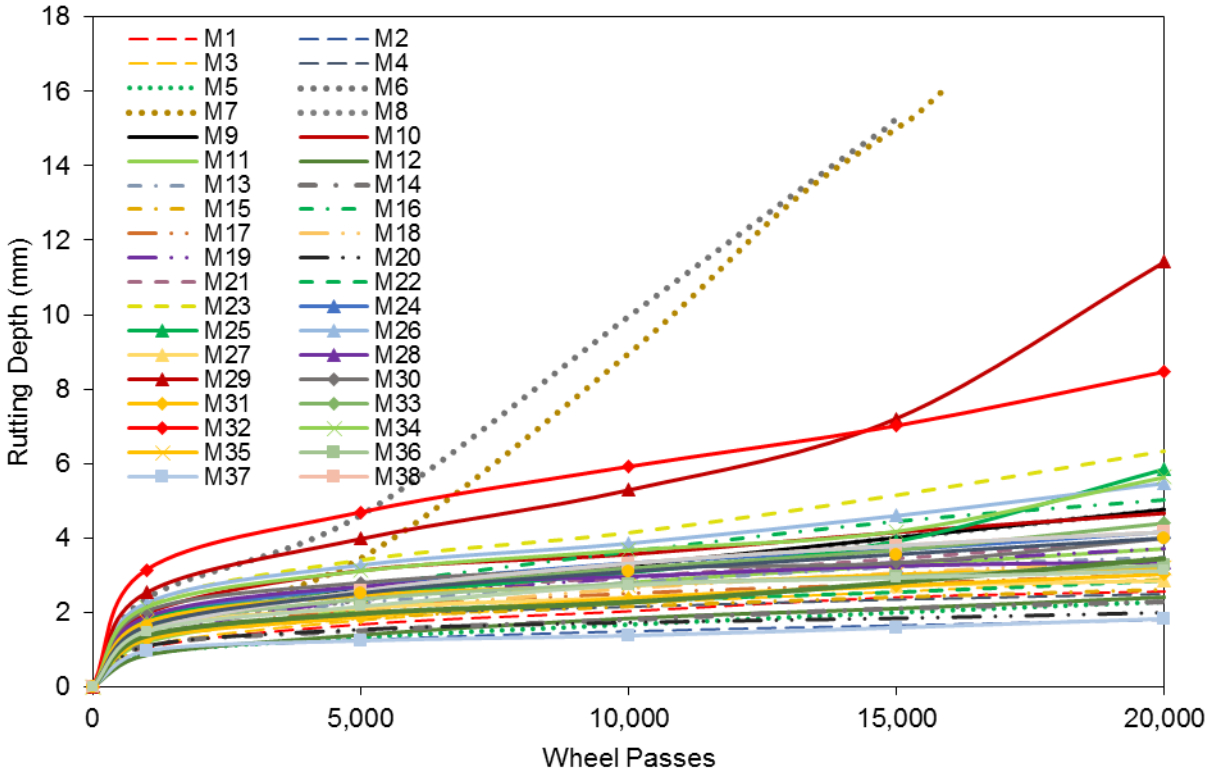

Figure 10: Generalized HWTD results

It can be clearly noticed from Table 4 and Figure 10 that mixtures 6 and 7 reached the stripping phase and wasn't able to finish the corresponding test (20,000 passes). Both mixtures were in presence of unique aggregates as shale and dacite. In addition, these mixtures were defined as finer AC mixtures. Not much can be said about the effect of binder PG and type of mixture. However, better results were expected for mixture 7 due to its higher PG grade of 76-28. In comparison to mixture 6, mixture 7 showed to have a slightly better performance. Comparing mixtures 1, 3, and 4, similar rutting depths maximum rutting depths were observed with better results in mixture 4. In the post-compaction phase, mixture 4 showed less resistance compared to the other 2 mixtures. This effect is closely related to the binder PG of the AC.

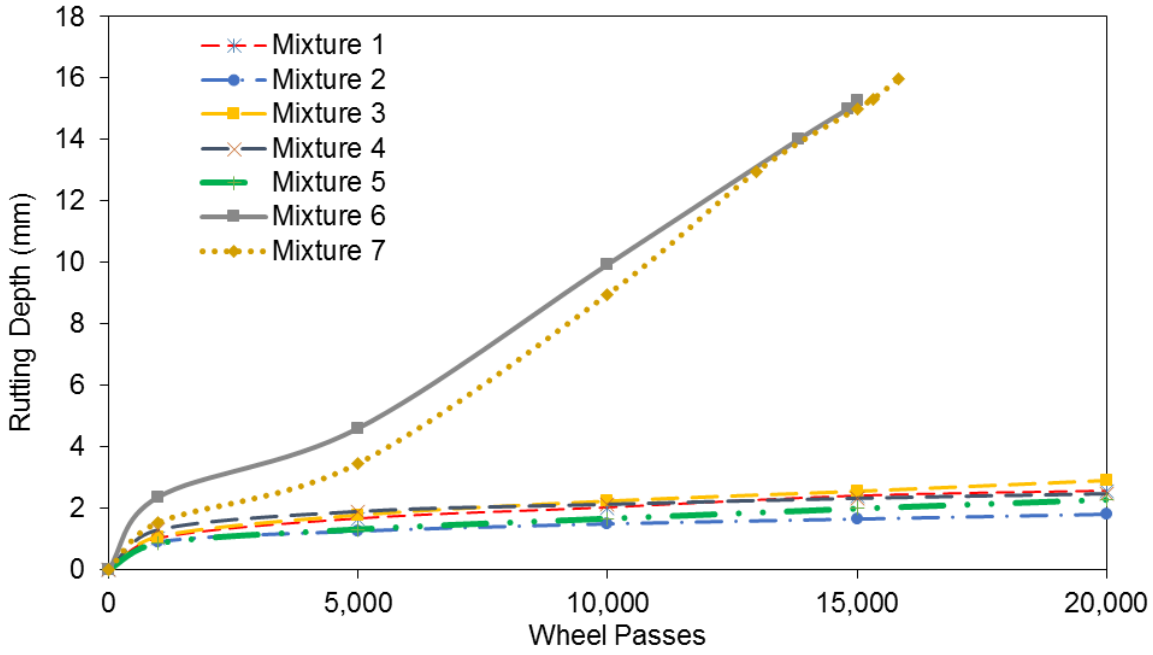

Figure 11: HWTD results for mixtures 1-7

In terms of creep slope, better performance was observed for mixture 4. From these observations, it can be assumed that mixtures with similar maximum rutting depth tend to have higher creep slopes if the rutting potential in the post-compaction phase is less. It can be seen from above that mixture 2 experiences the least amount of deformation (1.81 mm) among all the mixes illustrated in Figure 11. The mixture consists of 33 % RAP and aggregate type of limestone; which might be an attributing factor to its rutting resistance outcome. Mixture 2 results show higher post-compaction and creep slope; which coincides to the assumption made earlier about better performing mixtures such as mix 1, 3, and 4. Also, mixture 5 shows to be a better performing mixture with maximum impression of 2.30 mm. This may be due to its high PG grade of 76-22. Also, the WMA additive may have a contribution to the performance of the mixture.

As discussed earlier, mixture 8 to 12 have the same AC mixtures properties in terms of type of aggregate, gradation, binder PG and so on. These AC mixtures only differ in the type of HMA/WMA technology used. Table 5 lists the similarity of the AC properties and the different mixing technology used for each of the mixtures collected from SPS-10 site location.

Table 6: HMA/WMA mixtures collected from SPS-10 section

No. of Mixture	Type of Mixture	Gradation	Binder Grade Specified PG	Binder Grade Used PG	Type of Aggregate	RAP Content (%)	WMA Agent
8	HMA	SP III	76-22	70-28	Sand and Gravel	20	N/A
9	WMA	SP III	76-22	70-28	Sand and Gravel	20	Terex Foaming
10	WMA	SP III	76-22	70-28	Sand and Gravel	20	Evotherm
11	WMA	SP III	76-22	70-28	Sand and Gravel	20	Cecabase RT
12	WMA	SP III	76-22	70-28+	Sand and Gravel	20	Cecabase RT

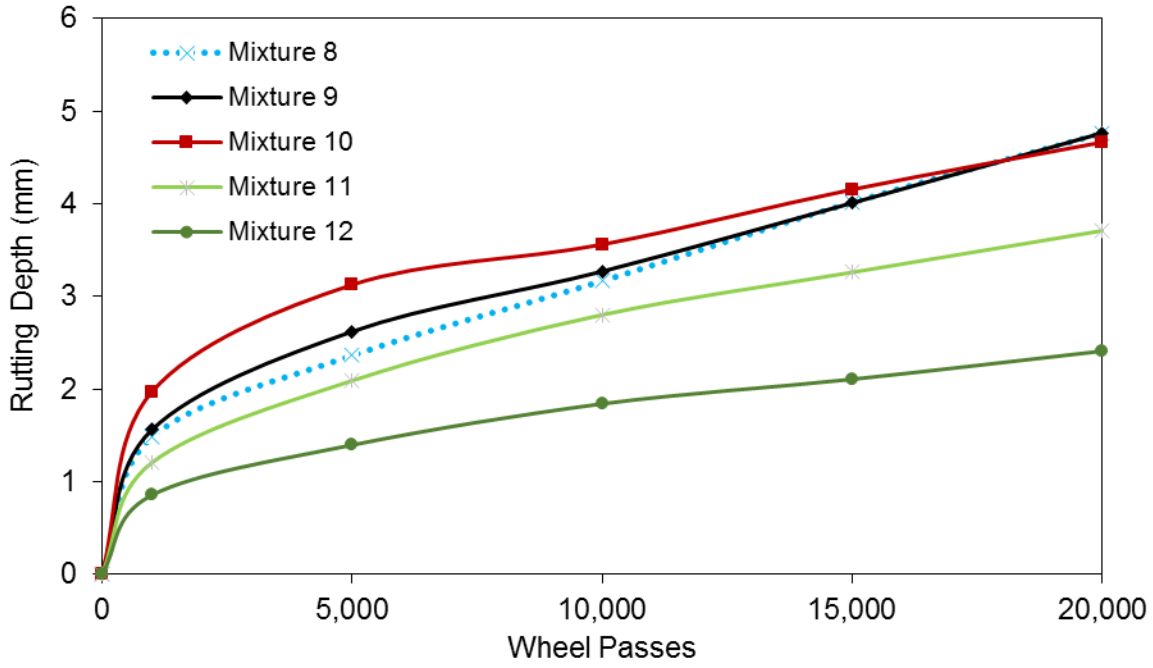

Figure 12: HWTD results for SPS-10 mixtures

As depicted in Figure 12, post-compaction phase and creep phase of mixture 8 and 9 behaved similar. A variation in rutting depth of approximately 0.1 mm and an insignificant variation in the creep slope were observed with better performance of the HMA mixture. A longer post-compaction phase was experienced for mixture 10. WMA mixture with Evotherm experienced a higher rutting depth when samples were under the densifying process. Once creep phase started to dominate the test, mixture 10 experienced a higher creep slope than mixture 8 and 9. A higher rutting depth was

observed for the mixture 10 until the 15,000 wheel passes approximately. Opposite trend was observed when number of passes increased and final rutting depth for this mixture was less than previous tested mixtures. In addition, mixture 10 showed better results in terms of creep slope. Critical phase for mixture 10 was observed in the post compaction phase while creep phase was critical for previous mixtures. Results for Evotherm showed same phenomena as results found by previous literature. Improvement in the creeping phase was observed compared to HMA control. In addition, the impact of Evotherm agent on WMA mixtures is significant when PG grades are higher than PG70-XX.

For the mixture 11, a significant improvement in the rutting depth results was observed in all HWTD phases compared to HMA and WMA mixtures with Foaming and Evotherm technology. As shown in Figure 12 and Table 5, creeping phase for mixtures 10 and 11 have the same trending reflected in the similar creep slope. For these two mixtures, differences were observed only in the post-compaction phase. Compared to mixtures 1 and 2, WMA with Cecabase RT showed better results in all HWTD phases. It was found that Cecabase RT showed better results as WMA agent.

Finally, WMA mixture with Cecabase RT and modified polymer showed the most significant results from all five mixtures. An important improvement in maximum impression depth and in HWTD phases was observed. The effect of a modified polymer in HWTD results between mixtures 11 and 12 is significant. The effect of modified polymer for rutting distresses is significant in WMA/HMA mixtures due the stiffness of the material.

From Figure 13, it was observed that rutting depths for mixtures 13, 14, 15, 17 and 18 are close in range and exhibited good performance against deformation, while mixture 16 shows a slightly lower rutting resistance and accumulated close to an additional 2 mm of depression in comparison to its closest counterpart. This may be due to its classification as a coarser AC mixture in comparison to the finer AC designation of mixes 13, 14, 15, 17 and 18. Also, from Table 3, mixture 16 has the lowest post-compaction slope and creep slope among the mixes mentioned. It was observed that as these two parameters decrease, so does the rutting resistance capability of the mixture. Comparing mixtures 15, 17, and 18, these mixtures are composed of hard aggregates basalt and quartzite. Mixture 15 better performance may be attributed to its high rap content of 35% and binder PG70-22 used. Mixture 17, despite having the same aggregate type and binder grade, its lower rap content of 15% may have resulted in the slightly lower performance. Not much can be said about the WMA additive of Maxam Aqua-Black Foaming, due to the fact that there are several mixes listed in Table 6 that contains the specified agent that have performed well. Compared to mix 15, the use of PG64-22 in mix 18 may have considerable effect to its slightly diminished performance despite having the same rap content. Lastly, even though with the use of lower binder grade of PG58-28, mixture 14 experienced the least amount of deformation (2.28 mm) and this might be a result of its combination of high classification as a finer AC mixture, elevated rap content of 35 % and the integration of WMA additive of Maxam Aqua-Black Foaming; which represents an opposite trend experienced in Mixture 17.

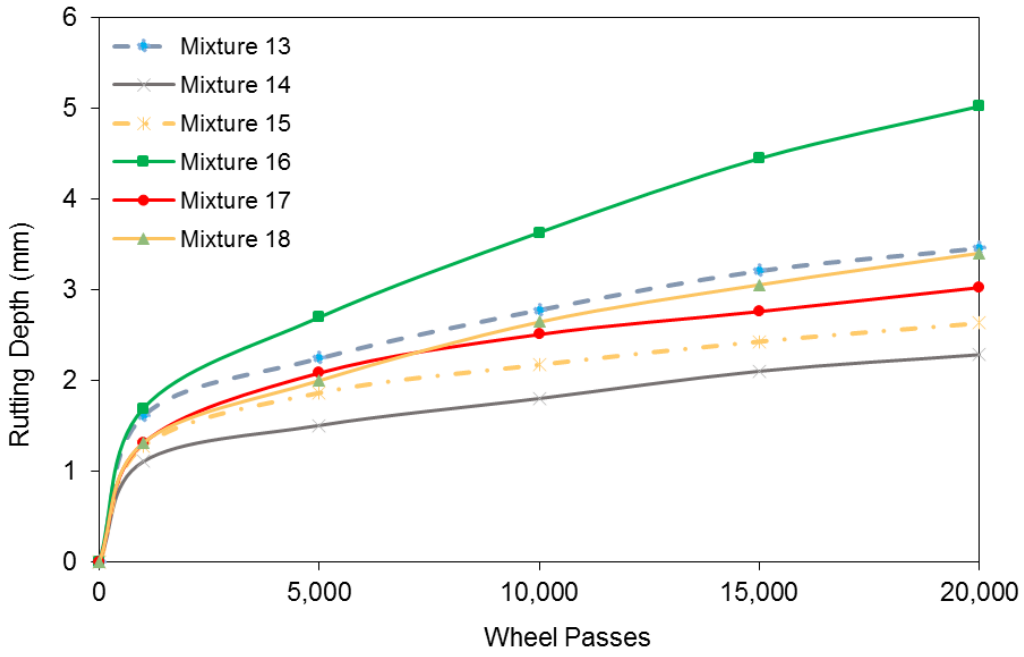

Figure 13: HWTD results for mix 13-18

From Figure 14, it was observed that mixtures 20 and 21, HMA type of the group, experienced the least amount of deformation compared to the WMA mixtures. This result might be attributed towards high content of reclaimed asphalt pavement amounting to 35%. Also, the slightly better rutting resistance was observed in mixture 20 which had a stiffer binder grade of PG64-22 compared to mixtures 22 utilization of PG58-28. Mixture 19 had lower rut depth amongst the WMA type mixtures. This might be attributed by the combination of 25% RAP content along with high binder grade of PG70-22. Mixture 21 result is very close in range with mixture 19's rut rate, considering that the mix is composed of SP-IV gradation, 25% RAP and PG64-22, as mentioned previously that finer AC mixtures tend to have higher rut resistance compared to coarser AC mixtures. Mixtures 21 and 23 experienced stripping during 14,250 and 10,200 passes respectively; premature stripping of mixture 23 compared to mixture 21 may be attributed to the fact that mixture 23 doesn't have the inclusion of RAP.

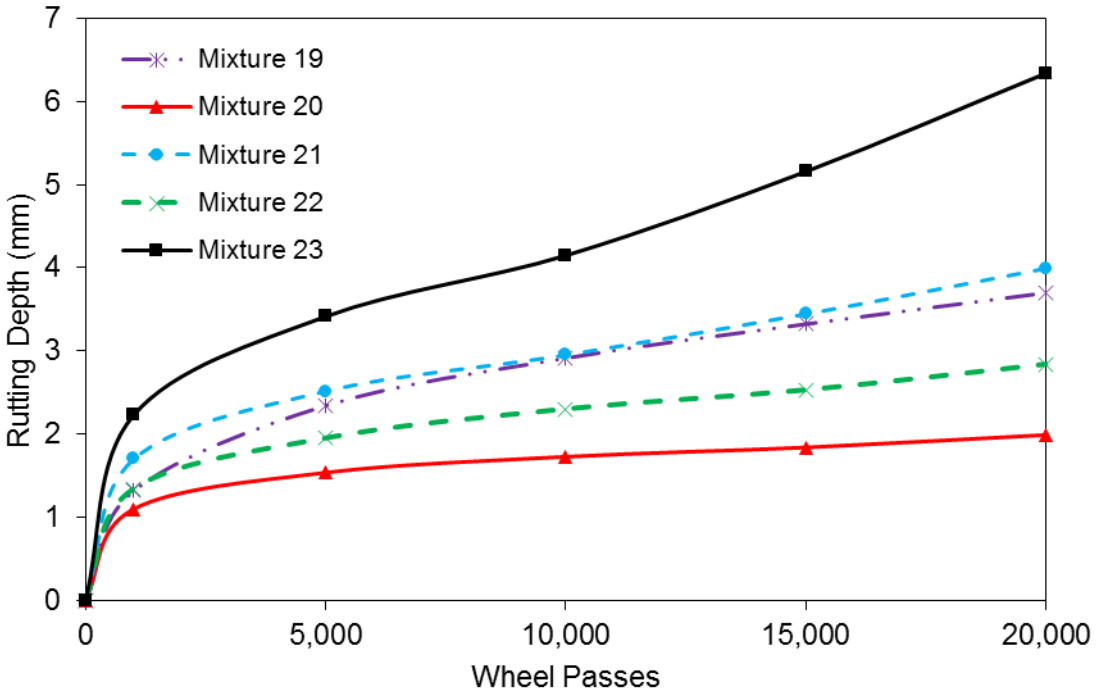

Figure 14: HWTD results for mix 19-23

From Figure 15, it was observed that mixture 29, HMA mixture with 20% RAP and a binder grade of PG64-28, experienced the most rut deformation amounting to 11.42 mm. Despite not having a significant rut failure compared to mixture 29, mixture 25 experienced a maximum impression of 5.85 mm. With the exception of mixtures 27 and 31, mixtures 24, 25, 29, 30, and 33 rut deformation plot indicated a stripping inflection plot for these mixes at 14,800, 13,050, 12,075, 15,100 and 13,550 passes, respectively. Mixture 29 nature of lowest rutting resistance was corresponded with the stripping slope of 1459 passes/mm out the tested mixes. But this mixture has a slightly better performance than mixtures 6 and 7, which contained unique aggregates. Better performance of mixture 25 can be attributed to inclusion of a high RAP content of 35%. Mixtures 27 and 31, mixes that utilized a higher binder grade PG76-XX and RAP content of 15% and 35% respectively, performed the best out the test group exhibiting high rutting resistance with the outcome of rut deformation values of 2.85 mm and 3.03 mm. The reason for mixture's 31 slightly diminished performance, compared to mixture 27, is the utilization of a softer binder of PG58-XX and the incorporation of Maxam foaming WMA additive; which might have led to the offset in rutting resistance.

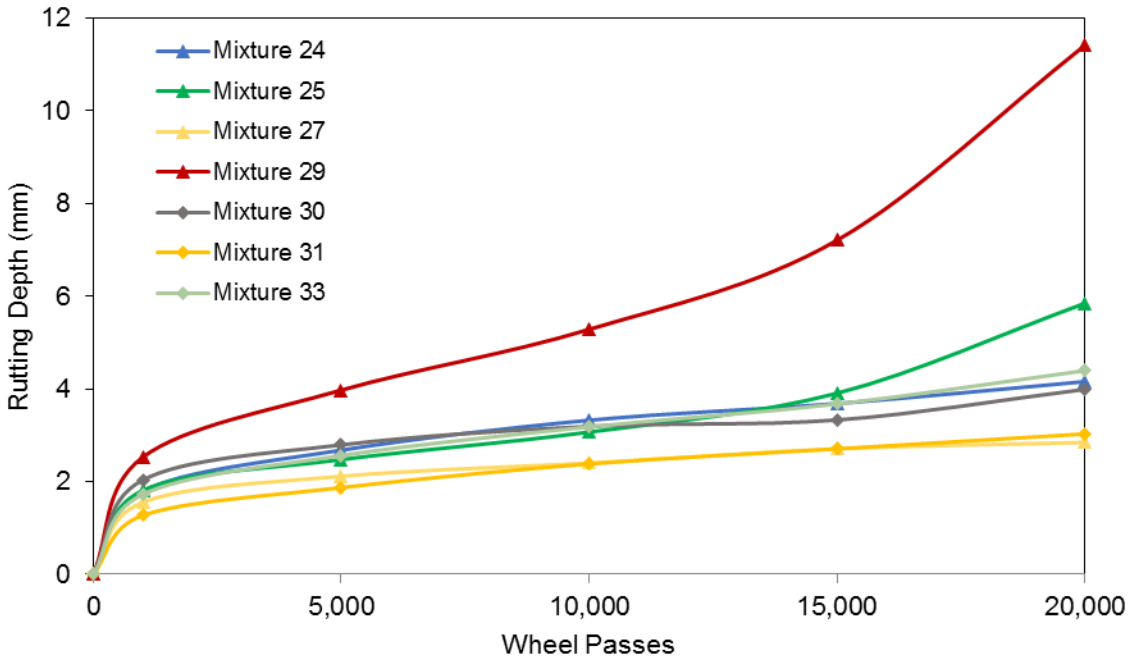

Figure 15: HWTD results for mixtures 24, 25, 27, 29, 30, 31, and 33

From Figure 16, only two out of the five mixes tested didn't demonstrate signs of stripping failure. Mix 28 and 35 rut depths of 3.35 and 3.20 mm are pretty close in range. The slight deformation experienced by mix 38 might be attributable to the fact that the mixes were tested at an elevated air void content of 6.61% compared to mix 35's 5.48%. Another factor to be weighed in is that mix 28 asphalt binder was modified through warm mix foaming process. Accounting for the fact that despite using a binder grade of PG70-22, mix 35's incorporation of a RAP percentage of 15% may have slightly increased the rutting resistance of the mixture. Mixtures 26, 32, and 34 experienced stripping, but mixture 32 displayed characteristics of weak rutting resistance by accumulating close to 8.5 mm in permanent deformation. The combination of a low binder grade of PG64-28 and warm mix modification of asphalt binder through foaming might have contributed to its failure. In regards to mixes 26 and 34, experiencing rut deformations of 5.47 mm and 5.63 mm respectively, are constructed with the same binder grade of PG70-22. It can be observed that mix 26 having 15% of RAP provides a slight advantage in rut resistance compared to mix 34.

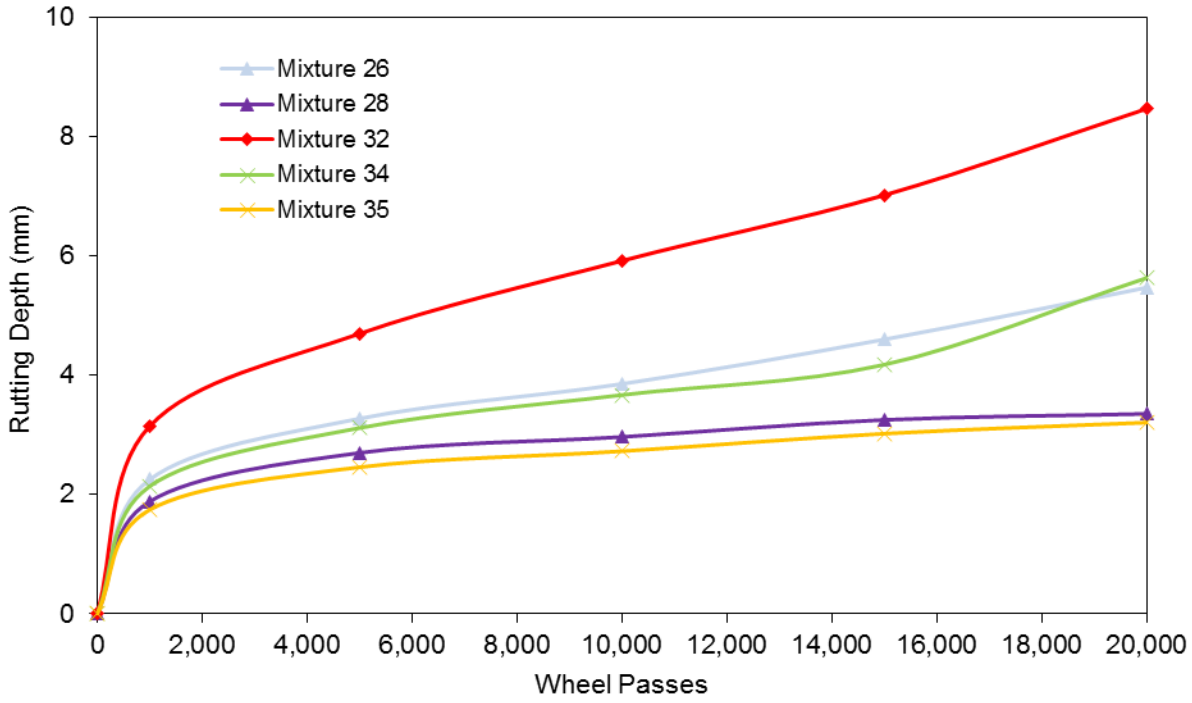

Figure 16: HWTD results for mixtures 26, 28, 32, 34, and 35

The HWTD test results for a total of nine SP-IV mixes are shown in figure 17. As can be seen from figure 17, mixture 37 exhibited characteristics of superior rutting resistance among the tested group of mixes, with a rut deformation value of 1.83 mm. Comparing this rut value with the other mixes tested beforehand, it presents the second best rutting resistance behind mixture 2, which consists of 33 % RAP, SP-III gradation, and aggregate type of limestone. It is worth noting that both mixtures are in the presence limestone aggregate type of limestone, which might be attributed to their enhanced resistance to permanent deformation. Despite mixture 37 consisting an elevated RAP percentage of 35%, its gradation makeup of SP-IV might have contributed to slight increase in deformation experienced by the asphalt concrete mixture. The maximum rut deformation was observed for mix 39 with a rut value of 4.98 mm. The rut deformation values for mix 40 was found to be 3.45 mm where 4.0 mm and 4.97 mm were observed for mix 41 and 39 respectively. Stripping was observed only for mixture 21 with a stripping slope of 3851 pass/mm and stripping inflection point of 14250 passes, and mixture 40 with a stripping slope of 8957 pass/mm and stripping inflection point of 10100 passes. The stripping potential experienced by mix 40 might be attributed to the less RAP content and lower PG binder grade.

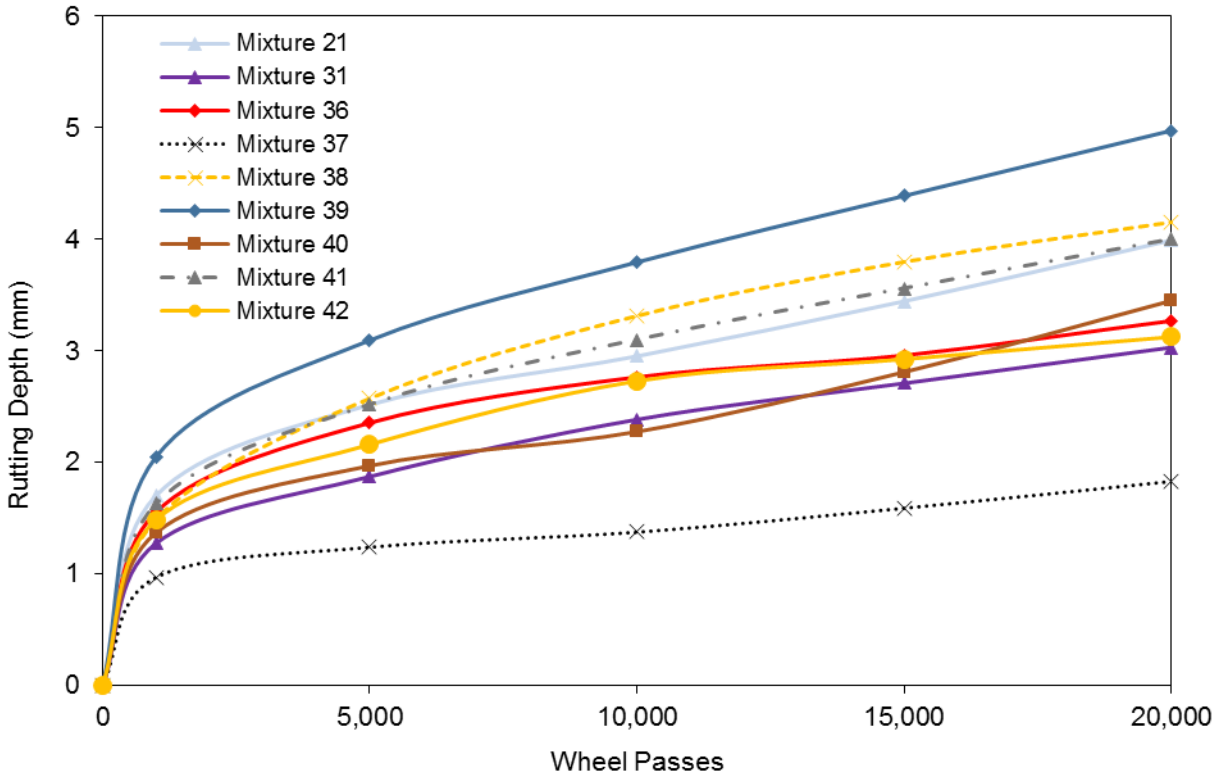

Figure 17: HWTD results for SP-IV mixes

Comparison of Field-Cored Mixture Performance with Laboratory Tested Values

Even though the HWTT has been gaining popularity and wide acceptance by some state highway agencies as a fast and reliable method to evaluate the rutting potential and moisture sensitivity of asphalt concrete mixtures, studies that correlate laboratory test results with field performance are very limited and not well established. The capability of this device to predict field performance therefore has not been sufficiently validated. According to a study conducted by Lu [33], which comprised of comparing HWTD test results with field-cored samples from 63 California pavement sections aged between 4 and 8 years of age, it was observed that laboratory results were incapable of clearly distinguishing sections with different field performance. Based on their analysis, both false and false negative results may occur where sections that performed well in the field showed good performance in the HWTT, but a few sections that performed poorly in the field also performed well in the HWTT. It was also observed that the potential weakness of this research is that the samples were taken from in-service pavements instead of from newly constructed pavements sections, this process might have likely added variations to the mix properties primarily due to the impacts of traffic loading, aging, and climate change.

On the contrary, a joint study by the FHWA and Virginia Transportation Research Council [34] evaluated the ability of three loaded wheel testers (LWTs) to predict rutting performance on AC mixtures placed at the full-scale pavement study WesTrack. The LWTs considered were this extensive evaluation were the Asphalt Pavement Analyzer

(APA), French Rut Tester (FRT), and HWTT. The scope of this study involved the evaluation of field performance data from 10 WesTrack pavement test sections comprising with varying binder content and air void percentages. Based on the data and analyses, it was found that the three devices examined provided a strong relationship with permanent deformation of the WesTrack sections studied. The HWTT had highest correlation of R^2 = 0.91, followed by the APA (R^2 = 0.90) and FRT (R^2 = 0.83).

The scope of this subtask is to evaluate the effectiveness of HWTT to distinguish mixture rutting performance with respect to their field-core counterparts. To fulfill this objective, a total of five pavement sections (3 with satisfactory rutting performance and 2 with bad rutting performance) were cored for examination of moisture damage and laboratory testing. Figure 18 depicts the process involved in collecting core samples from mixture 29 pavement test location. As described in table 7 and 8, the distribution of these coring sites covers different traffic, site location, mixture design characteristics and includes different mix performances. A minimum of four cores, all 150 mm in diameter, were taken at each site. Cores were then cut into specific dimensions for HWTT testing. The air void content of each specimen was measured prior initiating HWTT.

Table 7: Mixtures with satisfactory HWTT laboratory assessment

Mix No.	Location	Mile Post	Mix Summary	Material Type	PG Grade	HWTT Rut (mm)
18	NM-333	0.00-4.43	SP-III, 35%RAP	Quartzite	70-22	3.40
26	NM-314	2.94-3.47	SP-III, 15%RAP	Sand & Gravel	70-22	5.47
33	NM-6	18.53-23.64	SP-III, 25% RAP	Limestone	70-22	4.40

Table 8: Mixtures with poor HWTT laboratory assessment

Mix No.	Location	Mile Post	Mix Summary	Material Type	PG Grade	HWTT Rut (mm)
7	US-60	69.00-73.00	SP-III, EVOTHERM	Dacite	76-28	15.96
29	I-25/NM-14	276.00-278.00	SP-III, 15%RAP	Sand & Gravel	64-28	11.42

Figure 18: Field core collection from mixture 29 pavement test section location

Table 9: HWTD test results for field-cored mixtures

Mixture	Average Number of Passes	Maximum Impression (mm)	Samples Air Voids Average (%)	Post-Compaction Point Slope (pass/mm)	Creep Slope (pass/mm)	Stripping Slope (pass/mm)	SIP
7-FC	10,000	17.94	6.65	224	1360	475	6050
18-FC	20,000	5.77	8.75	544	4604	N/A	N/A
26-FC	20,000	3.78	8.04	725	7748	N/A	N/A
29-FC	20,000	6.59	3.85	454	4485	3256	16900
33-FC	20,000	7.51	9.18	303	4223	N/A	N/A

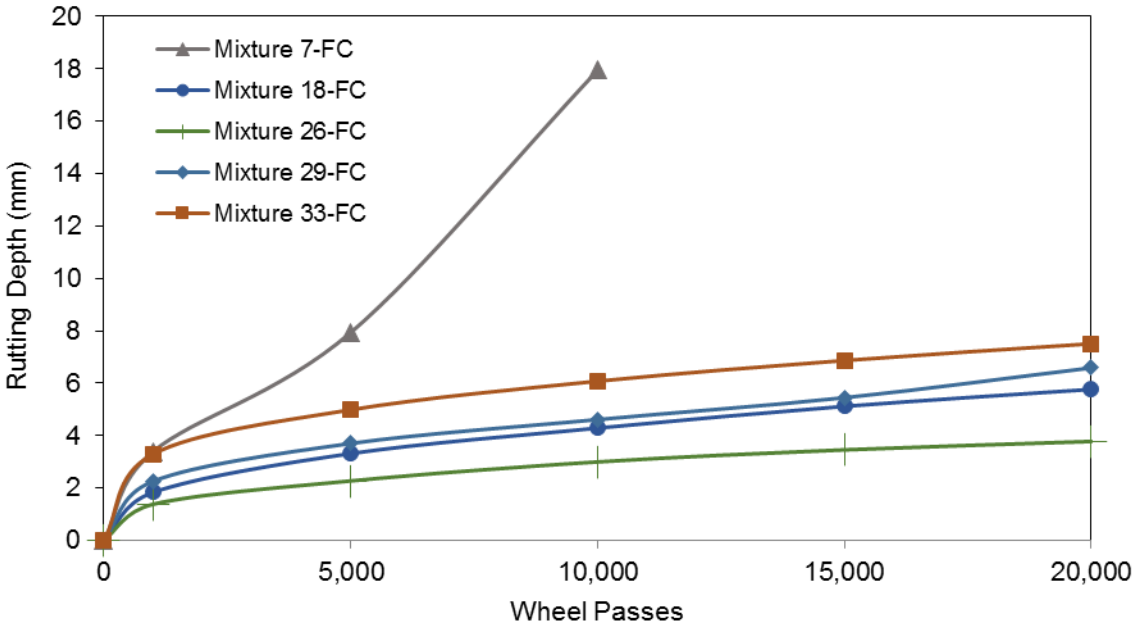

Figure 19: HWTD test results for field-cored mixtures

From Table 9 and Figure 19, it was observed that mixture 7 and mixture 29 exhibit characteristics of stripping. The rut progression curves from mixtures 7, 29, and 33 test results showed quick development of ruts in the initial few thousand wheel passes, which is due to densification and reduction of air void volume of mixes. For mixture 7, the slope of the rut progression curve changed significantly after reaching the SIP (6050 wheel passes) and in turn ended the testing procedure around 10,000 wheel passes where severe stripping and sample deterioration occurred. This particular mix showed the lowest rutting resistance in both testing scenarios: laboratory compacted and field-cored samples. These findings align with previous observations that these drastic failure in permanent deformation is associated to the use of Dacite as the aggregate type. In addition, the use of Evotherm as a binder modification process may have intensified the rutting rate of the mixture. Lastly, this specific mixtures was compacted in 2012. Accounting for pavement service life, the age of this pavement section might have resulted in oxidation of the pavement structure resulting in the weakening of the aggregate-binder bond.

On the other hand, the rapid rut accumulation in the post-compaction phase of mixture 33 may be due in part to its elevated air void content of 9.18%. Despite of that characteristic, no signs of stripping were incurred by the samples. With regards to mixture 29, a lower development of rutting was experienced in the post-compaction phase. This may be attributed to its low air void content of 3.85%. This material characteristic may limit the process of densification and providing more resistance to rutting. However, the mixture did demonstrate a stripping phase around the 16,900 wheel pass.

Acknowledging the fact that the field-cored samples experienced slightly higher rut values compared to their laboratory compacted counterparts, due to environmental and human factors (climate, construction practices, and traffic loading), this evaluation show

the ability of the HWTT to distinguish whether a particular mixture will perform satisfactorily or poor in the field.

Significance Test for UNM and NMDOT Hamburg Wheel Tracking Devices

Null Hypothesis: There is no difference between NMDOT and UNM Hamburg wheel tracking device results. If p value is equal or larger than 0.05 the null hypothesis can be accepted. Otherwise, we reject the null hypothesis.

Eight HWTD tests were performed by NMDOT and three by UNM with the same AC mixture using the same HWTD test configuration (20,000 passes and 50 °C).16 test results were recorded for NMDOT testing for both of the HWTD wheel paths.

For UNM testing, 6 test results were recorded. Table 10 summarizes the rutting depth at the 5 most significant number of wheel passes for each to the wheel test results.

Table 10: NMDOT HWTD results

Pass	T1	T1	T2	T2	T3	T3	T4	T4	T5	T5	T6	T6	T7	T7	T8	T8
0	0.0	0.0	0.0	0.0	0.0	0.0	0.0	0.0	0.0	0.0	0.0	0.0	0.0	0.0	0.0	0.0
1000	0.8	0.8	0.9	0.9	1.0	1.1	0.9	0.9	0.7	0.8	0.7	0.8	1.1	1.2	0.8	0.8
5000	1.3	1.3	1.6	1.7	1.9	1.8	1.6	1.5	1.2	1.3	1.3	1.3	2.1	2.2	1.3	1.3
10000	1.6	1.7	2.1	2.1	2.3	2.3	2.1	2.0	1.6	1.7	1.6	1.6	2.6	2.7	1.5	1.5
15000	1.8	1.9	2.4	2.5	2.5	2.5	2.3	2.2	1.8	1.9	1.8	1.9	2.9	3.0	1.7	1.7
20000	2.0	2.1	2.7	2.8	2.9	2.8	2.6	2.5	2.0	2.1	1.9	2.0	3.1	3.2	1.9	1.8

Table 11: UNM HWTD results

Pass	T1	T1	T2	T2	T3	T3
0	0	0	0	0	0	0
1000	1.20	0.98	0.93	1.22	1.16	1.03
5000	1.97	1.84	1.63	1.78	1.86	1.64
10000	2.53	2.20	2.05	2.14	2.42	2.12
15000	2.81	2.45	2.43	2.28	2.81	2.60
20000	3.16	2.70	2.72	2.41	3.23	3.28

For the significance test, a two tail significance test was used with homoscedastic variance. Variance is not constant but the difference does not increase with number of wheel passes, definition for homoscedastic variance.

The significance test results for UNM and NMDOT HWTD test results are given in Table 12. Results are expressed in p values.

Table 12: P-values

Pass	p
0	
1000	0.05
5000	0.17
10000	0.12
15000	0.09
20000	0.04

From the previous results, it can be observed that p value is equal or greater than 0.05 for all the analyzed passes besides the pass 20000. From these results we can accept the null hypothesis since 4 of the 5 wheel passes tested has met the condition. In conclusion, there is no significance difference between UNM and NMDOT HWTD results.

ASPHALT CONCRETE TENSILE STRENGTH RATIO (TSR) TESTING

Moisture-induced damage is the loss of adhesion between asphalt and aggregates in a mix (stripping) and/or the loss of cohesion within the asphalt mastic, where moisture enters the pavement through three mechanisms: infiltration, evaporation, and capillary rise [35]. For these instances, permeable pores provide the pathway for water to get inside the pavement and a study performed by Ahmad [36] aimed to find whether permeability is related to moisture damage of AC in the field and lab. His results conclude that moisture damage potential increases with the increase of permeable pores. It was also observed that pavements with decreasing permeability from the top to the bottom layers exhibit less damage.

Moisture damage in the United States is a big issue, as 34 out of 50 states are suffering from some sort of moisture related distress according to a survey conducted by Hicks [37]. In the field, moisture damage is initially identified by visual inspection of the pavements. But stripping, a major cause of distress in flexible pavements, generally occurs at interfaces and propagates upward. Therefore, visual inspection alone is not sufficient to identify moisture damage. The Modified Lottman Test has been developed to evaluate both moisture susceptibility and anti-stripping additives' effectiveness through mechanical testing [38].

The Indirect Tensile Strength (ITS) of asphalt mixtures is conducted by loading a cylindrical specimen across its vertical diametral plane at 50 mm/min (2 in./min) deformation rate and 25 °C test temperature; shown in Figure 20 below. The peak load at failure is recorded and used to calculate the Indirect Tensile (IDT) Strength of the specimen using Equation (1):

$$IDT = \frac{2*P}{\pi*D*t} \quad (1)$$

where *IDT* = indirect tensile strength (psi); *P* = maximum compressive strength noted on testing machine (Newton); *D* = diameter of sample (in.); *t* = thickness of sample (in.).

The value of ITS is used to evaluate the relative quality of mixes in conjunction with laboratory mix design testing and for estimating the potential for rutting or cracking. The results can also be used to determine the potential for field pavement moisture damage when results are obtained on both unconditioned and conditioned samples.

The index of Tensile Stress Ratio (TSR) can be used to measure the moisture susceptibility of the samples. A ratio of IDT for conditioned samples to unconditioned samples is the criterion to identify a moisture susceptibility of a mix. The TSR of wet to dry samples is calculated using Equation (2):

$$TSR = \frac{IDTwet}{IDTdry} \quad (2)$$

(a) (b)

Figure 20: Photographic view of IDT testing equipment

where IDT_{wet} = Average IDT of 3 wet conditioned samples; IDT_{dry} = Average IDT of 3 dry conditioned samples

According to the NMDOT mix design specifications [39] the minimum requirement of TSR is 85%.

For the purpose of this test portion, about 300 samples were prepared using the Superpave gyratory compactor following the AASHTO T 312 [26] test standard. The samples were compacted to diameter measurement of 150 mm (4 in.) specimens in order to meet the requirements of standard AASHTO T 283 [40]. All of them were not tested during this quarter. Cylinder samples are prepared to a height of 62±1 mm. The test can also be performed at 100 mm (6 in.) diameter samples with 3.75 in. height.

Samples' volumetric properties, theoretical maximum specific gravity (G_{mm}), air voids and bulk specific (G_{mb}) were determined at the UNM laboratory. The G_{mm}, G_{mb}, and air void were determined according to the AASHTO T 209 [27], AASHTO T 166 [28], and AASHTO T 269 [29] test protocols respectively. The resulting air voids range from 5.5% to 7.5%, which meets the desired criteria.

For the determination of indirect-tensile strength of dry and conditioned specimens, a total of six mixtures were tested at 25 ˚C using the lab available Indirect Tensile Test (IDT) machine. Prior to testing, in accordance to AASHTO T 283 [40] preparation of at least six specimens are required for each IDT test; half to be tested dry and the other half to be tested after partial saturation and moisture conditioning with a freeze-thaw cycle.

The dry subset of samples will be stored at room temperature for 24 $\pm$ 3 hours. At the end of the curing period, specimens shall be wrapped with plastic film or placed in a leak-proof plastic bag and then placed in a water bath at 25 ˚C for a duration of 2 hours $\pm$ 10 min. For the wet subset, specimen is saturated using a vibro-deairator for a short time (approximately 5-10 min); a device that applies vibration and suction

simultaneously. After saturation, the vacuum-saturated specimen shall be wrapped tightly with a plastic film in order to prevent any moisture loss. Then, this is followed by the placement of the wrapped sample into a leak-proof bag containing 10 $\pm$ 0.5 mL of water and seal the bag, which is shown in Figure 21(a). The plastic bags containing specimen were then placed in a freezer for 16 hours at -18 $\pm$ 3 ˚C for freezing. After the limit has been reached, the sample is then thawed in a hot water bath at a temperature of 60 ˚C for 24 hours (Figure 21(b)). This is immediately followed by 2 hours of conditioning at 25 ˚C.

(a) (b)

Figure 21: Photographic view of freeze-thaw specimen conditioning process for AASHTO T 283

Thus, in the AASHTO T 283 conditioning process, water is forced to enter inside the sample during saturation and to increase in volume during freezing. The increased volume of water causes increased pressure inside the pores of the sample causing damage. Thawing through the process of hot water bath for 24 hours also contributes to the softening of the binder, mastic and samples.

Test Results and Discussions

The following Table 13 represents the results of all the AC mixtures tested in the IDT Device. Due repeatability of results, each mixture data set was generalized.

Table 13: AASHTO T283 results

Mix	Average AV (dry condition)	Dry Tensile Strength (psi)	Average AV (wet condition)	Wet Tensile Strength (psi)	TSR (UNM)	TSR (Mix Design Chart)
1	6.4	210.5	6.6	145.4	0.69	0.89
2	6.3	202.3	6.6	138.4	0.68	0.95
3	6.0	244.8	6.0	179.5	0.73	0.89
4	7.3	214.5	7.4	154.8	0.72	0.89
8	6.7	165.3	6.9	144.1	0.87	0.94
9	5.3	97.3	5.6	141.5	1.45	0.86
10	6.1	180.7	5.3	187.8	1.04	0.87
11	7.0	160.3	6.1	158.7	0.99	0.87
12	6.2	135.6	5.5	189.1	1.39	0.88
13	5.9	307.2	5.8	250.5	0.82	1.14
15	6.0	183.5	5.8	139.2	0.76	0.94
16	7.2	118.0	6.5	164.8	1.4	0.92
17	5.9	218.1	6.2	151.1	0.69	0.9
18	5.8	168.7	6.1	120.3	0.71	0.89
20	6.9	231.4	6.5	169.8	0.73	0.95
21	6.3	180.4	6.6	125.8	0.70	0.91
22	6.2	214.1	6.4	156.1	0.73	0.94
23	5.5	121.5	5.8	91.2	0.75	0.87
24	5.9	173.7	6.6	145.6	0.84	0.91
25	5.9	212.2	6.3	157.6	0.74	0.9
26	6.2	165.2	6.7	102.9	0.62	0.91
27	6.9	142.4	6.7	121.3	0.85	0.88
28	6.9	215.0	7.1	161.2	0.75	0.93
29	7.1	132.8	6.8	179.6	1.35	0.93

Table 13: AASHTO T283 results (Continued)

Mix	Average AV (dry condition)	Dry Tensile Strength (psi)	Average AV (wet condition)	Wet Tensile Strength (psi)	TSR (UNM)	TSR (Mix Design Chart)
30	6.7	209.5	6.6	166.5	0.79	0.92
31	6.3	209.0	6.1	144.8	0.69	0.99
32	6.4	95.4	5.5	61.3	0.64	1.09
33	6.4	191.7	6.5	139.3	0.73	0.87
34	6.4	140.7	6.5	89.9	0.64	0.92
35	6.5	140.4	6.1	105.6	0.75	0.92
36	7.7	146.0	6.7	99.0	0.68	0.92
37	7.0	179.9	7.1	142.3	0.79	0.96
38	7.0	165.9	7.1	143.4	0.86	0.93
39	5.6	160.5	7.4	107.2	0.67	0.92
40	5.5	154.1	7.3	190.3	1.23	0.92
41	6.6	148.1	6.7	135.1	0.91	0.91

It can be inferred from the table above that 11 out of the 41 mixtures tested meet the specification requirements of NMDOT of a minimum TSR value of 85%. Mixture 24, TSR value of 0.84, came close to meeting the minimum requirement which can be easily interpreted as a pass, dramatically falls short to meet or exceed the TSR value of 0.91 reported in the mix design chart supplied by the NMDOT. Comparing the TSR values provided in the mix design charts to the TSR values generated from testing of laboratory prepared samples, only mixtures 9, 10, 11, 12, 16 and 40 results show a higher resistance to moisture susceptibility. Note that all the mixes except for mix 40 indicated contains WMA additives; where these results align with Gandhi's ([41] study of the effects of WMA additives on asphalt binder and mixture properties which found that WMA additives improved the TSR of the mixes. It should be noted that Mixtures 1 and 2 contain 35 % and 33 % of RAP respectively. According to Katman et al. [42] his study revealed that mixes with RAP are more resistant to moisture damage and have better fatigue resistance; due to the ability of RAP to absorb water. He also states that presence of bitumen coating the aggregate in RAP prevents water to fill the aggregate, thus aggregate adherence is not affected. But in the case of our test results, it shows otherwise. In regards to rut depth and TSR values, no significant correlation was observed between the two results.

Mixture 27 met the State's TSR value requirement, but didn't match up with the prescribed value in reference to mix design charts. However, mix 29 display of heightened strength under moisture conditioning cannot be justified by its use of a lower asphalt binder grade of PG64-28. The only measure to associate to its increased strength is the RAP component of 15%.

Comparing the SPS-10 mixtures, mixes 8 through 12 have the same mix design components such as gradation, 20% rap content, aggregate blend type and binder grade of PG70-28, but with the exception of the warm mix additives used for each respective mix. In reference to Table 4, Mix 8 does not contain any WMA agent, while mix 10 and mix 11 contains Evotherm and Cecabase RT respectively. Results from Table 13 show that both mixtures 8 and 10 meet the minimum TSR requirement, but mixture 8 falls short of the TSR ratio reported by the NMDOT mix design chart. On the other hand, mixture 10 has a significantly higher value of 1.04 in comparison to the 0.87 NMDOT value. In correlation with the HWTD data, similar rut depth and good TSR values were observed for mixtures 8 and 10; where mixture 10 performed slightly better than mixture 8. This might be attributed to the Evotherm agent present in the mix. On the other hand, despite a significantly higher rutting resistance in mixture 11 compared to mixes 8 and 10, opposite trend was observed in TSR ratio. Among the SPS-10 mixtures assessed for rutting deformation, it was observed that Cecabase RT additive showed to improve the performance of mixtures 11 and 12 in aspects of rutting resistance and all HWTD phases.

From table 13, the average tensile strength of dry subset samples for SPS-10 section 1 to Section 5 are 165.3 psi, 97.3 psi, 180.7 psi, 160.3 psi, and 135.9 psi, respectively. Thus, it is seen that mixture with Evotherm showed maximum tensile strength, followed by HMA, Cecabase mixture 2 with polymer modified binder, Cecabase mixture 1 and at last, foaming. On the other hand, the average tensile strength of wet subset samples are 144.1 psi, 141.5 psi, 187.9 psi, 158.7 psi, and 189.1 psi, respectively. Thus, it is seen that Cecabase mixture 2 showed maximum tensile strength value in wet condition, followed by Evotherm, Cecabase 2, HMA, and Foaming. So, the trend is different in dry and wet condition. Thus, the ratio between wet conditioned tensile strength and dry condition tensile strength is considered the key parameter of moisture damage resistance or stripping resistance. Based on the New Mexico specification, all the samples passed in the TSR tests. Based on the TSR value, Foaming section showed highest stripping resistance, followed by Cecabase 2, Evotherm, HMA, and Cecabase 1.

The current findings from table 13 suggest that the indirect tensile strength test may not be the best choice for the purpose of assessing and controlling moisture damage in asphalt mixtures. The inconsistencies in the results could be that the moisture conditioning used in AASHTO T 283 may not simulate actual field conditions well. Another reason to consider is that the time gap between the collections of the HMA materials to the completion of the specified test in the laboratory, samples might have experienced asphalt binder oxidation. This is hypothesized to be a major contributor to age-related pavement failure [43] which might have attributed to the decrease of the TSR values for most of the tested samples.

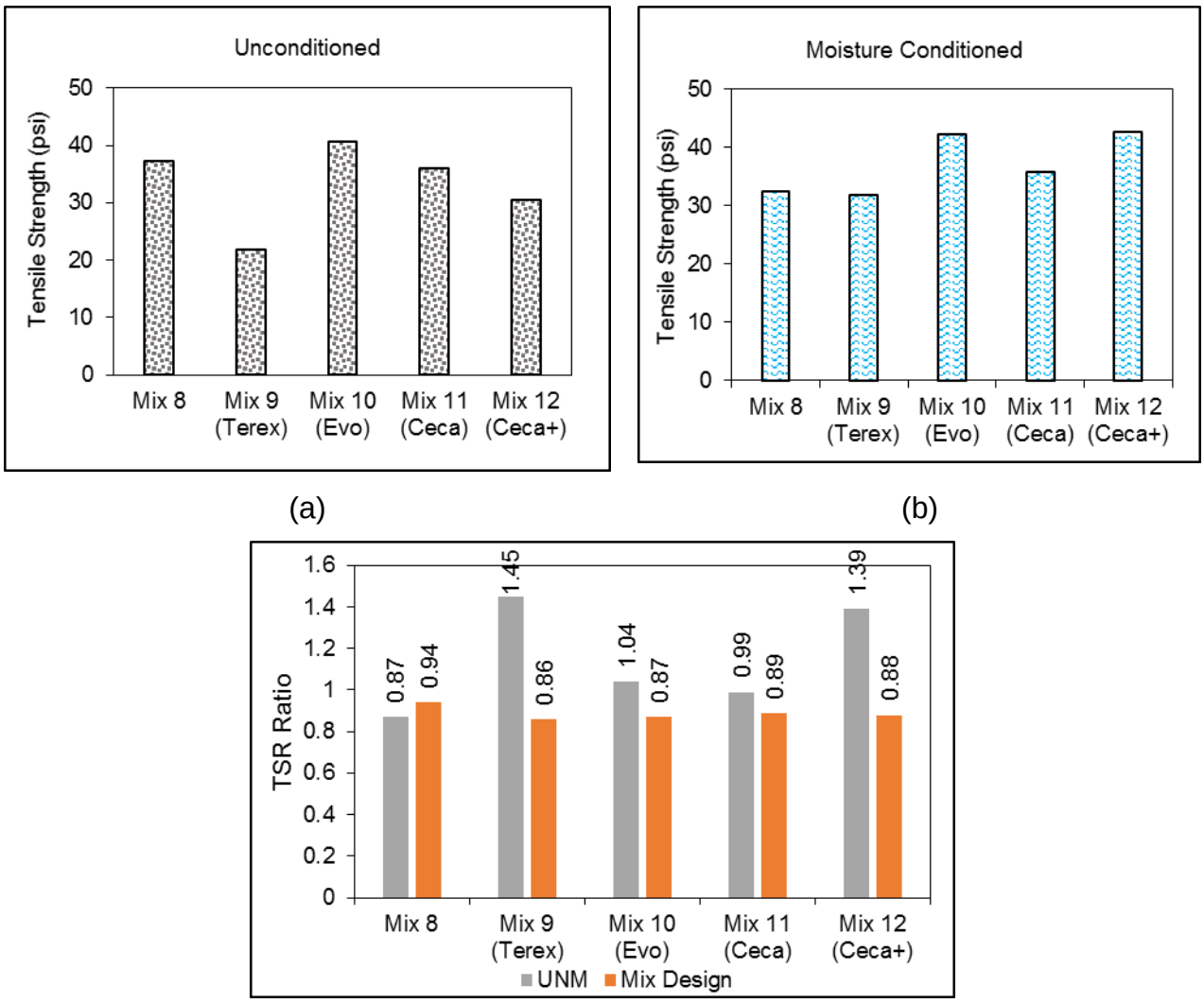

Figure 22: (a) Dry Tensile strength, (b) wet tensile strength, and (c) laboratory TSR values compared to mix design chart values

Table 14 presents a comparison of TSR test results conducted at UNM and NMDOT laboratory for mixture 41.Comparing the tensile strength in wet and dry condition, it was observed that there is no significant difference between the UNM and NMDOT test results for both condition. Figure 23 illustrates the TSR values obtained from laboratory test at UNM and NMDOT. TSR value was found to be 0.91 at UNM laboratory whereas 0.92 at NMDOT.

Table 14: AASHTO T283 results for mix 41

Mix	Sample No.	AV* (%)	Dry Tensile Strength (psi)	AV* (%)	Dry Tensile Strength (psi)	AV* (%)	Wet Tensile Strength (psi)	AV* (%)	Wet Tensile Strength (psi)
		NMDOT	NMDOT	UNM	UNM	NMDOT	NMDOT	UNM	UNM
41	1	7.5	127.4	7.6	129	7.5	128.7	6.9	146.1
41	2	7.0	169.6	6.4	156.4	7.0	153.7	6.6	132.4
41	3	7.4	151.5	6.3	158.9	6.8	130	6.7	127
	Avg.	7.3	149.5	6.8	148.1	7.1	137.5	6.7	135.2

*AV=Average air void

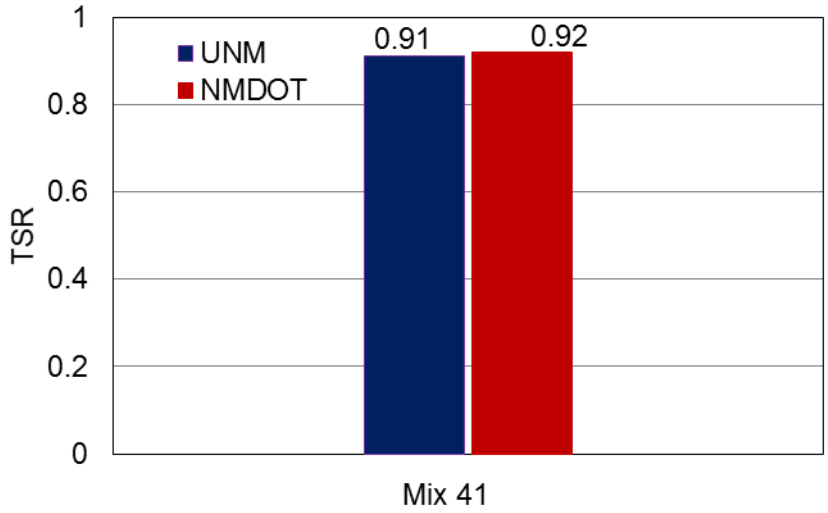

Figure 23: TSR test results for mix 41

TSR test was also conducted in UNM and NMDOT laboratory for mix 37.Table 15 presents a comparison of TSR test results. Figure 24 illustrates the TSR values obtained from laboratory test at UNM and NMDOT. TSR value was found to be 0.0.79 at UNM laboratory whereas 0.71 at NMDOT.

Table 15: AASHTO T283 results for mix 37

Mix	Sample No.	AV* (%)	Dry Tensile Strength (psi)	AV* (%)	Dry Tensile Strength (psi)	AV* (%)	Wet Tensile Strength (psi)	AV* (%)	Wet Tensile Strength (psi)
		NMDOT	NMDOT	UNM	UNM	NMDOT	NMDOT	UNM	UNM
37	1	6.5	196.7	6.8	169.6	7.1	136.3	6.9	143.3
37	2	5.8	187.9	7.2	173.1	7.0	153.7	7.3	131.2
37	3	5.2	199.8	7.1	197.1	7.7	126	7.1	152.1
	Avg.	5.8	194.8	7.0	179.9	7.3	138.6	7.1	142.3

*AV=Average air void

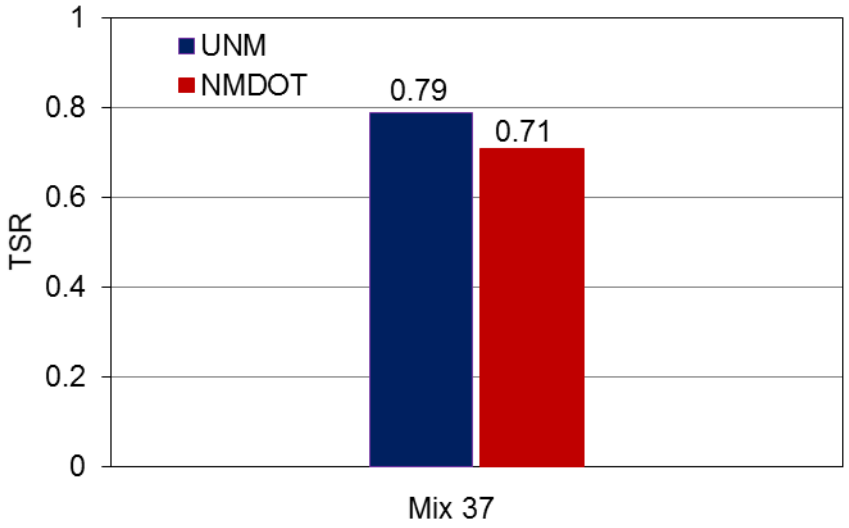

Figure 24: TSR test results for mix 37

Correlation between the TSR and HWTD test

It can be clearly noticed from Table 5 that eleven out of the forty-two mixes exhibited characteristic of stripping potentials indicating that these mixes were more prone to moisture damage than the rest of the mixes. The TSR is a laboratory testing procedure used to measure the moisture susceptibility of the AC mixes. The stripping number of these eleven mixes obtained from the HWTD test were correlated with their wet tensile strength from IDT test. Figure 25 depicts the relationship between these two parameters. A mixture having higher stripping number is expected to have higher wet tensile strength. It is observed from Figure 25 that there is no sensible correlation between them.

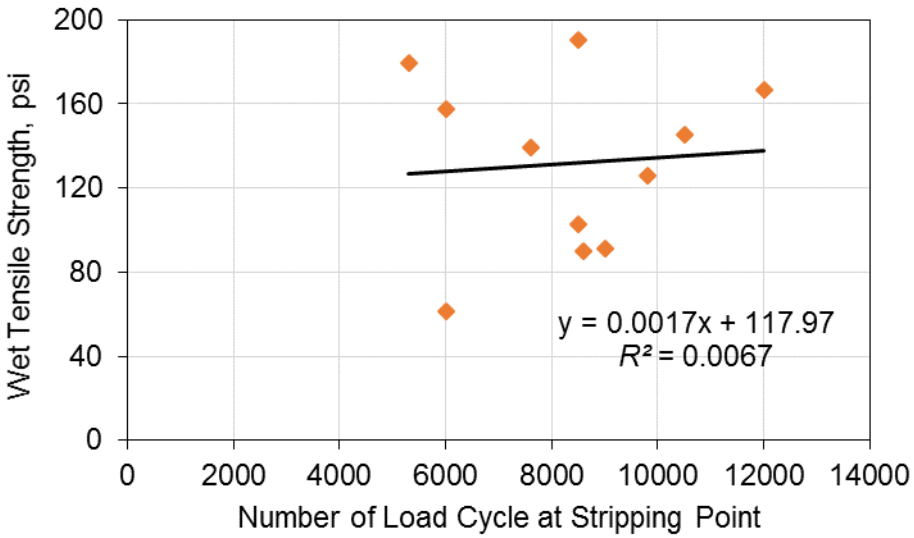

Figure 25: Wet tensile strength with stripping point

LABORATORY TESTING FOR BINDER G* AND δ

This test method covers the determination of the dynamic shear modulus and phase angle of asphalt binder when tested in dynamic (oscillatory) shear using parallel plate test geometry. Oscillatory loading frequencies using this standard can range from 1 to 100 rad/s using a sinusoidal waveform. Specification testing performed at a test frequency of 10 rad. This test method is intended for determining the linear viscoelastic properties of asphalt binders as required for specification testing and is not intended as a comprehensive procedure for the full characterization of the viscoelastic properties of asphalt binder. Test specimens 2 mm thick by 8 mm in diameter are formed between parallel metal plates. During testing, one of the parallel plates is oscillated with respect to the other at pre-selected frequencies and rotational deformation amplitudes (strain control) (or torque amplitudes (stress control)). The required stress or strain amplitude depends upon the value of the complex shear modulus of the asphalt binder being tested. The required amplitudes have been selected to ensure that the measurements are within the region of linear behavior.

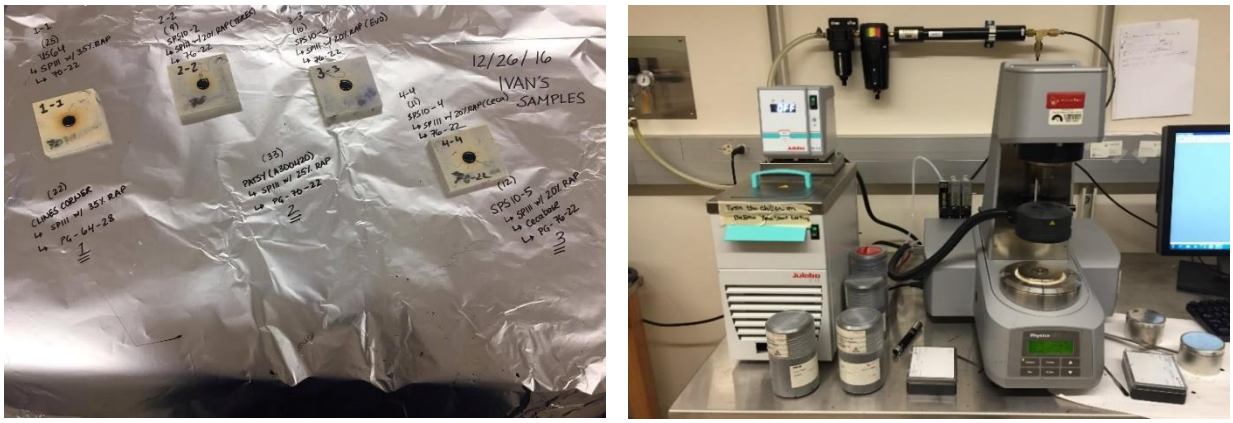

(a) (b)

Figure 26: a) 8 mm binder test specimens for DSR testing b) Anton-Paar DSR setup

For the purpose of this study, aged materials in accordance with AASHTO T 240 [44] will be tested in the DSR. Since asphalt behavior depends on both time and temperature, the ideal test for asphalt would evaluate both. The devices, which measure both these properties, are generically known as dynamic shear rheometers, oscillatory shear rheometers, or dynamic rheometers. By adapting these devices for use with asphalt, both time and temperature effects can be evaluated. When used to test asphalt binders, dynamic shear rheometers, or DSRs, measure the rheological properties (dynamic shear modulus, phase angle, etc.) at both high and intermediate temperatures (Figure 26).

DSR operation mainly consists of an asphalt that is sandwiched between a fixed plate and a plate that oscillates back and forth as shown in Figure 27. The oscillating plate starts at point A and moves to point B. From point B the oscillating plate moves back,

passing point A on its way to point C. From point C the plate moves back to point A. This movement comprises one cycle of oscillation. All SuperPave DSR tests are conducted at a frequency of 10 radians per second, which is equal to about 1.59 Hz; where the specified DSR oscillation rate is meant to simulate the shearing action corresponding to a traffic speed of about 55 mph.

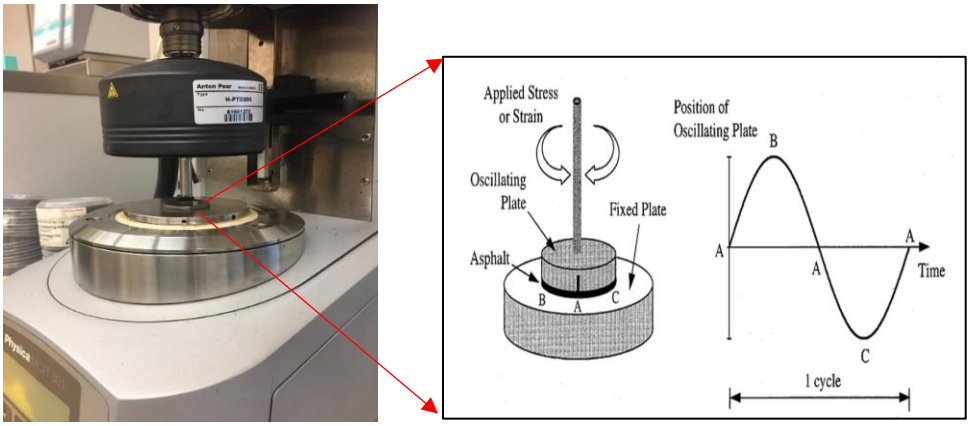

(a) (b)

Figure 27: Principle of DSR operation with sample, with stress-strain response of a viscoelastic material

This test is used to characterize the viscous and elastic behavior of asphalt binders at high and intermediate temperatures. It does this by measuring the complex shear modulus (G*) and phase angle (δ) of asphalt binders. G* is a measure of the total resistance of a material to deforming when repeatedly sheared. It consists of two parts: a part that is elastic (recoverable) and a part that is viscous (non-recoverable). δ is an indicator of the relative amounts of recoverable and non-recoverable deformation. Together, the complex shear modulus and the phase angle define the resistance to shear deformation of the asphalt binder in the linear viscoelastic region. G* and δ are used as predictors of HMA rutting; where rutting is the main concern early in any pavement service life.

In order to resist rutting, an asphalt binder should be stiff (it should not deform too much) and it should be elastic (it should be able to return to its original shape after load deformation). Therefore, the complex shear modulus elastic portion (G*/sinδ) should be large. Traditionally, SuperPave specification requires a minimum value for the elastic component of the complex shear modulus be meet (Table 16). Intuitively, the higher the G* value, the stiffer the asphalt binder is able to resist deformation, and lower the δ value, the greater the elastic portion of G* is able to recover its original shape after being deformed by a load. However, the scope of this project requires the testing for G* and δ values to be used in the |G*|-based Witczack model to predict dynamic modulus (E*) values; which provides insight into a material's viscous properties. The binder samples are then tested at different temperatures of 40, 55, 70, 85, 100, 115, and 130°F in accordance to AASHTO T 342 [45].

Table 16: Superpave specification on DSR test for rutting parameter

Parameter	Unaged Binder	RTFO aged Binder
G*/sinδ	≥ 1 kPa	≥ 2.2 kPa

Asphalt binders collected from the asphalt plant for Mixtures 2, 4, 7, 8, and 13 were tested. Table 17 provides information in regards to the mixtures' properties and Table 18 represents the rheological results for the tested binders in the DSR. Figure 28 shows the complex shear modulus and phase angle of the RTFO aged binder with temperature.

Table 17: Materials collected

Test Code	Mixture	Type	Mix Summary	Binder Grade Used	Binder Grade Specified	Asphalt Source
D2A1	2	HMA	SP-III w/ 33%RAP	64-22	76-22	Western Refining
D4A1	4	HMA	SP-III	64-28	64-28	NuStar
D6A1	7	WMA	SP-III (EVOTHERM)	76-28	76-28	Holly Frontier
D4A4	8	HMA	SP-III w/ 20%RAP	70-28	76-22	Holly Frontier
D4A9	13	WMA	SP-III (TEREX)	76-22	76-22	Holly Frontier

Table 18: Rheological properties for the tested binders

Binder Grade Used	Temperature (°F)	G* (kPa)	δ (°)	G*/sinδ (kPa)
PG 64-22	40	18671.3	31.6	35594.5
PG 64-22	55	8209.42	34.7	14403
PG 64-22	70	2961.87	39.9	4619.31
PG 64-22	85	898.76	46.6	1236.61
PG 64-22	100	309.43	53	387.63
PG 64-22	115	86.5	60	99.87
PG 64-22	130	24.94	67.2	27.05
PG 64-28	40	21321	43	31280.1
PG 64-28	55	6322.77	51	8141.64
PG 64-28	70	1713.8	57.6	2029.56
PG 64-28	85	435.94	62.8	490.05
PG 64-28	100	117.45	66.9	127.68
PG 64-28	115	34.65	70.9	36.68
PG 64-28	130	11.23	74.8	11.63
PG 70-28	40	15311	40.8	23455.8
PG 70-28	55	5154.88	45.3	7253.48
PG 70-28	70	1577.52	49.5	2073.96
PG 70-28	85	477.27	52.8	598.87
PG 70-28	100	149.57	55.3	181.88
PG 70-28	115	50.49	57.5	59.84
PG 70-28	130	17.97	60	20.74
PG 76-22	40	12585	42.7	18557.5
PG 76-22	55	3965.9	49.7	5202.34
PG 76-22	70	1097.48	56.2	1321.16
PG 76-22	85	291.81	61.2	333.06
PG 76-22	100	80.11	64.6	88.69
PG 76-22	115	25.58	67.1	27.76
PG 76-22	130	9.06	69.2	9.69
PG 76-28	40	18600	40.8	28465.6
PG 76-28	55	6240	47.6	8450.07
PG 76-28	70	1810	53.9	2240.13
PG 76-28	85	477	58	562.47
PG 76-28	100	140	59.1	163.16
PG 76-28	115	48.4	58.4	56.83
PG 76-28	130	18.8	57.2	22.37

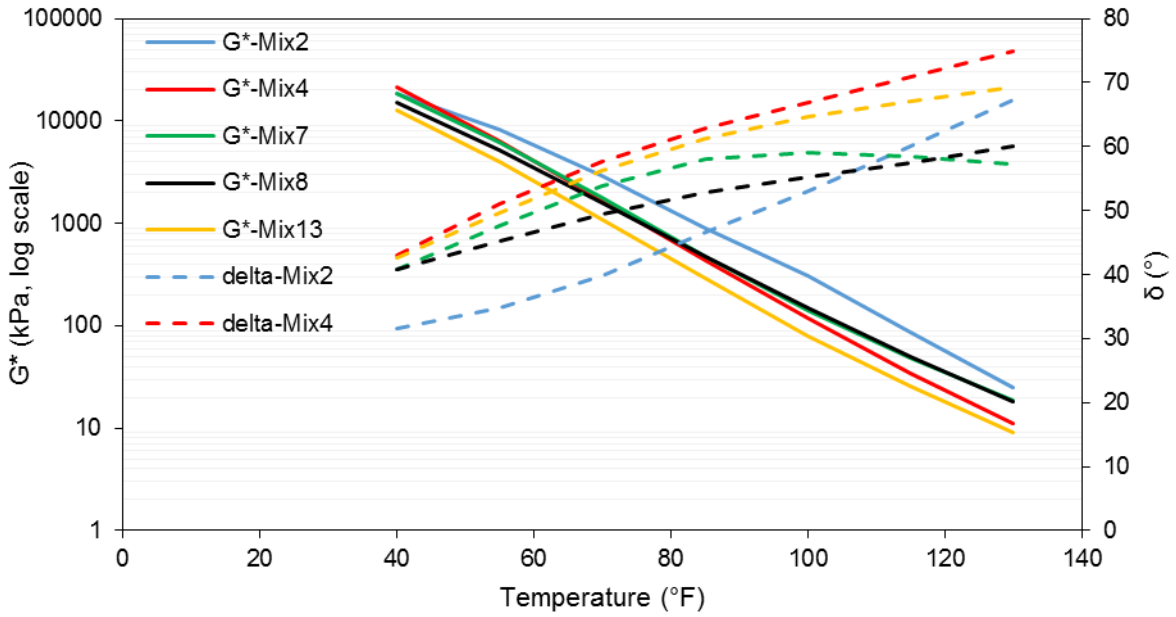

Figure 28: Complex shear modulus and phase angle of asphalt binders tested in DSR

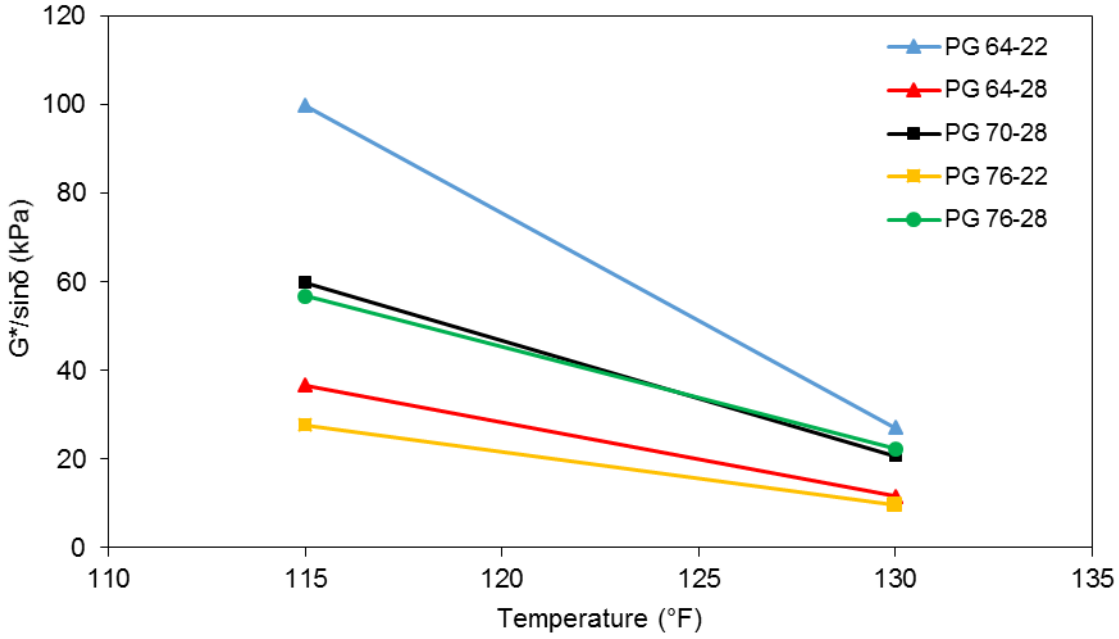

Figure 29: G*/sinδ vs Temperature for RTFO-aged binders

For the purpose of correlating binder results with HWTD results, a closer examination of the G*/sinδ values between the temperatures of 115°F and 130°F could provide insight (Figure 29). The reason for selecting this temperature range is that the HWTD test is performed at 50°C, which lies between the specified temperature ranges when converted into °F.

Table 19: G*/sinδ and rut depth comparison for tested mixtures

Mix	Type	Mix Summary	Binder PG	G*/sinδ - 115°F	G*/sinδ - 130°F	Rut Depth (mm)
2	HMA	SP-III w/ 33% RAP	64-22	99.87	27.05	1.81
4	HMA	SP-III	64-28	36.68	11.63	2.48
7	WMA	SP-III - Evotherm	76-28	59.84	20.74	15.96
8	HMA	SP-III w/ 20% RAP	70-28	27.76	9.76	4.76
13	WMA	SP-III - Terex Foaming	76-22	56.83	22.37	3.46

From Table 19, Mixture 2 experiences the best performance against rutting deformation. It can be seen that the complex shear modulus for the corresponding mix at the two specified temperatures are the highest among the tested group. Not much can be discussed about Mixture 7 due to the fact that its high rutting failure was attributed mainly to its composition of unique aggregates of Dacite, which was identified earlier. Complex shear modulus values for Mixture 7 and Mixture 8 are very close to one another, despite having similar binder grade of PG76-XX, the slight difference in values may be a result of the WMA agents present in both mixes.

Comparing Mixture 2 and Mixture 8, they contain 33% and 20% RAP content respectively. Mixture 2 shows to have significantly higher values in both rut depth and complex shear modulus; this may be attributed to the elevated RAP content resulting into a stiffer binder.

As most of the collected mixes contain high contents of RAP, it would be beneficial to study the effects of RAP on properties of the plant produced mixtures due to possible blending. According to a study conducted by Mcdaniel et al. [46] it was found that asphalt binders recovered from plant produced mixes showed that as the RAP content increased, the high temperature grade of the recovered binder also increased by 1 to 3 degree Celsius. Also, a blending analysis using comparison of measured mix moduli to predicted moduli suggested that significant blending of the RAP and virgin binder occurred in 16 of the 20 mixes that was tested during the study.

In order to evaluate these effects, extraction and recovery of asphalt binder from asphalt concrete is an approach to be considered. The process is elaborately explained and showed in the following. Extraction of asphalt binder is performed following AASHTO D2172 [47]: Standard Test Methods for Quantitative Extraction of Bitumen from Bituminous Paving Mixtures and AASHTO D5404 [48]: Standard Practice for Recovery of Asphalt from Solution Using the Rotary Evaporator respectively.

Figure 30(b) shows the sample emerged in 600 mL of Trichloroethylene solvent and kept covered for 45 minutes. The bowl was mounted securely in the centrifuge, where a filter paper was introduced on top of the bowl in order to capture the fines. The bowl was clamped tightly to start the centrifuge slowly and followed with an increased speed to 3600 rev/min, as shown in Figure 30(c). When the solvent flow ceases to drain, the centrifuge is stopped completely. The addition of another 200 mL of Trichloroethylene solvent is poured into the asphalt mixture for binder extraction as shown in Figure. These steps were repeated until the extract was not less than straw color.

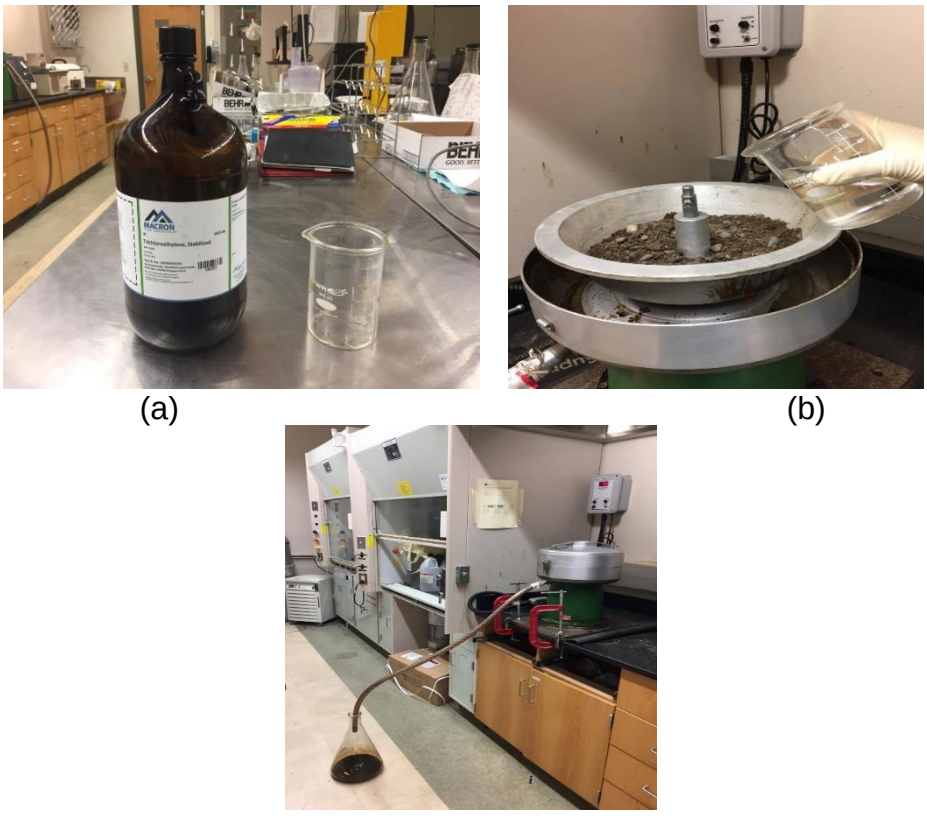

(a) (b)

(c)

Figure 30: Binder solvent extraction in centrifuge phase I

The following step involves the introduction of the extract in another centrifuge (AASHTO D1856), shown in Figure 31, to a centrifuge charge of no less than 30 minutes with 770 times of gravity with a small flow rate of 150 mL/min. The procedure allows the removal of fines which were not separated using the initial centrifuge process.


(a) (b)

Figure 31: Binder solvent extraction in centrifuge phase II for removal of fines

Binder recovery from solvent extract was achieved through the process of using the rotary evaporator in accordance to AASHTO D5404 (Figure 30). At first, the oil bath was heated to 140°C and a vacuum of 50 mm of Hg was introduced into the system. The vacuum allows introducing a 600mL of asphalt solvent extract solution in the distillation flask by the sample line. A nitrogen flow of 500mL/min was begun to reduce further aging of the binder sample. The distillation flask started to rotate at a speed 40 rpm and lowered into the heated oil bath. The vacuum pressure, oil bath temperature and condenser temperature can be found in Figure 32.

Figure 32: Recovery of asphalt binder (rotavapor)

The remaining amount of solvent extract was introduced in the distillation flask as the solvent in the flask becomes very low. When the bulk of the solution was recovered from the extract the distillation flask lowered 1.5 in in the oil bath, the vacuum was reduced to 80 m of Hg, the system introduced to a higher nitrogen flow of 600 mL/min and a higher rotation of 45 rpm for a duration of 10 minutes.

As shown in Figure 32, the last step of the procedure includes the binder recovery from the volumetric flask into a small aluminum container at an oven temperature of 165°C.

Figure 33: Asphalt binder recovery post-rotavapor process

Asphalt binders from Mixtures 8, 9, 10, 11, 12, 22, 25 and 33 were extracted and tested for complex shear modulus and phase angle were performed. Table 20 provides information in regards to the mixtures' properties and Table 21 represents the rheological results for the tested binders in the DSR. Figure 34 shows the complex shear modulus and phase angle of the extracted binder with temperature.

Table 20: Binder extraction from HMA/WMA Mixes

Test Code	Mixture	Type	Mix Summary	Binder Grade Used	Binder Grade Specified	Asphalt Source
D4A4	8	HMA	SP-III w/ 20%RAP	70-28	76-22	Holly Frontier
D4A5	9	WMA	SP-III w/ 20%RAP (TEREX)	70-28	76-22	Holly Frontier
D4A6	10	WMA	SP-III w/ 20%RAP (Evotherm)	70-28	76-22	Holly Frontier
D4A7	11	WMA	SP-III w/ 20%RAP (Cecabase)	70-28	76-22	Holly Frontier
D4A8	12	WMA	SP-III w/ 20%RAP (Cecabase+)	70-28	76-22*	Holly Frontier
D5A1	22	HMA	SP-III w/ 35%RAP	58-28	64-28	Western Refining
D5A2	25	HMA	SP-III w/ 35%RAP	58-28	70-22	Western Refining
D3A10	33	HMA	SP-III w/ 25%RAP	64-22	70-22	Western Refining

Table 21: Rheological properties for extracted binders

Mixture	Temperature (°F)	G* (kPa)	δ (°)	G*/sinδ (kPa)
8	40	21136.6	37.3	34879.5
8	55	8083.81	43.8	11679.4
8	70	2682.77	50.7	3466.82
8	85	774.08	57.5	917.82
8	100	222.48	63.3	249.04
8	115	66	68.7	70.84
8	130	21.17	73.4	22.09
9	40	29907.7	34.6	52668.9
9	55	11873.9	40.7	18208.7
9	70	4106.41	47.4	5578.63
9	85	1223.56	54.1	1510.49
9	100	359.1	60	414.65
9	115	107.63	65.2	118.56
9	130	34.45	69.9	36.68
10	40	17270.7	38.5	27743.5
10	55	6617.39	44.7	9407.79
10	70	2212.15	51.1	2842.49
10	85	649.78	57.3	772.16
10	100	191.88	62.7	215.94
10	115	58.42	67.6	63.19
10	130	19.28	72.1	20.27
11	40	18267.3	38.8	29152.9
11	55	6768.23	45.6	9473.04
11	70	2164.9	52.6	2725.15
11	85	604.73	59.3	703.29
11	100	169.05	65.1	186.37
11	115	49.47	70.3	52.54
11	130	15.9	74.9	16.47

Table 21: Rheological properties for extracted binders (continued)

Mixture	Temperature (°F)	G* (kPa)	δ (°)	G*/sinδ (kPa)
12	40	33178	30.8	64795.4
12	55	14311.1	36.2	24231.3
12	70	5418.12	42.3	8050.54
12	85	1779.23	48.5	2375.61
12	100	570.6	53.7	708.01
12	115	184.29	57.6	218.27
12	130	65.03	59.9	75.17
22	40	8695.5	43.6	12609.1
22	55	3107.51	50.1	4050.64
22	70	965.21	56.8	1153.5
22	85	267.81	63.4	299.51
22	100	76.16	69.3	81.41
22	115	22.92	74.8	23.75
22	130	7.64	79.3	7.77
25	40	16703.8	40.1	25932.6
25	55	6055.2	47.3	8239.33
25	70	1877.57	54.9	2294.9
25	85	489.94	62.4	552.85
25	100	126.18	69	135.16
25	115	33.92	75	35.12
25	130	10.29	79.8	10.46
33	40	25050.6	35.7	42928.6
33	55	10007.6	41.8	15014.4
33	70	3433.16	48.6	4576.87
33	85	1000.78	55.7	1211.45
33	100	283.3	62.1	320.56
33	115	81.6	68.1	87.94
33	130	25.32	73.5	26.4

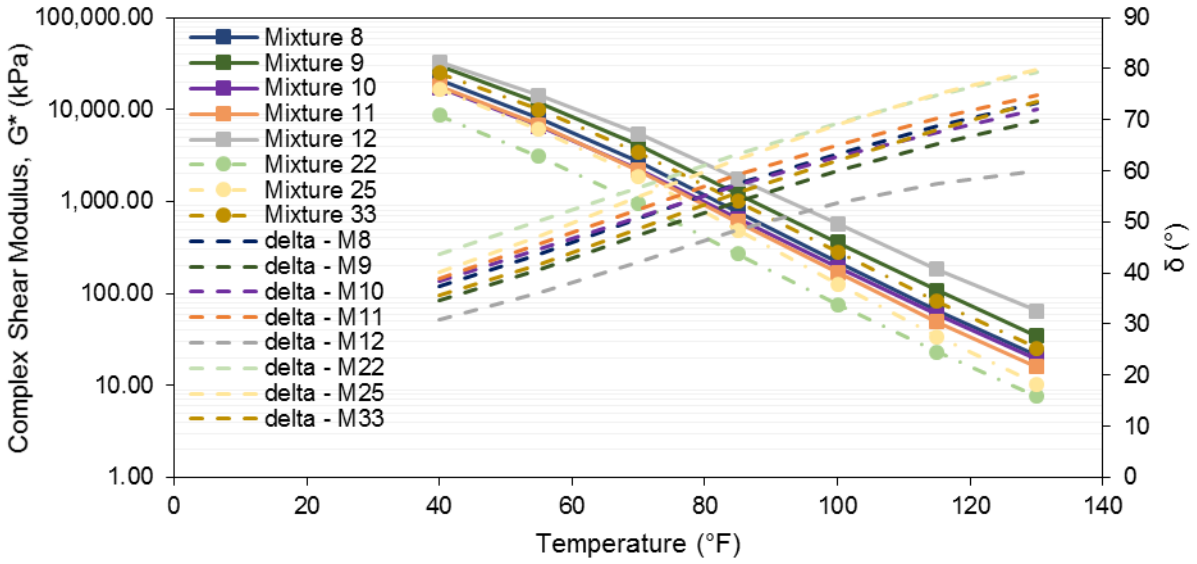

Figure 34: Complex shear modulus and phase angle of extracted binders tested in DSR

As mentioned previously, the higher the G* value, the stiffer the asphalt binder is able to resist deformation. Comparing the G* retrieved for mixes 8-12 against the rheological properties of virgin binder grade PG70-XX, it is clearly noticeable that mixture incorporated with RAP and WMA additives display higher G* values across the tested temperatures. According to Li et al. [49] experimental results indicate that asphalt mixtures containing RAP have higher complex shear modulus values than the control mixtures containing no RAP.

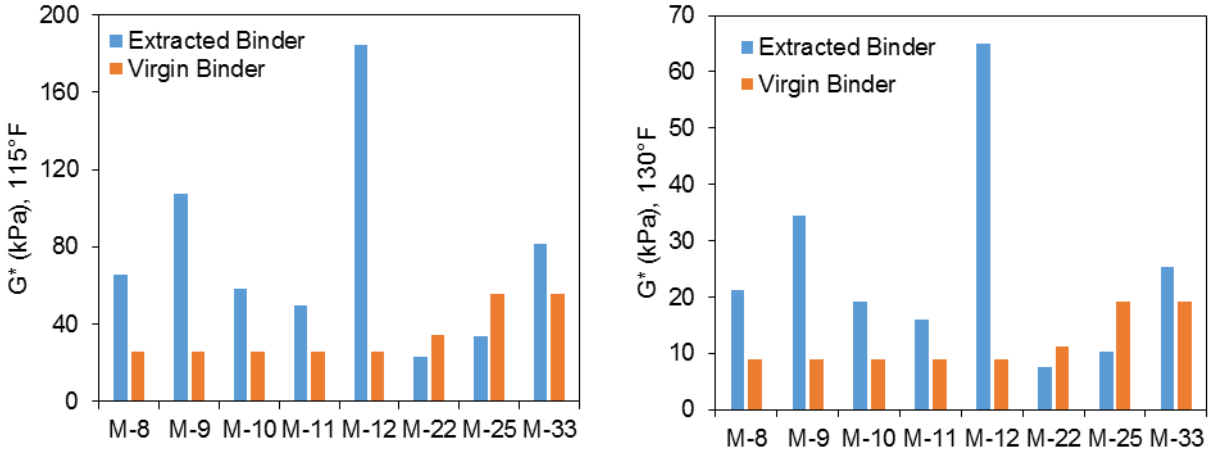

Figure 35: G* of as-recovered binders in comparison to virgin RTFO-aged binders at 115°F and 130°F

It is quite evident from Figure 35 that the complex shear modulus of extracted binder for SPS-10 mixtures and mix 33 show an elevated value. Comparing the results for mix 9

and mix 12 to the virgin RTFO-aged rheological property, the percent increase in G* are close to 300 and 600%. This clearly illustrates that the parameters tested from virgin RTFO-aged binders of varying binder performance grade doesn't accurately depict the actual binder behavior. On the other hand, values retrieved from mixtures 22 and 25 display an opposite trend, experiencing a decrease of 40% in value of complex shear modulus. This may be attributed to unsuccessful blending of RAP within the binder system.

To completely characterize the flow characteristics of the recovered binders, master curves were constructed for the as-recovered and Rolling Thin Film Oven (RTFO)-aged virgin binders. The master curve of an asphalt binder provides a relationship between the binder stiffness and reduced frequency over a range of temperatures and frequencies; making it possible to predict viscoelastic properties over a wide frequency range and also to predict viscoelastic properties at any temperature [50]. In order to create a master curve, the stiffness of an asphalt binder at multiple temperatures and frequencies is measured. Then, this is followed by fitting the data into a viscoelastic model applied to asphalt binders. For the purpose of this study, master curves will be constructed for mixtures 8 through 12. The reason for the selection is that this particular cluster of mixes utilizes the same material components for design, with the exception of modification with various warm mix additives. Also, it is worth noting that these mixes are incorporated with 20% RAP and it would be a great insight to identify the occurrence of RAP blending and the effects of WMA to the rheological properties of the binders.

As shown in Figure 36, it was observed that all mixtures modified with various warm mix additives and RAP of 20% display rheological characteristics of higher complex shear modulus across the frequency range. This is to be expected as RAP is added to asphalt binder, resulting in a stiffer binder mixture.

Despite the fact that asphalt bitumen make up 4 to 8 % of a pavement mix structure, it provides a level of rigidity, structural bonding, resilience, and absorbance which holds the total pavement mixture together as a solid body [51]. However, with higher traffic densities and effects of environmental exposure, binder flows and dissipates energy with time [52]. As a result, asphalt binder experience a variety of thermomechanical demands; where pavement defects transpire such as rutting at high temperatures due to thermal susceptibility of asphalt [53]. The resistance of asphalt mixtures to rut deformation is related to the stiffness of bitumen, mix volumetric, and the bonding interaction between bitumen and aggregate [54-56]. The asphalt contribution to permanent deformation process has traditionally been handled by looking at the asphalt binder's consistency based on softening point and penetration tests [57-59]. Nowadays, with the addition of Reclaimed Asphalt Pavement (RAP) materials, polymer modified asphalts, and warm mix agents, the asphalt rutting characterizations attained through these empirical tests is insufficient. It would be beneficial to study the effects of such added materials on the properties of the plant produced mixtures and determining the fundamental rheological properties is the proper manner to characterize the asphalt binder's rutting behavior.

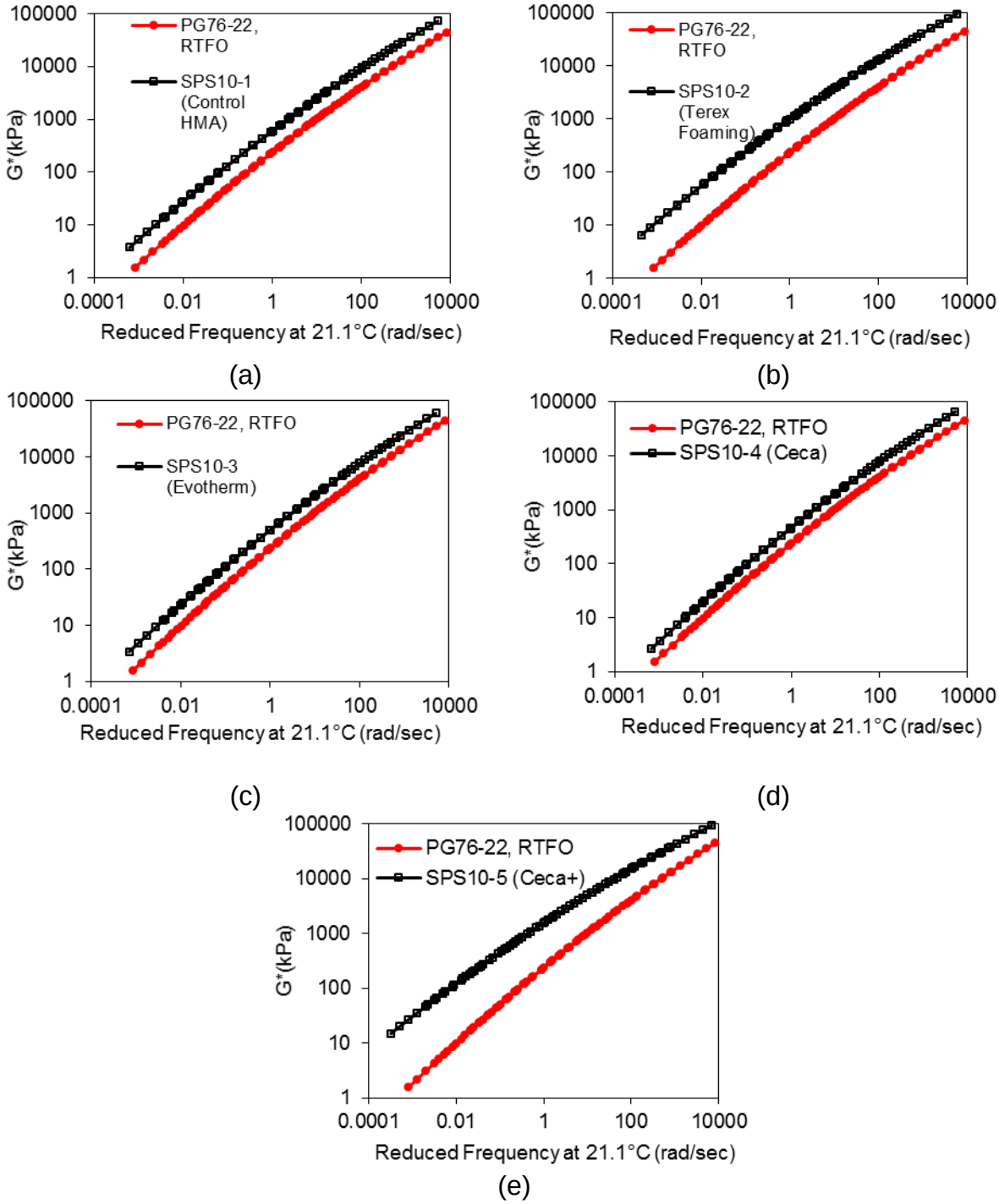

Figure 36: Master curves for as-recovered binders for mix 8-12 in comparison to PG76-22 (RTFO-aged)

To better understand the effects of these warm mix additives on the mixtures performance, frequency temperature sweep and multiple stress-creep recovery tests were employed to investigate the rutting resistance, using high temperature rheological properties of warm mix-modified binders. Two approaches were considered for this task: the Superpave rutting specification parameter (G*/sinδ) and multiple stress-creep

recovery, where both test methods were conducted at a fixed temperature of 50°C using a dynamic shear rheometer. By using these specific approaches, the rheological rut properties of modified asphalt binders were determined and then correlated with Hamburg Wheel Track Testing (HWTT) results performed at 50°C.

The MSCR test aims at measuring the permanent deformation properties of asphalt binders. In order to provide a new high temperature binder specification that more accurately indicates the rutting performance of the bitumen and is blind to modification, this test was developed by the U.S Federal Highway Administration [60]. The test is typically performed at the maximum PG (performance grade) temperature of each binder. But for this study, tests were conducted at 50°C in order to correlate results with the HWTT. In accordance with AASHTO TP70, the percent recovery (% R) and non-recoverable creep compliance (Jnr) are determined and reported as average results. The MSCR test consists a total of 10 cycles of creep and recovery - 1 s loading time of a constant shear load and followed by 9 s unloading time at stress levels of 0.1 and 3.2 kPa. A typical creep and recovery curve in MSCR test is shown in Figure 37.

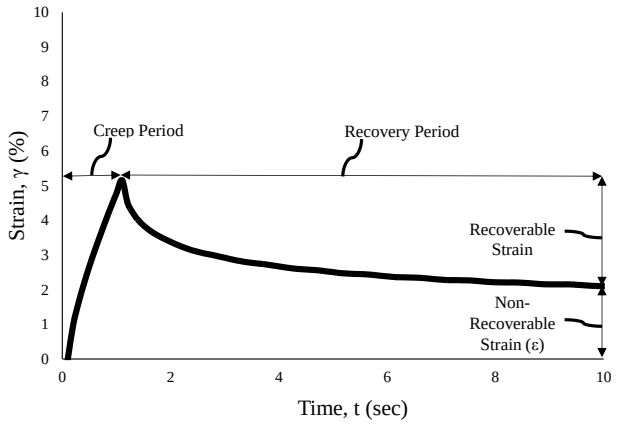

Figure 37: A typical creep and recovery curve in MSCR test

At each stress level, ten cycles are applied with no time lag and corresponding strain values are recorded. The percent recovery is calculated through the use of equation 3, where e_r and e_t represent the recoverable deformation and total deformation, respectively. For each of the ten cycles at a creep stress (σ, Pa), the non-recoverable creep compliance, J_{nr} (kPa-1) is given by equation 4, where e_{nr} and σ are the non-recoverable deformation and test stress level, respectively. Finally, J_{nr} is determined at 3.2 kPa using equation 5.

$$\%R = \frac{e_r}{e_t} * 100 \tag{3}$$

$$J_{nr}(\sigma, N) = \frac{e_{nr}}{\sigma} \tag{4}$$

$$J_{nr}(\sigma) = \frac{SUM(J_{nr}(\sigma, N))}{10} \tag{5}$$

It was observed that all forms of warm mix modification was observed to increase the superpave rutting parameter (Figure 38(a)). For example, G*/sinδ value for binders with

Terex® foaming, Evotherm®, Cecbase®, and Cecabase®+ was found to be approximately 27.90, 20.47, 19.90,and 91.83 kPa, respectively, compared to 11.70 kPa for control HMA. Results indicate that the addition of Cecabase® with polymer modification increased G*/sinδ substantially. From these results, Cecabase®+ is recognized to be the most effective additive in improving rutting resistance followed by Terex® foaming, Evotherm®, and Cecabase® unmodified. Based on the simple regression analysis (Figure 38(b)), a good correlation of R^2 = 0.91 was observed between the maximum rut depth and rheological parameter values of these mixtures.

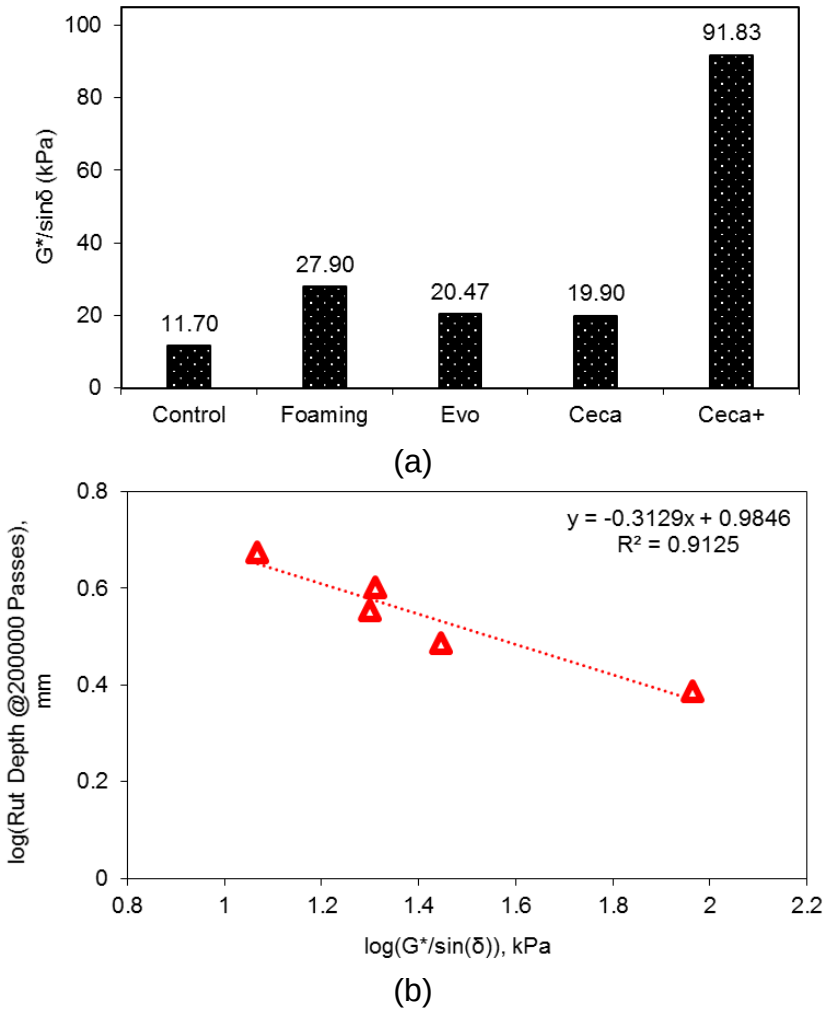

Figure 38: Superpave rutting parameter results

With respect to MSCR test evaluation, the J_{nr} value of control HMA was found to be 0.59 kPa^{-1} (Figure 39(a)). The J_{nr} values of the extracted binders with Terex®, Evotherm®, Cecabase®, and Cecabase®+ was found to be 0.15, 0.46, 0.23, and 0.02, respectively. Lower J_{nr} values were observed for all WMA modified mixtures in comparison to control HMA. This indicates increased rut resistance. As shown in Figure 39(b), the % Recovery value of the control sample was found to be 13.47. The % Recovery values of the extracted binders with the presence of Terex®, Evotherm®, Cecabase®, and Cecabase®+ was found to be 32.58, 18.14, 23.71, and 77.54, respectively. This also indicates increased rutting resistance compared to the control

sample. Based on the lowered J_{nr} and heightened % Recovery values from the incorporation of Cecabase®+, the influence of polymerization is exhibited through the decreased rutting potential.

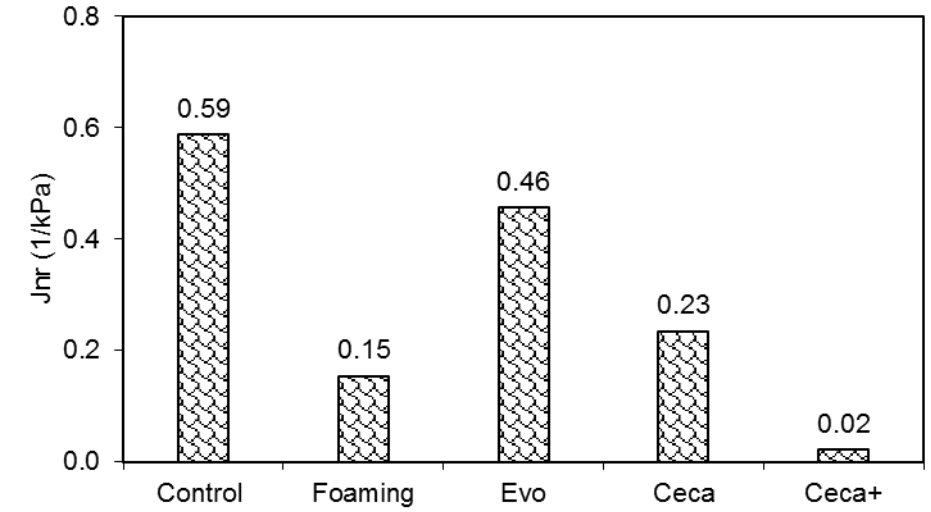

(a)

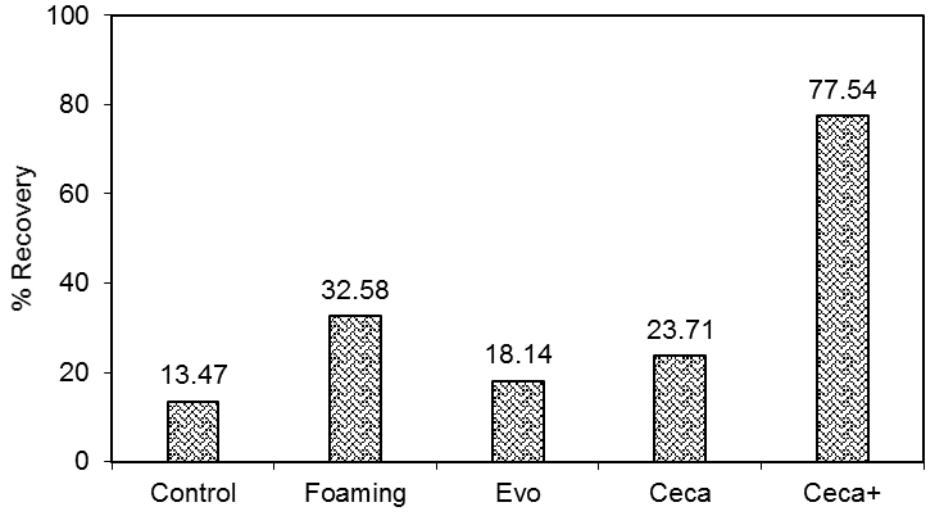

(b)

Figure 39: MSCR parameter results

As shown in Figure 40, a simple linear regression analyses were performed between the two parameter results obtained from this test method in contrast to HWTT, As shown in Figure 39, a correlation value of R^2 = 0.96 and R^2 = 0.77 were found for J_{nr} and % Recovery, respectively. Hence, indicating the non-recoverable creep compliance parameter as a reliable measure when it comes to evaluating rutting resistance, out of the MSCR parameters.

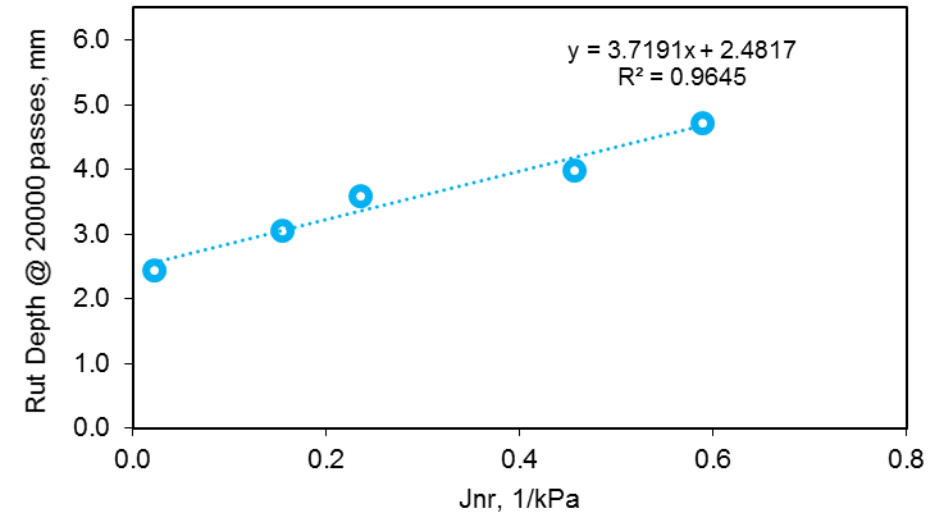

(a)

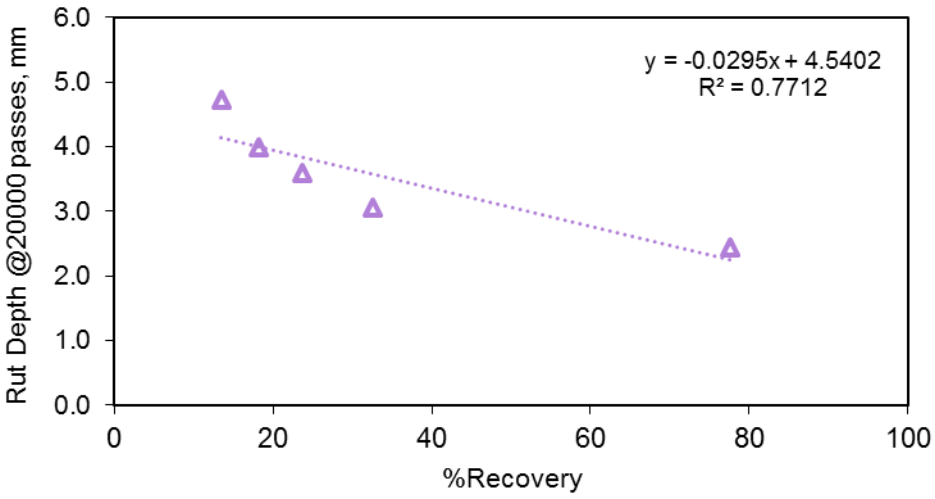

(b)

Figure 40: Simple linear regression analysis of MSCR results with respect to HWTT

Based on the J_{nr} values, the order of rut resistance for the extracted binders can be seen as (i) Cecabase®+, (ii) Terex® Foam, (iii) Cecabase®, (iv) Evotherm®, and (v) Control. This ranking order shows that compared to the control HMA sample, WMA modification improves the rutting potential of the mixtures.

PREDICTING E* AND CORRELATING IT WITH HWTD

In this task, mixture volumetric data and binder shear modulus and phase angle obtained in the previous chapter will be utilized to predict mix E* using the $|G_b^*|$-based Witczak equation. As part of the structural design processes to optimize field performance of asphalt concrete mixtures, various laboratory tests such as the Hamburg Wheel Tracking Test (HWTT) and Dynamic Modulus (DM) have been proposed and developed for use as a simple performance test to characterize the rutting resistance potential of asphalt concrete mixes. The purpose of dynamic modulus testing is to define the materials stress to strain relationship under continuous sinusoidal loading, where the stiffness of the aspahlt mixture is measured under dynamic loading at various temperatures and frequencies, thus it is used to determine which mixes may be more susceptible to performance issues such as rutting. As the task does not prescribe the testing of dynamic modulus, the only approach is to utilize an E* prediction model for mixes used in this study and attempt to correlate findings with HWTT results.,

The $|G_b^*|$-based Witczak model, also known as Witczak-Bari model [61] was presented in 2006 as a newly revised version of the widely used Witczak-Andrei predictive model; where the complex shear modulus (G_b^*) and phase angle (δ_b) of binder replaced the viscosity, from the current A-VTS relationship, as direct inputs, because G_b^* can more effectively describe binder stiffness with changing in temperature and loading time. This was developed using the Bari database of 7400 measured $|E^*|$ values obtained from 346 different asphalt concrete mixtures. $|G_b^*|$-based Witczak equation can be as:

$$Log|E^*| = -0.349 + 0.754\cdot(|G_b^*|^{-0.0052})\cdot$$
$$[6.65 - 0.032\cdot P_{200} + 0.0027\cdot P_{200}^{\ 2} + 0.011\cdot P_a - 0.0001\cdot P_4^2 + 0.006\cdot P_{38} - 0.00014\cdot P_{38}^2 - 0.08\cdot V_a - \quad (6)$$
$$1.06\left(\frac{V_{beff}}{V_{beff}+V_a}\right)] + \frac{2.56 + 0.03\cdot V_a + 0.71\cdot\left(\frac{V_{beff}}{V_{beff}+V_a}\right) + 0.012\cdot P_{38} - 0.0001\cdot P_{38}^{\ 2} - 0.01\cdot P_{34}}{1+e^{(-0.7814-0.5785\log|G_b^*|+0.8834\log\delta_b)}}$$

Where:

$|E^*|$ = Asphalt mix dynamic modulus (10^5 psi)
$|G_b^*|$ = Dynamic shear modulus (psi)
δ_b = Phase angle (degree)
V_a = Air voids in the mix (% by volume)
V_{beff} = Effective binder content (% by volume)
P_{200} = % Passing #200 sieve (0.075 mm)
P_4 = Cumulative % retained on #4 sieve (4.75 mm)
P_{38} = Cumulative % retained on 3/8 inch sieve (9.5 mm)
P_{34} = Cumulative % retained on 3/4 sieve (19 mm)

However, a number of studies were conducted to evaluate the performance of the model mentioned above. According to a study conducted by Singh et al. [62] the accuracy of the $|G_b^*|$-based Witczak equation is poor when compared to other available

|*E**| models. Also, El-Badawy et al. [63] reported that the |G_b*|-based Witczak model produces less accurate and relatively higher biased estimates of |*E**| than η-based Witczak model (equation 7).

$$Log|E^*| = -1.249937 + 0.029232 \cdot P_{200} - 0.001767(P_{200})^2 - 0.002841 \cdot P_4 - 0.058097 \cdot V_a - 0.802208 \frac{V_{beff}}{V_{beff} + V_a} + \frac{[3.8719977 - 0.0021 \cdot P_4 + 0.003958 \cdot P_{38} - 0.000017(P_{38})^2 + 0.005470 \cdot P_{34}}{1 + e^{(-0.6033133 - 0.313351 \log f - 0.393532 \log \eta)}} \quad (7)$$

Where:

|*E**| = Asphalt mix dynamic modulus (10^5 psi);
η = Binder viscosity (10^6 poise);
f = Loading Frequency (Hz);
V_a = Air voids in the mix (% by volume);
V_{beff} = Effective binder content (% by volume);
P_{200} = % Passing #200 sieve (0.075 mm);
P_4 = Cumulative % retained on #4 sieve (4.75 mm);
P_{38} = Cumulative % retained on 3/8-inch sieve (9.5 mm);
P_{34} = Cumulative % retained on 3/4-inch sieve (19 mm).

Several studies also indicate the shortcomings of the η-based Witczak model. It was found that the |*E**| predicted by the equation above estimates lower dynamic modulus values at higher temperatures and higher values at lower temperatures. Zaman et al. [64] reported that this model significantly underestimates |*E**| values when the DSR test data is used.

Rahman et al. [65] developed a predictive model to estimate the dynamic modulus values of asphalt concrete mixtures typically produced in New Mexico. The following equation is as follows:

$$Log|E^*| = \delta_{E^*} + \frac{\alpha_{E^*|}}{1 + e^{\beta_{E^*} + \gamma_{E^*} * \log(f)}} \quad (8)$$

Note that the |*E**| is kept in angular frequency space, so that the angular loading frequency associated with a certain pair of |G_b*| and δ_b can be readily used in the equation to estimate the dynamic modulus of the asphalt concrete mix for that particular angular frequency of loading.

where:

$$\delta_{E^*} = -3.31676767 + 0.15223521(F_m)^2 - 1.78427544(F_m) - 0.00508589(C_u) - 0.50580886(V_a)^2 + 5.731483(V_a) + 0.02629492(V_{beff})^2 - 0.61189577(V_{beff}) \quad (9)$$

$$\alpha_{E^*} = -0.81621932 - 0.26422402(F_m)^2 + 3.07887763(F_m) + 0.00633059(C_u) + 0.28170835(V_a)^2 - 3.2881344(V_a) - 0.03350841(V_{beff})^2 + 0.72041062(V_{beff}) \quad (10)$$

$$\beta_{E^*} = 0.26881379(F_m)^2 - 3.16127514(F_m) - 0.43917071(V_a)^2 + 5.14118364(V_a) + 0.05136617(V_{beff})^2 - 1.15376261(V_{beff}) + 0.01434329 \log \eta \quad (11)$$

$$\gamma_{E^*|} = -1.39453189 - 0.0512783(F_m) + 0.00003869(C_u)^2 - 0.00290191(C_u) - 0.05321409(V_a)^2 + 0.5285461(V_a)$$

(12)

The variables affecting |*E**| of mixes considered in this study are the following: fineness modulus (F_m), uniformity coefficient (C_u) for the aggregate used in the asphalt concrete mixtures; effective binder content (V_{beff}), air void content (V_a), the viscosity of the binder (η), and the loading frequency (f). The definitions of F_m, C_u, and η are given below;

$$F_m = \frac{\sum_{i=1}^{N} CPR_i}{100} \quad (13)$$

$$C_u = \frac{D_{60}}{D_{10}} \quad (14)$$

$$\eta = \left(\frac{|G_b^*|}{\omega}\right)\left(\frac{1}{\sin\delta_b}\right)^{a_0 + a_1\omega + a_2\omega^2} \quad (15)$$

where:

η = Binder viscosity (cP);
$|G_b^*|$ = Binder shear modulus (Pa);
δ_b = Binder phase angle (degree);
ω = Angular frequency used to measure G_b^* and δ_b (radians/sec);
a_o, a_1, and a_2 = Fitting parameters, respectively, 3.63922, 0.13137, and -0.0009;

For ω = 10 rad/sec [where $f = \omega/(2\pi)$ = 10/(2*3.14) = 1.59 Hz], which is the specified test frequency in the Superpave PG system.

A total of 13 standard sieves will be used for sieve analyses of the aggregate blends. The designations and the opening sizes are presented in Table 22.

Table 22: Standard sieves used

Sieve Designation	Sieve opening (mm)
2 inch	50.00
1.5 inch	37.50
1 inch	25.00
¾ inch	19.00
½ inch	12.50
3/8 inch	9.50
No. 4	4.75
No. 8	2.36
No. 16	1.18
No. 30	0.60
No. 50	0.30
No. 100	0.15
No. 200	0.075

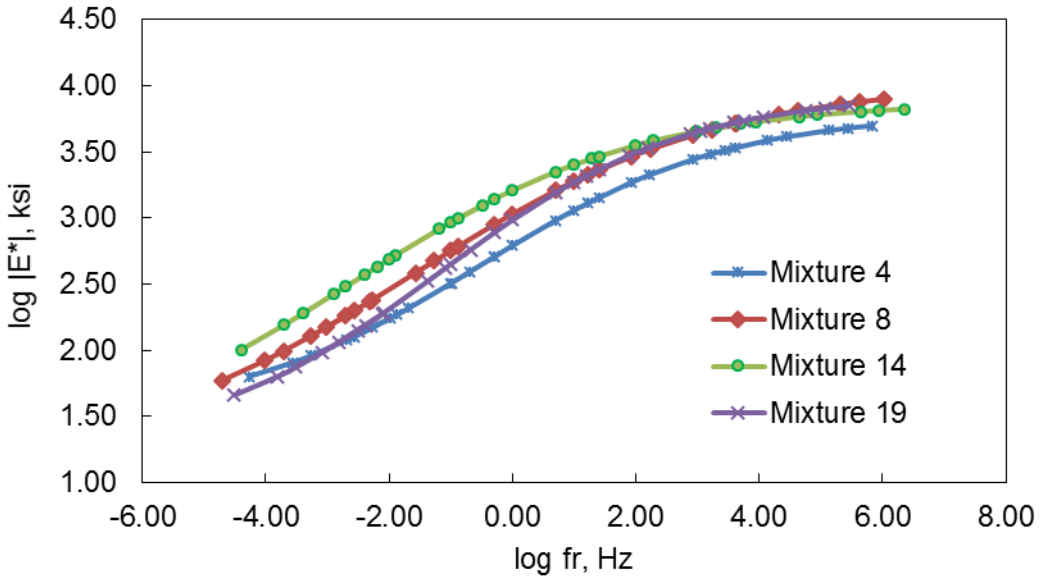

Figure 41: Dynamic modulus master curves at 21.1°C for mixtures 4, 8, 14 and 19 considered in this study

The objective of this subtask is to validate the accuracy of the newly developed regression-based |*E**| predictive model for the asphalt concrete mixtures typically used in New Mexico. As shown in Figure 41, tested dynamic modulus data for mixtures 4, 8, 14, and 19 were considered in this assessment. A variety of binder performance grades are used in these mixtures depending on the regional climate associated with the pavement operation site.

As shown in Figure 42, the newly developed |*E**| prediction model has a fairly good coefficient of determination of R^2=0.956 in normal or arithmetic scale. Again, in logarithmic scale, the coefficient of determination is R^2=0.961, which is excellent for this type of models where numerous complexities are involved. Both of the plots show that the |*E**| data points are around the line of equality without any significant bias. Therefore, it can be said that the discussed predictive model provides a fairly good estimation of |*E**| of asphalt concrete mixtures of New Mexico.

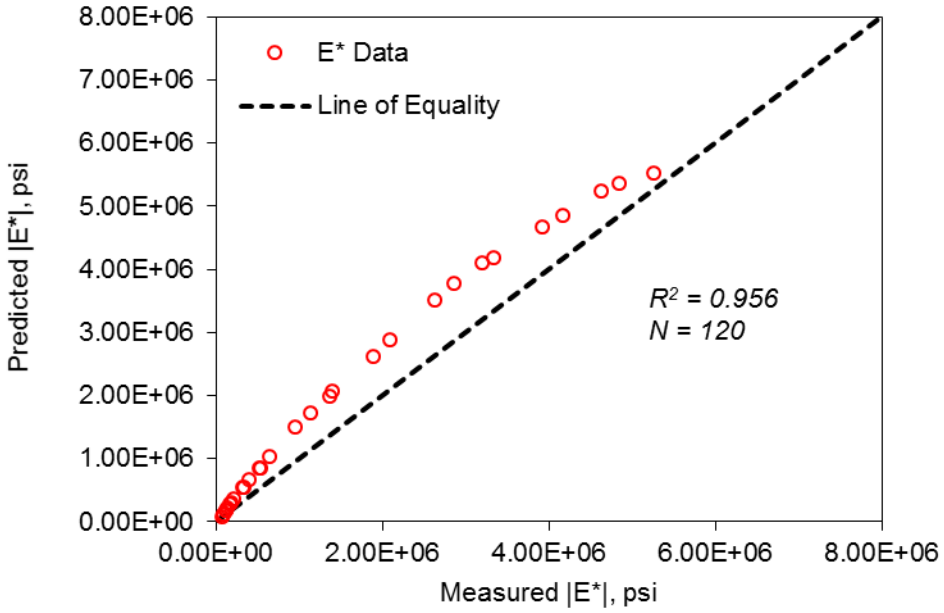

(a)

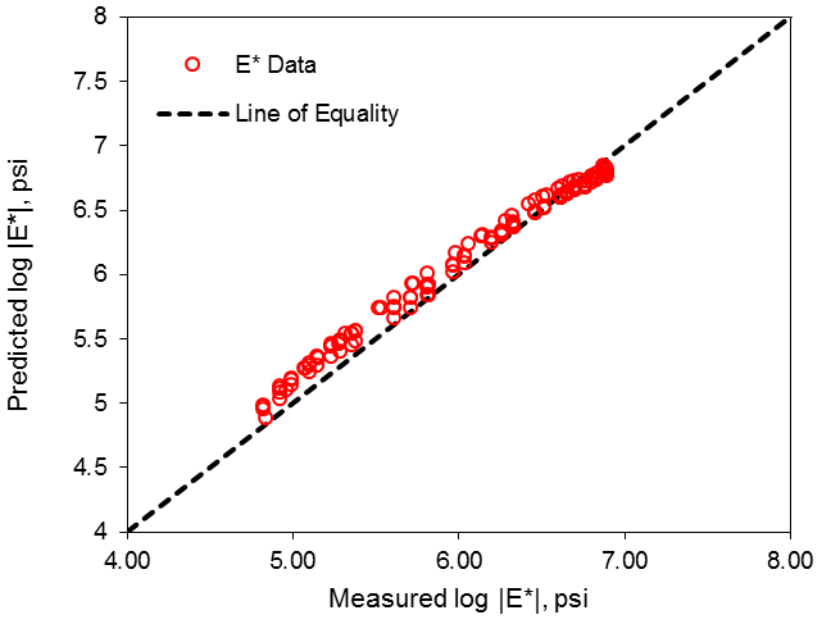

(b)

Figure 42: |*E**| Predicted by the new η-based model versus measured |*E**| plot in a) normal or arithmetic scale, and b) in logarithmic scale.

MEPDG RUT PREDICTION AND COMPARISON WITH HWTD RUTTING

Developed under multiple NCHRP projects including 1-37A, 1-40 and 9-30A over the past fifteen years, the AASHTO Mechanistic-Empirical Pavement Design Guide (MEPDG) is emerging as a mainstream pavement design method throughout North America. The method established a direct tie between pavement distresses and various design inputs including material properties, pavement structures, traffic loadings, and climate and so on. The design method has been packaged in a user-friendly working platform now called the AASHTOWare Pavement.

In this task, the predicted E* data and/or mix volumetrics with G* and δ data will be used in MEDPG at level 3 and 2 to determine AC rutting of the mixtures collected within a specified pavement geometry. HWTD laboratory test results will be compared with the MEPDG predicted rutting. This is reasonable during the time of this study due to the lack of availability of field rutting values for this mixes.

A predictive rutting system was developed to evaluate the permanent deformation within all rut susceptible layers in the pavement within the analysis period. Individual layer rut depths are predicted for each layer as a function of time and traffic repetition. This also allow for the prediction of the total pavement rut depth, with time and traffic repetitions. Regardless of the material type considered, there are generally three distinct stages for the permanent deformation behavior of pavement materials under a given set of material, load and environmental conditions.

The MEDPG software relates rut depth to the vertical permanent deformation of different structural layers. The mechanistic analysis initializes with first calculating the resilient strain in each analysis layer based on elastic layer theory. After the resilient strains are obtained, the plastic strain of each analysis layer is then calculated by using one of the three empirical rutting models, depending upon which material is used in the analysis layer. Since the three rutting models were all established based on laboratory experiments, they are subject to further calibrations. The AC rutting model is expressed in equation as:

$$\frac{\varepsilon_{p,AC,i}}{\varepsilon_{r,AC,i}} = k_z \beta_{AC} 10^{-3.3541} T_i^{1.5606\beta_T} N^{0.4791\beta_N} \quad (16)$$

Where $\varepsilon_{r,AC,i}$ denotes the resilient strain of AC at the mid-depth of the i^{th} analysis layer under a specific traffic load. $\varepsilon_{p,AC,i}$ is the corresponding accumulated plastic strain, k_z is the depth confinement factor as a function of total asphalt layer thickness and depth to computational point, T_i is the temperature at the i^{th} analysis layer in Fahrenheit degree, *N* is the number of load repetitions. Lastly, β_{AC}, β_T, β_N represent the calibration factors, which equal to 1.0 by default. Note that β_{AC} is also known as AC-scale factor, and the β_T, β_N are called temperature and traffic exponents, respectively.

Figure 43 shows the MEPDG rut analysis for the following fifteen HMA/WMA mixes and Table 23 lists the generalized rut results simulated for pavement life cycle of 20 years. It can be seen that mixture 5 experiences the most rut deformation of 13.42 mm out of the studied group. Compared to the rutting values retrieved from testing of laboratory compacted samples, mixture 5 displays a high rutting resistance equaling to a rut value of 2.3 mm after the performance of 20,000 wheel passes.

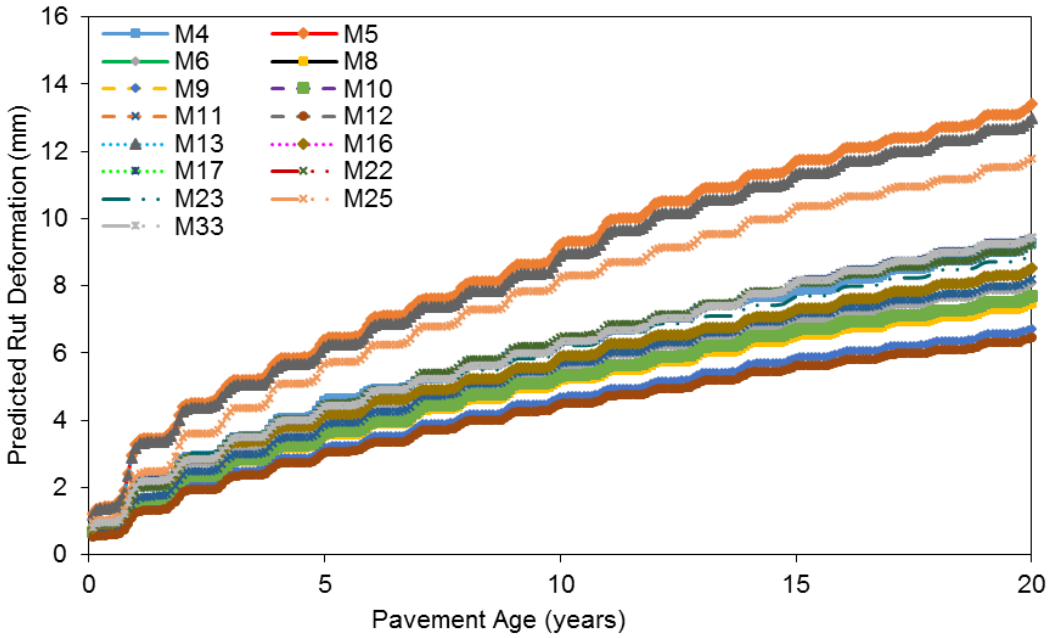

Figure 43: MEPDG Level 2 analysis rut prediction

Table 23: MEPDG rut prediction data

Mix	1 year	5 years	10 years	20 years	UNM Max. Rut
4	2.12	4.58	6.33	9.28	2.48
5	3.29	6.39	9.23	13.42	2.3
6	1.93	3.95	5.59	8.08	15.27
8	1.48	3.52	5.18	7.46	4.76
9	1.33	3.19	4.67	6.72	4.77
10	1.52	3.61	5.32	7.69	4.67
11	1.62	3.86	5.69	8.19	3.71
12	1.23	3.03	4.47	6.46	2.41
13	3.18	6.18	8.91	12.98	3.46
16	2.03	4.15	5.88	8.51	5.02
17	2.03	4.4	6.31	9.45	3.02
22	1.87	4.46	6.47	9.21	2.84
23	2.13	4.35	6.17	8.93	6.34
25	2.32	5.66	8.23	11.78	5.85
33	2.02	4.39	6.3	9.43	4.4

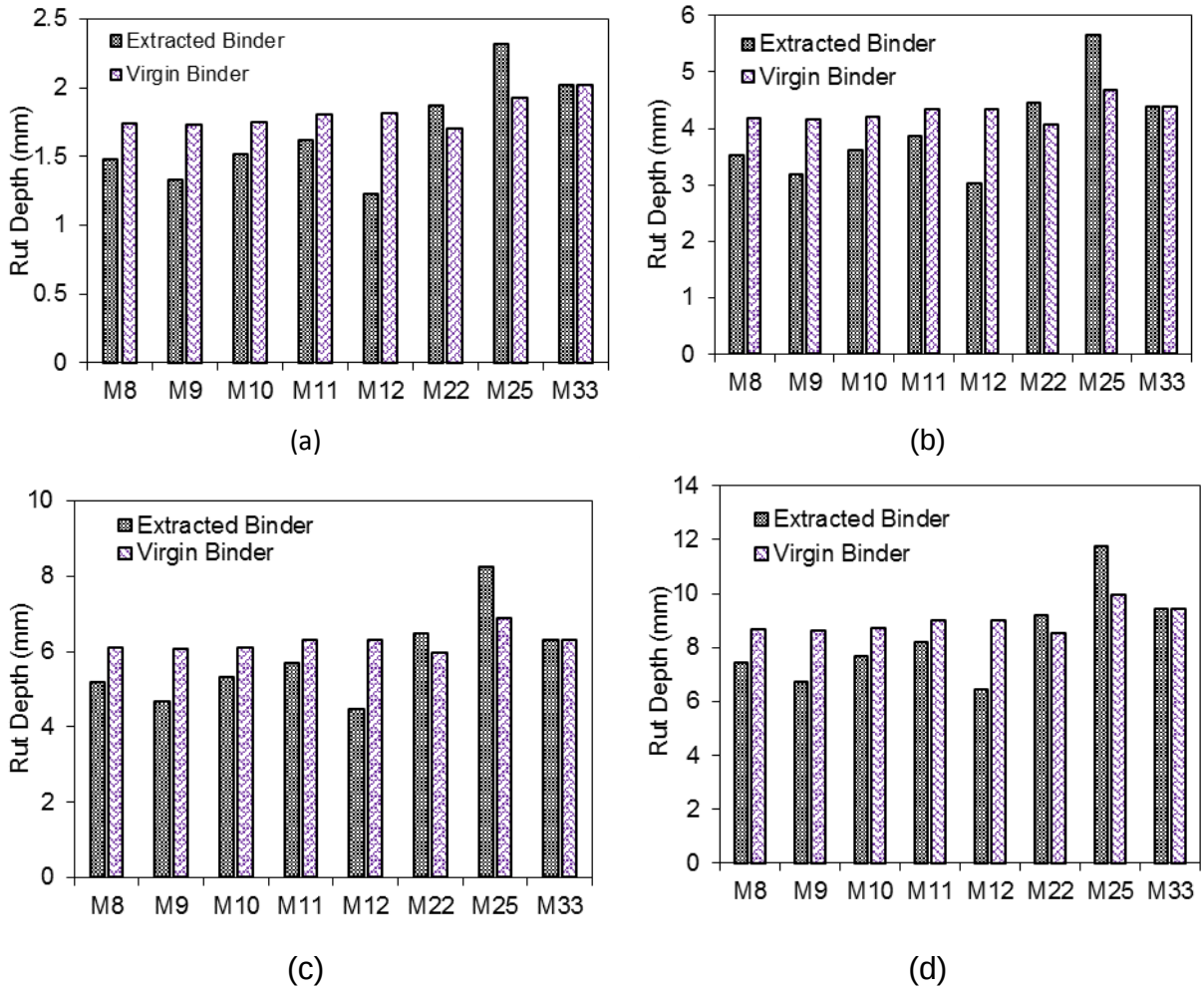

Figure 44: MEPDG rut prediction simulation for (a) 1st year, (b) 5th year, (c) 10th year, and (d) 20th Year

As discussed in earlier in this report, extracted binders from the SPS-10 group of mixtures along with mixture 22, 25, and 33 were tested for G* and δ, where these two parameters will be used to perform a level 2 analysis in order to measure long term performance. As shown in Figure 44, an analysis of as-recovered and virgin RTFO-aged binder for each respective mixture has been simulated for 20 year life cycle. It was observed that despite having the similar design components with the exception of WMA additives, the simulation with virgin binder properties displays an elevated permanent deformation value for all five mixtures. However, as-recovered binder properties show that the incorporation of RAP and WMA does mitigate the rutting susceptibility of mixtures. On the other hand, actual binder input simulation for mixtures 22 and 25 results in an increased rut deformation compared to the virgin binder simulation. As mentioned in the concluding remarks in task 4 of this report, this decrease in rutting resistance might be attributed to the unsuccessful blending of RAP within the binder system, thus not experiencing the expected stiffening effect.

Figure 45 illustrates the MEPDG rut analysis for all the SP IV mixes collected so far for this study. The analysis was performed for a design life of 20 years and employing the binder shear modulus, phase angle, and volumetric properties of the mixture determined in task 4. It is observed from figure 45, mixture 39 shows the highest rut deformation of 14.69 mm and mix 38 shows the second highest rut deformation of 12.78 mm after 20 years of pavement service life. The rut depths of all the other mixes are appeared to be very close to each other.

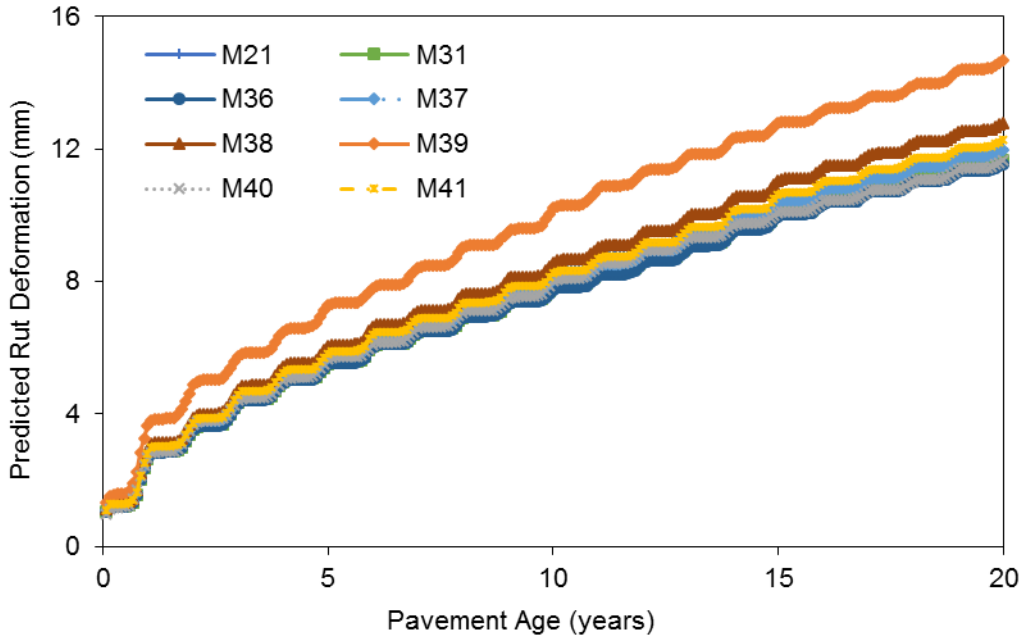

Figure 45: MEPDG Level 2 analysis rut prediction for SP IV Mixes

Table 24 presents a comparison of MEPDG rut depth with the laboratory measured rut deformation. As can be seen from table 24, the highest rut depth was observed for mixture 39 (4.98 mm) followed by mixture 38 (4.16 mm) which are consistent with the MEPDG analysis value. The MEPDG analysis yields higher rut depth after 20 years of pavement service life compared to the laboratory measured value for all the tested mixtures.

Table 24: MEPDG rut prediction data in mm

Mix	1 year	5 years	10 years	20 years	UNM Max. Rut
21	2.68	5.86	8.28	11.99	3.99
31	2.64	5.51	7.83	11.67	3.03
36	2.63	5.49	7.77	11.55	3.27
37	2.74	5.72	8.07	11.99	1.83
38	2.89	6.03	8.58	12.78	4.16
39	3.65	7.27	10.21	14.69	4.98
40	2.7	5.65	8.02	11.65	3.45
41	2.8	5.83	8.26	12.27	4.0

HWTD SPECIFICATION DEVELOPMENT FOR NEW MEXICO

Due to excessive rutting deformation incurred by mix 6 and 7, rut specification limit for SP-III was developed based on the HWTD laboratory test results for the other 31 mixes. Table 25 summarizes the maximum and minimum rut depth incurred by the mixes at various number of wheel passes. A total of 6 mixes have PG 64-XX binder grade and the maximum and minimum rut depth are measured 2.2 mm and 5.3 mm respectively from HWTD test at 10,000 wheel passes. The allowable maximum rut impression depth for PG 64-XX AC mixes at 10,000 wheel passes is developed based on the maximum rut values of the 6 mixes. The rut specification limits for other PG binder mixes are developed by employing the same principle.

Table 25: Maximum and minimum rut depth (mm) at various wheel passes

Binder Grade	Total Mixes	5000 (Passes)	10000 (Passes)	15000 (Passes)	20000 (Passes)
64-XX	6	2.0 - 4.0	2.2 - 5.3	2.4 - 7.1	2.5 - 11.4
70-XX	10	1.5 - 3.6	1.7 - 4.3	1.8 - 5.3	1.9 - 7.0
76-XX	15	1.3 - 3.1	1.5 - 3.6	1.6 - 4.1	1.8 - 4.8

Based on the HWTD laboratory test results, the New Mexico DOT is recommended to follow table 26 as a criteria to measure the quality of rut resistance of SP-III mixtures. If the reported rut depth is higher than the prescribed maximum rut value, the mix will be considered as failed. For example, the rut value of an SP-III mix involved with any of the following binder PG grade exceeds the maximum rut value, this mixture will be assessed as a failure.

Table 26: Rut specification limits for SP-III mixes

Binder Grade	HWTT Number of Wheel Passes	Test Temperature (°C)	Max Rut Value (mm)
64-XX	10000	50	5.5
64-XX	15000	50	7.0
64-XX	20000	50	11.5
70-XX	10000	50	4.5
70-XX	15000	50	5.5
70-XX	20000	50	7.0
76-XX	10000	50	3.5
76-XX	15000	50	4.0
76-XX	20000	50	5.0

Nine total SP-IV mixtures were collected and tested in this study. The rut specification for SP-IV mixtures was developed based on these test results. The rut specification for SP-IV mixtures is presented in Table 27. The New Mexico DOT is recommended to follow Table 26 as a criteria to measure the quality of rut resistance of SP-IV mixtures. If the reported rut depth is higher than the prescribed maximum rut value, the mix will be considered as failed. For example, the rut value of an SP-IV mix involved with any of the following binder PG grade exceeds the maximum rut value, this mixture will be assessed as a failure.

Table 27: Rut specification limits for SP-IV mixes

Binder Grade	HWTT Number of Wheel Passes	Test Temperature (°C)	Max Rut Value (mm)
64-XX	10000	50	5.5
64-XX	15000	50	6.0
64-XX	20000	50	6.5
70-XX	10000	50	4.5
70-XX	15000	50	5.0
70-XX	20000	50	5.5
76-XX	10000	50	3.5
76-XX	15000	50	4.0
76-XX	20000	50	4.5

CONCLUSIONS AND RECOMMENDATIONS

General

This research project conducts a comprehensive study to measure and minimize the rutting and stripping potentials of AC mixes using Hamburg Wheel Tracking Device. HWTD and TSR tests were conducted on the collected forty-two AC mixes. DSR and MSCR tests were also conducted on the virgin and extracted binder of several mixes. Several pavement sections were analyzed in MEPDG software and the resulting rut depth after the pavement design life were compared with the laboratory rut deformation.

Conclusions

Based on the overall tasks in this research project the following conclusions can be drawn:

- Given the HWTD test results conducted on the collected forty-two AC mixes, it was observed that the laboratory rut deformation was sensitive to aggregate type, PG binder grade, and RAP content. It was also found that SP-IV mixes experience less rutting compared to SP-III mixes.
- TSR test was conducted to assess the moisture susceptibility of the collected mixes. Of the collected forty-two mixes eleven mixes exhibited characteristic of stripping potentials. Attempt was made to correlate the moisture susceptibility of these mixes obtained from TSR test with the stripping potentials of the HWTD test results. This study found no strong correlation between them.
- Of the collected forty two mixes five were collected from the specific pavement study sections-10. These five mixes having the same mix design only differ in WMA additives and polymer modified binder. The HWTD results demonstrated that WMA additives enhance the rutting potentials of the mixtures.
- Several pavement sections were modeled and analyzed in MEPDG software. The obtained rut values after twenty years of pavement design life were compared with the laboratory HWTD test results. The MEPDG rut values are found to be higher than that of the HWTD test results.
- A detailed specification for the NMDOT was developed to evaluate the quality of rut resistance of both the SP-III and SP-IV mixes.

Recommendations

Recommendations are made to perform further research in the following area:

- The rut specification for SP-IV mixes was developed based on the HWTD test results for only nine mixes. The HWTD test should be conducted on more mixes in order to generate a detailed specification for SP-IV mixes.

- Field rut performance of the selected pavement sections can be monitored each year and compared it with the laboratory test results.

REFERENCES

[1] Solaimanian, M. and Pendola, G. (2011). “Aggregate Behavior in the Hamburg Wheel Tracking Device” Texas Department of Transportation.

[2] Sel, I., Yildirim, Y. and Ozhan, H. (2014). “Effect of Test Temperature on Hamburg Wheel-Tracking Device Testing” Journal of Materials in Civil Engineering, DOI: 10.1061/(ASCE)MT.1943-5533.0001036.

[3] Lu, Q. (2005). “Investigation of conditions for Moisture Damage in Asphalt Concrete and Appropriate Laboratory Test Methods” University of California Transportation Center.

[4] Yildirim, Y. and Stokoe, K. (2006). “Analysis of Hamburg Wheel Tracking Device Results in Relation to Field Performance” Report No. FHWA/TX-06/0-4185-5, Texas Department of Transportation.

[5] Izzo, R. and Tahmoressi, M. (1998). “Evaluation of the Use of the Hamburg Wheel Tracking Device for Moisutre Susceptibility of Hot Mix Asphalt” Report No. DHT-45, Texas Department of Transportation.

[6] Khandal, P., and Cooley, A. (2002). “Coarse versus Fine-Graded Superpave Mixtures Comparative Evaluation of Resistance to Rutting” Publication No. NCAT Report 02-02. National Center for Asphalt Technology.

[7] Gokhale, S., Choubane, B., Sholar, G., and Moseley, H. (2006). “Evaluation of Coarse and Fine Graded Superpave Mixtures under Accelerated Pavement Testing.” Publication No. FL/DOT/SMO/06-494. Florida Department of Transportation.

[8] Golalipour, A., Jamshidi, E., Niazi, Y., Afsharikia, Z., and Khadem, M. (2012). “Effect of Aggregate Gradation on Rutting Asphalt Pavements.” In Procedia Social and Behavioral Sciences. Vol 53, pp. 440-449.

[9] Manal A., and Attia, M. (2013). “Impact of Aggregate Gradation and Type of Hot Mix Asphalt Rutting in Egypt.” In International Journal of Engineering Research and Application, Vol. 3, Issue 4, pp. 2249-2258.

[10] Habeeb, H., Chandra, S., and Nashaat, Y. (2012). “Estimation of Moisture Damage and Permanent Deformation in Asphalt Mixture from Aggregate Gradation.” In KSCE Journal of Civil Enginering, Vol. 18(6), pp. 1655-1663.

[11] Kanitpong, K., Charoentham, N., and Likitlersuang, S. (2012). “Investigation on the Effects of Gradation and Aggregate Type to Moisture Damage of Warm Mix Asphalt Modified with Sasobit.” In International Journal of Pavement, Vol. 13:5, pp. 451-458.

[12] Tarefder, R. and Zaman, M. (2002). Evaluation of Rutting Potential of Hot Mix Asphalt Using the Asphalt Pavement Analyzer. Publication No. Final Report Item 2153; ORA 125-6660. Oklahoma Department of Transportation.

[13] Aschenbrener, T. and Currier, G, (1993). “Influence of Testing Variables on the Results from the Hamburg Wheel-Tracking Device” Report No. COOT -D1D-R-93-22, Colorado Department of Transportation, Denver, Colorado.

[14] Kassem, E., Masad, E., Lytton, R., and Chowdhury, A. (2011). “Influence of Air Voids on Mechanical Properties of Asphalt Mixtures.” In Journal of Road Materials and Pavement Designs, Vol. 12, pp. 493-524.

[15] Zaumanis, M. (2011) Warm Mix Asphalt Investigation. MSc. Thesis, Technical University of Denmark.

[16] Perkins, S. (2009) “Synthesis of Warm Mix Asphalt Paving Strategies for use in Montana Highway Construction.” Publication No. FHWA/MT-09-009/8117-38. Montana Department of Transportation.

[17] Liva, G., and McBroom, D. (2009). “Warm Mix Asphalt.” Research Report. Montana Department of Transportation.

[18] Hurley, G., and Prowell, B. (2006). “Evaluation of Evotherm for use in Warm Mix Asphalt” Publication No. NCAT Report 06-02. National Center for Asphalt Technology.

[19] Aschenbrener, T., Schiebel, B., and West, R. (2011). “Three-Year Evaluation of the Colorado Department of Transportation’s Warm-Mix Asphalt Experimental Feature on I-70 in Silverthorne, Colorado.” Publication No. NCAT Final Report 11-02. National Center for Asphalt Technology.

[20] Jones, D., Wu, R., Tsai, B., and Harvey, T. (2011). “Warm-Mix Asphalt Study: Test Track Construction and First-Level Analysis of Phase 3a HVS and Laboratory Testing. (Mix Design #1).” Publication No. CA13-2221A. California Department of Transportation.

[21] AASHTO T 2-10 (2010). “Standard Practice for Sampling Aggregates” Standard Specifications for Transportation Materials and Methods of Sampling and Testing, 31st Edition. AASHTO, Washington, D.C.

[22] AASHTO T 168 (2011). “Standard Method of Test for Sampling Bituminous Paving Mixtures" Standard Specifications for Transportation Materials and Methods of Sampling and Testing, AASHTO, Washington, D.C.

[23] AASHTO M 323-12 (2012). Standard specification for superpave volumetric mix design. Standard Specifications for Transportation Materials and Methods of Sampling and Testing.

[24] Roberts, F.L., Kandhal, P.S., Brown, E.R., Lee, D.Y., and Kennedy, T.W. (1996). Hot Mix Asphalt Materials, Mixture Design, and Construction. National Asphalt Paving Association Education Foundation (NAPA).

[25] FHWA (2011). “The multiple stress creep recovery (MSCR) procedure.” (FHWA-HIF-11-038). Office of Pavement Technology. Washington, DC: U.S. Department of Transportation, Federal Highway Administration.

[26] AASHTO T 312 (2011). “Standard Method of Test for Preparing and Determining the Density of Hot Mix Asphalt (HMA) Specimens by Means of the Superpave Gyratory Compactor" Standard Specifications for Transportation Materials and Methods of Sampling and Testing, AASHTO, Washington, D.C.

[27] AASHTO T 209 (2011). “Standard Method of Test for Theoretical Maximum Specific Gravity (Gmm) and Density of Hot Mix Asphalt (HMA)” Standard Specifications for

Transportation Materials and Methods of Sampling and Testing, AASHTO, Washington, D.C.

[28] AASHTO T 166 (2005). “Standard Method of Test for Bulk Specific Gravity (Gmb) of Compacted Hot Mix Asphalt (HMA) Using Saturated Surface-Dry Specimens" Standard Specifications for Transportation Materials and Methods of Sampling and Testing, AASHTO, Washington, D.C.

[29] AASHTO T 269 (2014). “Standard Method of Test for Percent Air Voids in Compacted Dense and Open Asphalt Mixtures” Standard Specifications for Transportation Materials and Methods of Sampling and Testing, AASHTO, Washington, D.C.

[30] AASHTO T 324-11 (2011). “Standard Method of Test for Hamburg Wheel-Track Testing of Compacted Hot-Mix Asphalt (HMA).” Standard Specifications for Transportation Materials and Methods of Sampling and Testing, 31st Edition. AASHTO, Washington, D.C.

[31] AASHTO TP 79-09 (2009). “Standard Method of Test for Determining the Dynamic Modulus and Flow Number for Hot Mix Asphalt (HMA) Using the Asphalt Mixture Performance Tester (AMPT).’ Standard Specifications for Transportation Materials and Methods of Sampling and Testing, 29th Edition. AASHTO, Washington, D.C.

[32] Yildirim, Y., Jayawickrama, P., Hossain, M., Alhabshi, A., Yildirim, C., Fortier Smit, A. and Little, D. (2007). “Hamburg Wheel Tracking Database Analysis” Report 0-1707-7, Texas Department of Transportation, Austin, TX.

[33] AASHTO T 168 (2011). “Standard Method of Test for Sampling Bituminous Paving Mixtures" Standard Specifications for Transportation Materials and Methods of Sampling and Testing, AASHTO, Washington, D.C.

[34] Williams, R., & Prowell, B. (1999). “Comparison of laboratory wheel-tracking test results with Wes Track performance.” Transportation Research Record: Journal of the Transportation Research Board, 1681, 121-128.

[35] Mercado, E.A. (2007). “Influence of fundamental material properties and air void structure on moisture damage of asphalt mixes.” PhD Thesis submitted to Texas A&M University.

[36] Ahmad, M. (2013). “Permeability and Moisture Damage Characteristics of Asphalt Pavements.” PhD Thesis submitted to University of New Mexico.

[37] Hicks, R.G. (1991). “Moisture Damage in Asphalt Concrete: Synthesis of Highway Practice.” NCHRP Report 175.

[38] Apeagyei, A.K., Buttlar, W.G., and Dempsey, B.J. (2006). “Moisture Damage Evaluation of Asphalt Mixtures using AASHTO T283 and DC(T) Fracture Test.” 10th International Conference on Asphalt Pavements – August 12-17, 2006, Quebec City, Canada, Vol. 1, pp. 740-51.

[39] New Mexico Department of Transportation (2014). “Standard Specifications for Highway and Bridge Construction.” 2014th Edition, pp. 213.

[40] AASHTO T 283-14 (2014). “Standard Method of Test for Resistance of Compacted Asphalt Mixtures to Moisture-Induced Damage” Standard Specifications for Transportation Materials and Methods of Sampling and Testing, AASHTO, Washington, D.C.

[41] Gandhi, T. (2008). “Effects of warm asphalt additives on asphalt binder and mixture properties.” Thesis.

[42] Katman, H.Y., Ibrahim, M.R., Matori, M.Y., Norhisham, S., Ismail, N., and Che Omar, R. (2012). “Tensile Strength of Reclaimed Asphalt Pavement.” International Journal of Civil & Environmental Engineering IJCEE-IJENS Vol: 12 No: 03.

[43] Jung, S.H. (2006). “The Effects of Asphalt Binder Oxidation on Hot Mix Asphalt Concrete Mixture Rheology and Fatigue Performance.” PhD Thesis submitted to Texas A&M University.

[44] AASHTO T 240 (2014). “Effect of Heat and Air on a Moving Film of Asphalt Binder (Rolling Thin-Film Oven Test)” Standard Specifications for Transportation Materials and Methods of Sampling and Testing, AASHTO, Washington, D.C.

[45] AASHTO T 342-11 (2011). “Standard Method of Test for Determining Dynamic Modulus of Hot Mix Asphalt (HMA).” Standard Specifications for Transportation Materials and Methods of Sampling and Testing, 31st Edition. AASHTO, Washington, D.C.

[46] McDaniel, R. S., Shah, A., Huber, G. A., & Copeland, A. (2012). “Effects of reclaimed asphalt pavement content and virgin binder grade on properties of plant produced mixtures”. Road Materials and Pavement Design, 13(sup1), 161-182.

[47] AASHTO D 2172 (2010). “Standard Test Methods for Quantitative Extraction of Bitumen from Bituminous Paving Mixtures” Standard Specifications for Transportation Materials and Methods of Sampling and Testing, 31st Edition. AASHTO, Washington, D.C.

[48] AASHTO D 5404 (2010). “Standard Practice for Recovery of Asphalt from Solution Using the Rotary Evaporator” Standard Specifications for Transportation Materials and Methods of Sampling and Testing, 31st Edition. AASHTO, Washington, D.C.

[49] Li, X., Marasteanu, M., Williams, R., & Clyne, T. (2008). “Effect of reclaimed asphalt pavement (proportion and type) and binder grade on asphalt mixtures.” Transportation Research Record: Journal of the Transportation Research Board, (2051), 90-97.

[50] Booshehrian, Abbas, Walaa S. Mogawer, and Ramon Bonaquist. "How to construct an asphalt binder master curve and assess the degree of blending between RAP and virgin binders." Journal of Materials in Civil Engineering 25, no. 12 (2012): 1813-1821.

[51] Bahia, H.U., Hanson, D.I., Zeng, M., Zhai, H., Khatri, M.A. and Anderson, R.M., “Characterization of modified asphalt binders in superpave mix design”, (No. Project 9-10 FY'96), 2001.

[52] Tabatabaee, H.A. and Bahia, H.U., “Establishing use of asphalt binder cracking tests for prevention of pavement cracking”, Road Materials and Pavement Design, 15(sup1), 2014, pp.279-299.

[53] Pérez-Lepe, A., Martınez-Boza, F.J., Gallegos, C., González, O., Muñoz, M.E. and Santamarıa, A., “Influence of the processing conditions on the rheological behaviour of polymer-modified bitumen”, Fuel, Vol. 82, No. 11, 2003, pp.1339-1348.

[54] Gómez-Meijide, B., and I. Pérez (2016). “Binder–aggregate Adhesion and Resistance to Permanent Deformation of Bitumen-Emulsion-Stabilized Materials Made with Construction and Demolition Waste Aggregates.” Journal of Cleaner Production 129: 125–133.

[55] Remišová, Eva, and Viera Zatkalíková (2016). “Evaluation of Bituminous Binder in Relation to Resistance to Permanent Deformation.” Procedia Engineering 153. XXV Polish – Russian – Slovak Seminar “Theoretical Foundation of Civil Engineering”: 584–589.

[56] Ling, Cheng, Amir Arshadi, and Hussain Bahia (2017). “Importance of Binder Modification Type and Aggregate Structure on Rutting Resistance of Asphalt Mixtures Using Image-Based Multi-Scale Modelling.” Road Materials and Pavement Design 18(4): 785–799.

[57] Morea, F., J. O. Agnusdei, and R. Zerbino (2010). “Comparison of Methods for Measuring Zero Shear Viscosity in Asphalts.” Materials and Structures 43(4): 499–507.

[58] Silva, Hugo M. R. D., Joel R. M. Oliveira, Joana Peralta, and Salah E. Zoorob (2010). “Optimization of Warm Mix Asphalts Using Different Blends of Binders and Synthetic Paraffin Wax Contents.” Construction and Building Materials 24(9): 1621–1631.

[59] Ziari, Hasan, Rezvan Babagoli, and Ali Akbari (2015). “Investigation of Fatigue and Rutting Performance of Hot Mix Asphalt Mixtures Prepared by Bentonite-Modified Bitumen.” Road Materials and Pavement Design 16(1): 101–118.

[60] FHWA (2011). “The multiple stress creep recovery (MSCR) procedure.” (FHWA-HIF-11-038). Office of Pavement Technology. Washington, DC: U.S. Department of Transportation, Federal Highway Administration.

[61] Giuliana, G., Nicolosi, V., & Festa, B. (2012). “Predictive Formulas of Complex Modulus for High Air Void Content Mixes”. In Transportation Research Board 91st Annual Meeting.

[62] Singh, D., Zaman, M., & Commuri, S. (2011). “Evaluation of predictive models for estimating dynamic modulus of hot-mix asphalt in Oklahoma”.Transportation Research Record: Journal of the Transportation Research Board, (2210), 57-72.

[63] El-Badawy, S., Bayomy, F., & Awed, A. (2012). “Performance of MEPDG dynamic modulus predictive models for asphalt concrete mixtures: local calibration for Idaho”. Journal of Materials in Civil Engineering, 24(11), 1412-1421.

[64] Zaman, M., & Hossain, Z. (2012). “Behavior of selected warm mix asphalt additive modified binders and prediction of dynamic modulus of the mixes”. Journal of Testing and Evaluation, 41(1), 1-12.

[65] Rahman, A. S. M. A., Hasan M. Faisal, and Rafiqul A. Tarefder. "Application of a Numerical Interconversion Technique to Determine the Effect of Aging on Linear

Viscoelastic Material Functions of Asphalt Concrete". Transportation Research Board 94th Annual Meeting. No. 15-5672. 2015.